Nobel Symposium on Free Electron Laser Research
14^{th}-18^{th} June, 2015
Sigtunahöjden, Sweden

SACLA and FERMI: New opportunities for atomic, molecular and cluster science

Kiyoshi Ueda

Tohoku University, Sendai 980-8577, Japan

Nobel Symposium on Free Electron Laser Research
14th-18th June, 2015
Sigtunahöjden, Sweden

SACLA : New opportunities for atomic, molecular and cluster science

Kiyoshi Ueda
Tohoku University, Sendai 980-8577, Japan

Nobel Symposium on Free Electron Laser Research
14th-18th June, 2015
Sigtunahöjden, Sweden

SACLA and FERMI: New opportunities for atomic, molecular and cluster science

Kiyoshi Ueda

Tohoku University, Sendai 980-8577, Japan

SACLA

Masaki

We appreciate your support for our SLiT-J (3GeV ring+FEL) project!

FERMI

Coherent control via phase controlled multicolor FEL!

Carlo

EUV-X FELs in the world

Swiss FEL (2017), Korean FEL, Shanghai FEL, etc., are coming!

Outline

- From SCSS (SASE EUVFEL) to FERMI (seeded EUVFEL)
  – Interatomic Colombic decay (ICD) vs nanoplasma formation
  – ICD cascades, inelastic scattering of ICD electrons in neon clusters
  – Two-photon excitation of ICD states and the time-resolved study in neon dimers
  – Coherent control for photoionization of the neon atom by phase-controlled two-color (w-2w) pulses

- to SACLA (SASE hard X-ray FEL)
  – Deep inner-shell multi-photon ionization of Ar and Xe atoms
  – Photoion-photoion coincidence imaging following deep inner-shell multi-photon ionization of CH3I and 5I-uracil
  – Electron spectroscopy on cold nanoplasma formation from argon, krypton and xenon clusters
  – Single-shot imaging of xenon nano-clusters
  – IR-probe experiment of XFEL-ignited nanoplasma dynamics

SCSS test accelerator : EUV-FEL (20-24 eV)

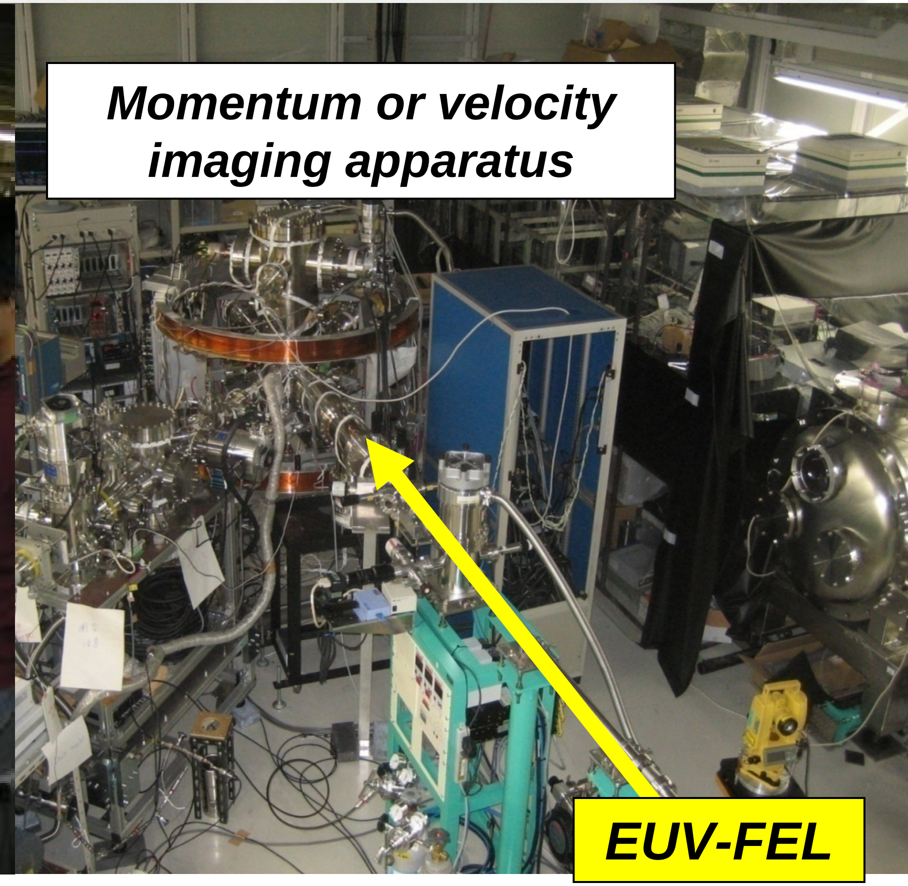

Multiple ionization of rare gas clusters: with M. Yao's group

EUV-pump EUV-probe: with J. Ullrich's group

Electron spectroscopy with VMI: with M. Vrakking's group

Linear FEL power dependence of energetic Ne+ yields

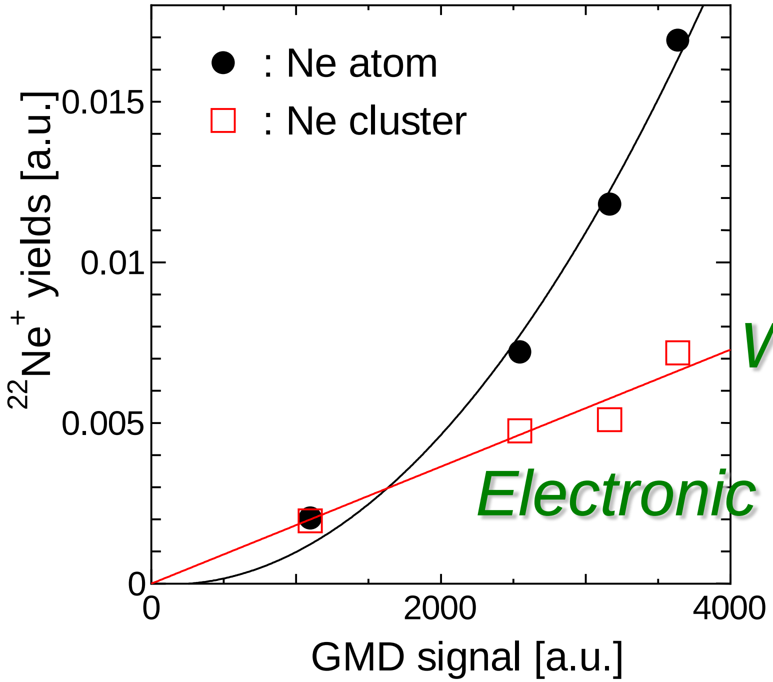

WHY?

Electronic decay ?

Interatomic Coulombic decay in multiply excited clusters

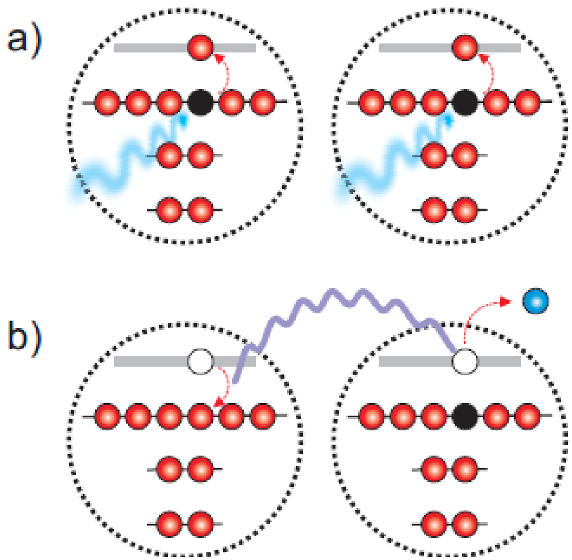

*Kuleff et al. PRL **105**, 043004 (2010).*

We found linear FEL-power dependence of energetic Ne^+ yields ejected from clusters (<N>=1000), in sharp contract with quadratic FEL-power dependence of Ne^+ yields from the atomic beam.

K. Nagaya, A. Sugishima, H. Iwayama, H. Murakami, M. Yao, H. Fukuzawa, X.-J. Liu, K. Motomura, K. Ueda, N. Saito, L. Foucar, A. Rudenko, M. Kurka, K.-U. Kuehnel, J. Ullrich, A. Czasch, R. Doerner, R. Feifel, M. Nagasono, A. Higashiya, M. Yabashi, T. Ishikawa, T. Togashi,, H. Kimura, and H. Ohashi,
*J. Phys. B: At. Mol. Opt. Phys. **46**, 164023 (2013)*

Thermal emission from Ne clusters

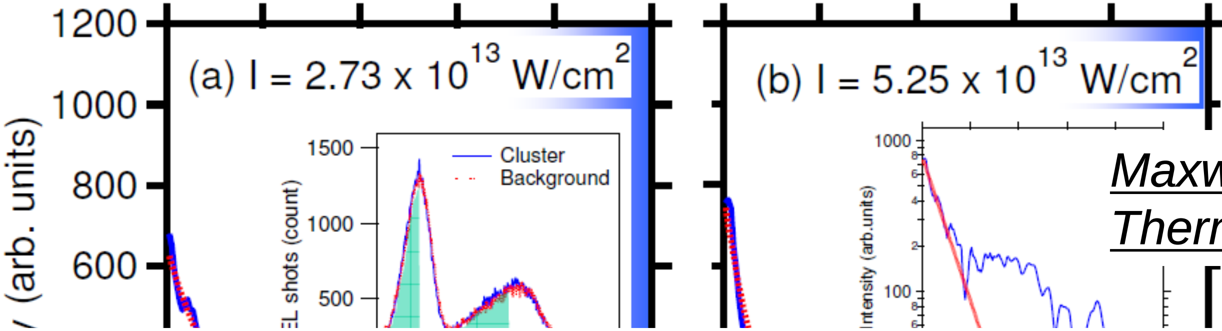

Maxwell-Boltzmann distribution
Thermal emission (Te ~ 2eV)

S. Yase, K. Nagaya, Y. Mizoguchi, M. Yao, H. Fukuzawa, K. Motomura, A. Yamada, Ri Ma, K. Ueda, N. Saito, M. Nagasono, T. Togashi, K. Tono, M. Yabashi, T. Ishikawa, H. Ohashi, and Y. Senba Phys. Rev. A ***88****, 043203 (2013).*

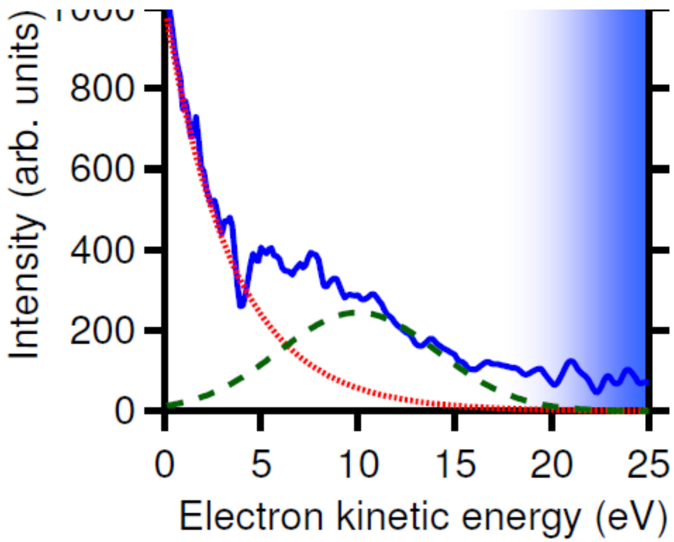

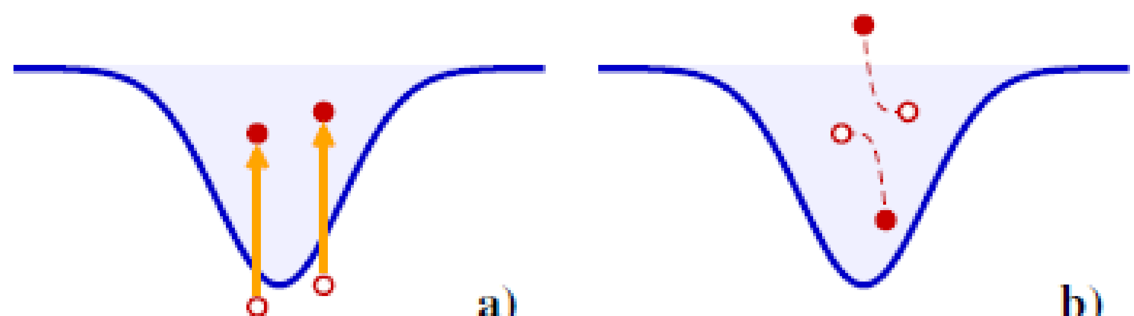

collisions between "free" electrons

Bostedt et al. NJP ***12****, 083004 (2010).*

Evidence of ICD cascades

3d +3d → 3p + e(ICD)

3d + 3d → 3s + e(ICD)

3s + 3s → 2p + e(ICD)

3d +3d → 2p + e(ICD)

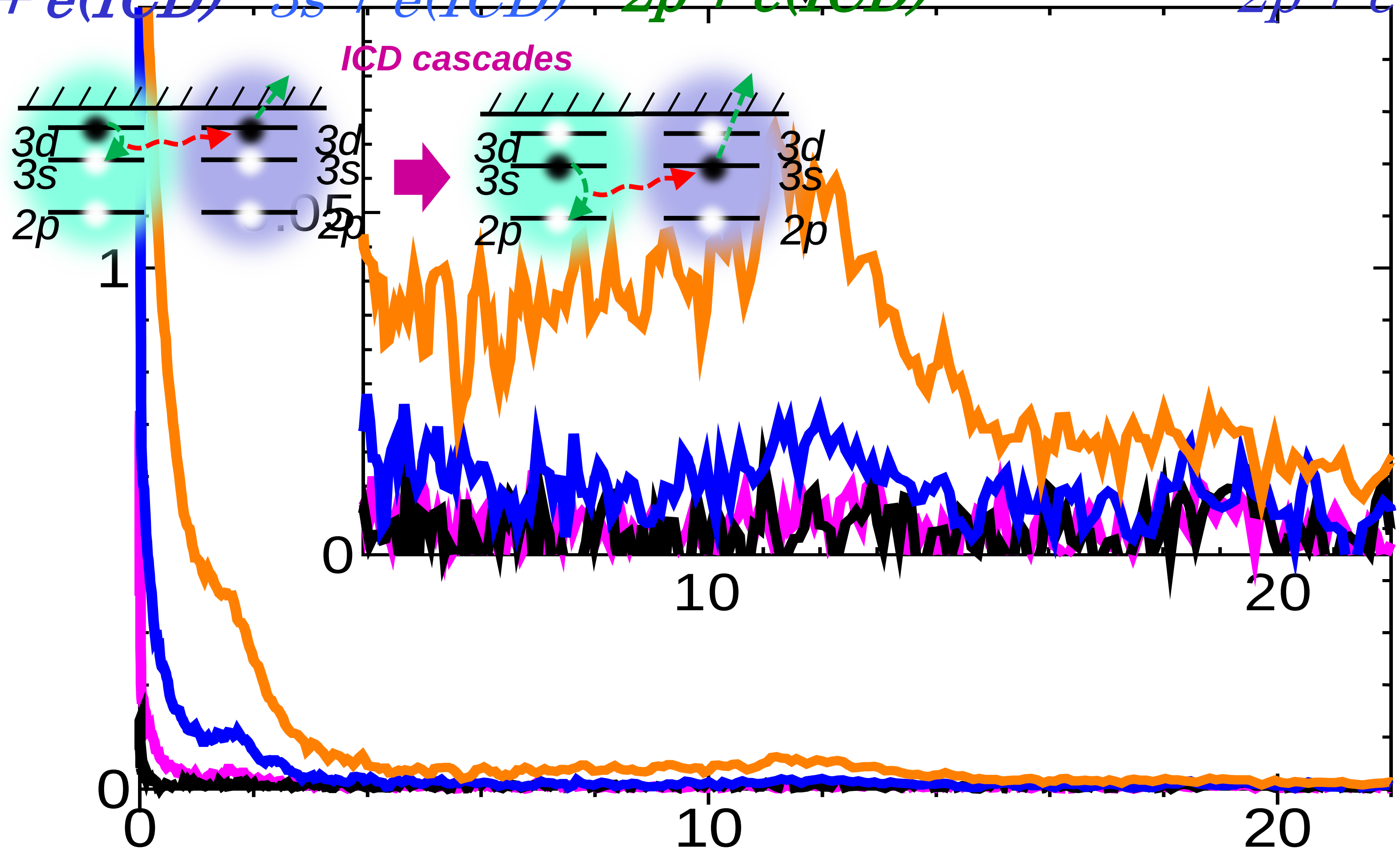

ICD cascades: experiment and theory

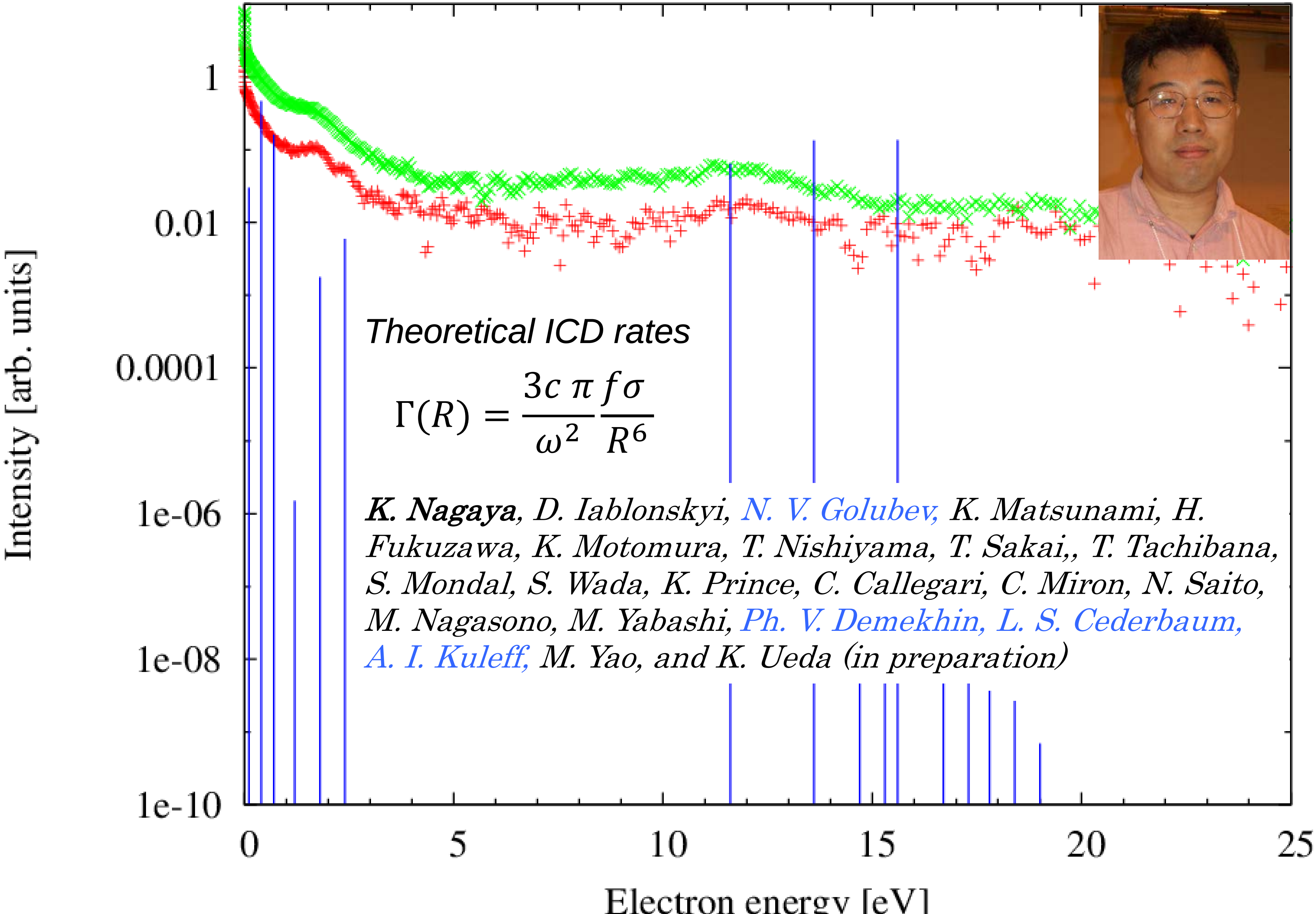

Theoretical ICD rates

$$\Gamma(R) = \frac{3c\,\pi}{\omega^2}\frac{f\,\sigma}{R^6}$$

K. Nagaya, *D. Iablonskyi, N. V. Golubev, K. Matsunami, H. Fukuzawa, K. Motomura, T. Nishiyama, T. Sakai,, T. Tachibana, S. Mondal, S. Wada, K. Prince, C. Callegari, C. Miron, N. Saito, M. Nagasono, M. Yabashi, Ph. V. Demekhin, L. S. Cederbaum, A. I. Kuleff, M. Yao, and K. Ueda (in preparation)*

Absorption spectra of neon clusters

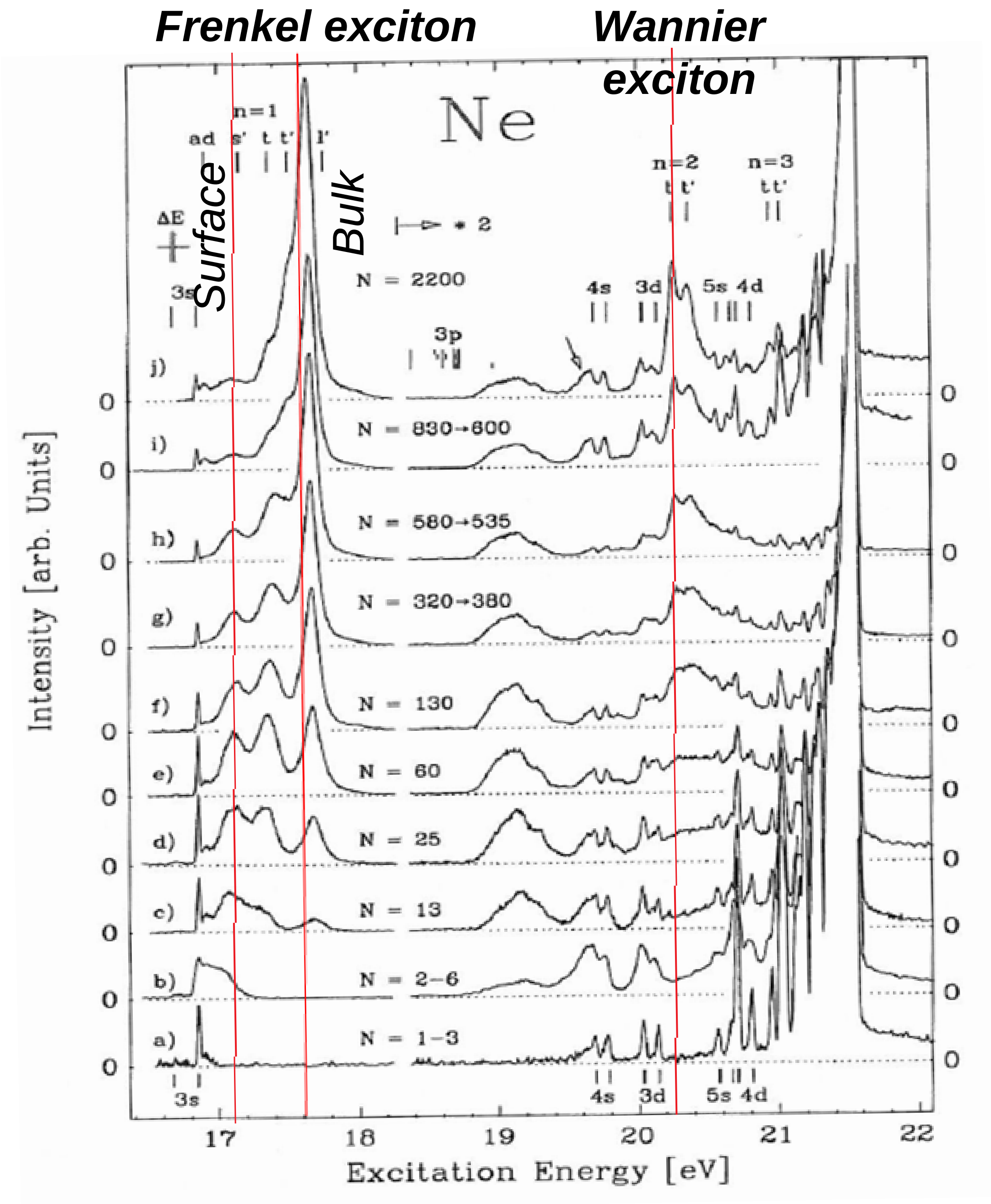

M. Joppien, Ph.D. thesis
Universität Hamburg (1994)

FERMI@ELETTRA: seeded FEL source

Operation for users started in December 2012

3rd harmonic of Ti:Sa laser or OPA → *Modulator* → *Radiator*

Photon energy range: 19-62 eV

Pulse duration: < 100 fs

Pulse Energy: < 100 μJ

Photon energy tunability

$\Delta\omega_{XUV} \sim 20\ meV$

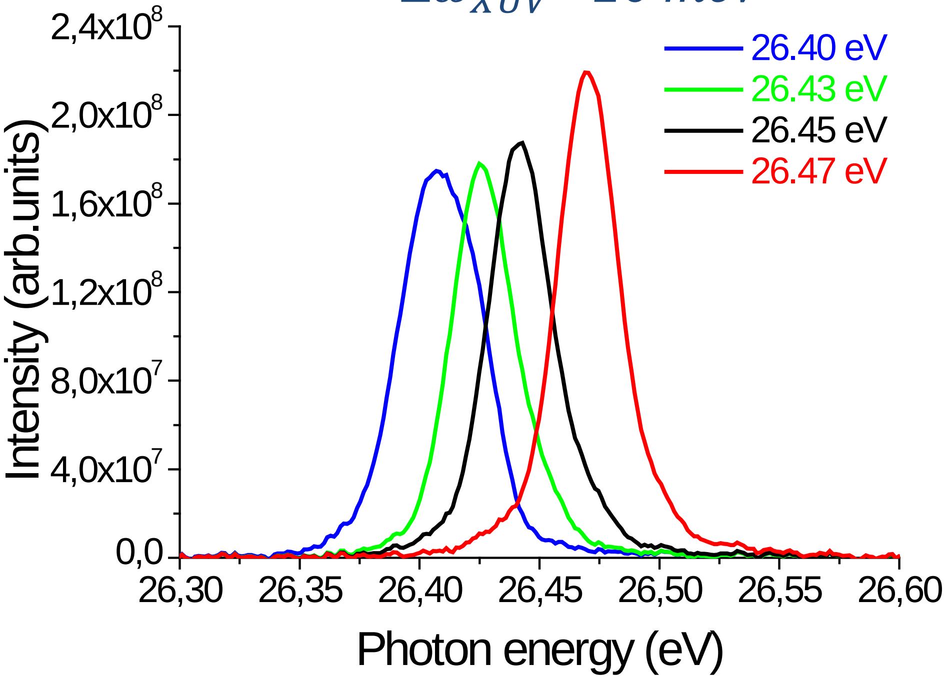

Ideal source for investigating nonlinear resonant effects!

Surface Frenkel exciton ($2p^6 \rightarrow 2p^5 3s$ @17.12eV)

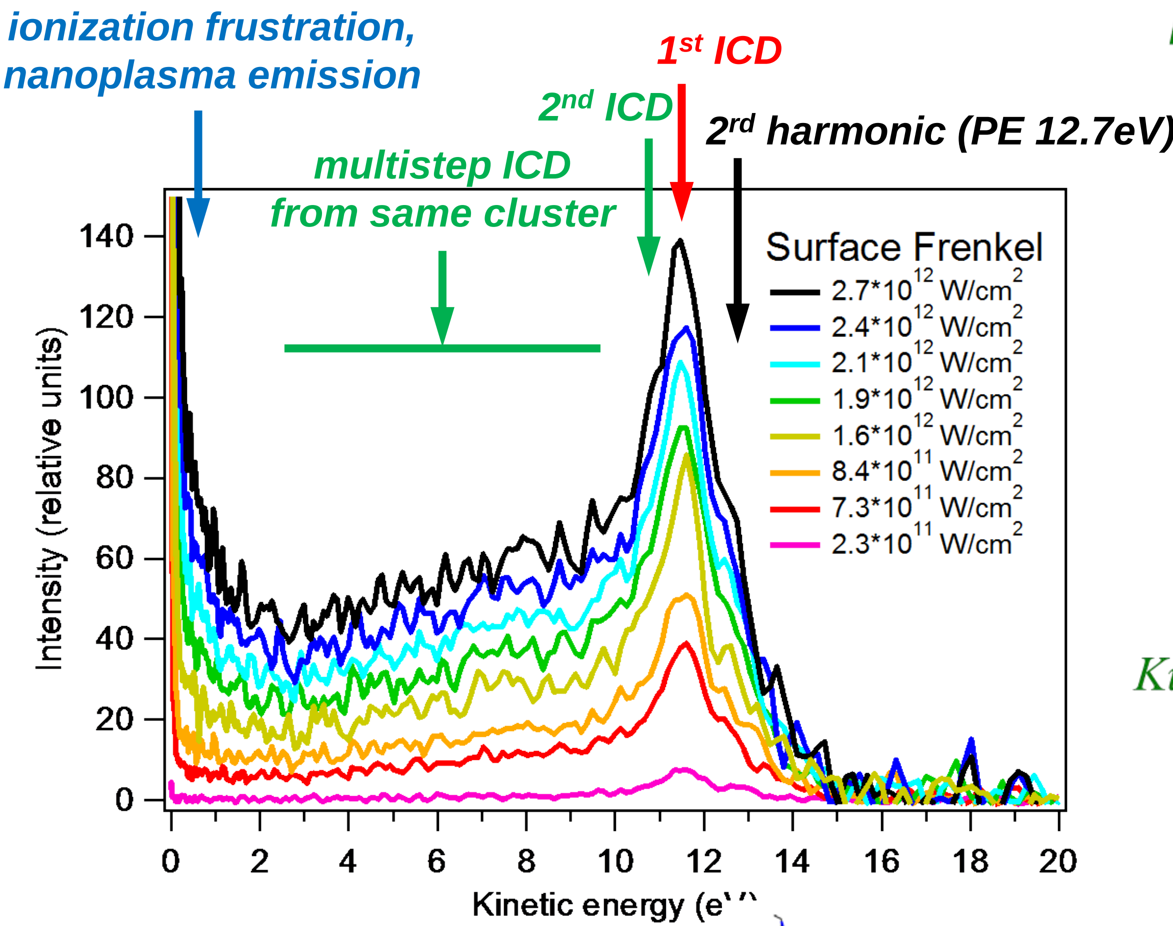

Interatomic Coulombic decay in multiply excited clusters

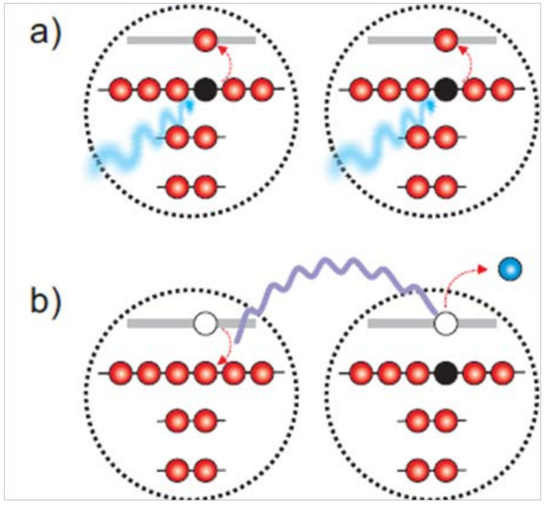

Kuleff et al. PRL ***105****, 043004 (2010).*

Electrons are bounded to the individual atomic ions.

Multistep direct ionization of Ar_{147} clusters

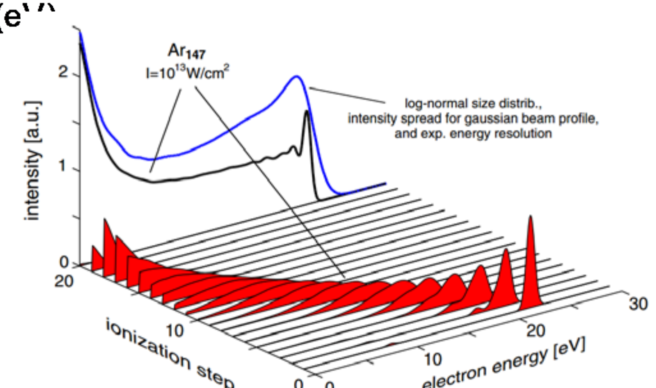

C. Bostedt et al., Phys. Rev. Lett. ***100****, 133401 (2008)*

Bulk Frenkel exciton ($2p^6 \rightarrow 2p^5 3s$ @17.65eV)

ICD:

$3s+3s \rightarrow 2p+e$

Internal inelastic scattering ICD:

$3s+3s+3s \rightarrow 2p+3p+e$ (knock-up)

$3s+3s+3s \rightarrow 2p+e+e$ (knock-off)

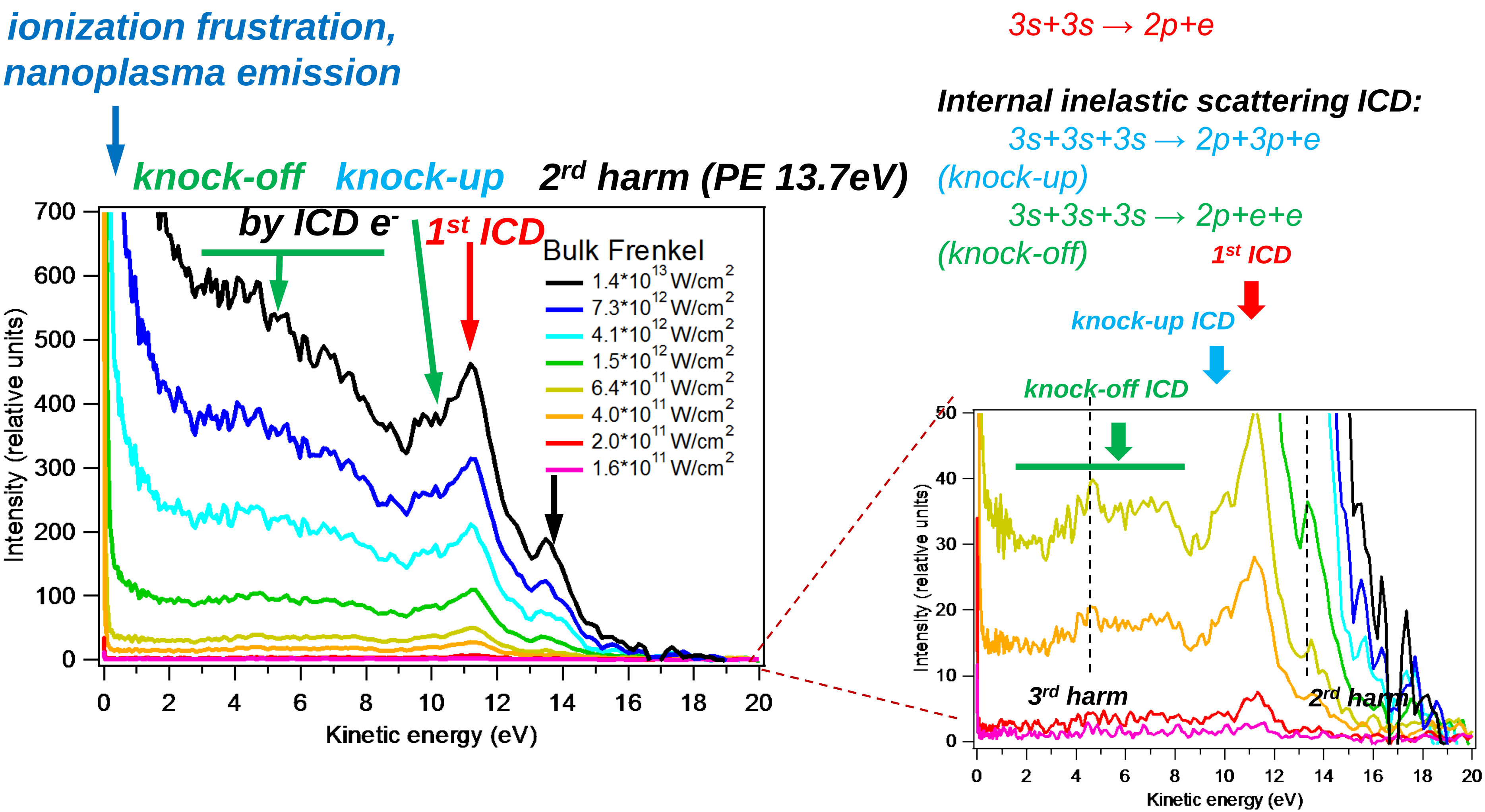

Wannier exciton $(2p^6 \rightarrow 2p^5 3d$ @20.26eV)

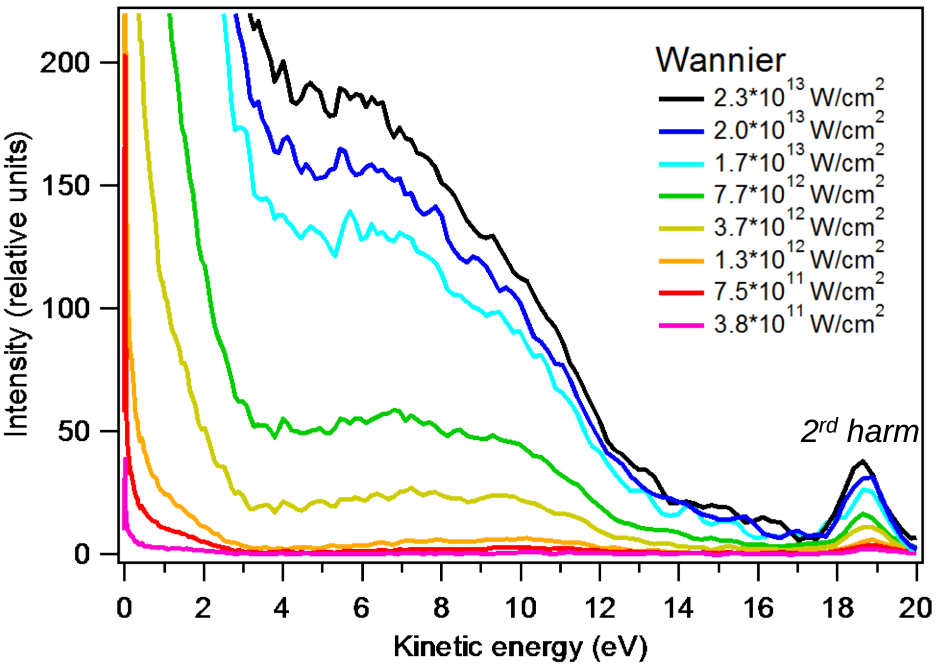

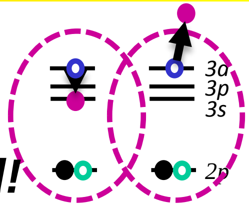

2-body ICD:

3d+3d → 2p+e ***– quenched!***

3d+3d → 3s+e(~1.3eV) – intra-Rydberg ICD

3s+3s → 2p+e – cascade ICD

Internal inelastic scattering ICD:

numerous knock-up and knock-off CD channels

intra-Rydberg ICD
(super Coster-Kronig)

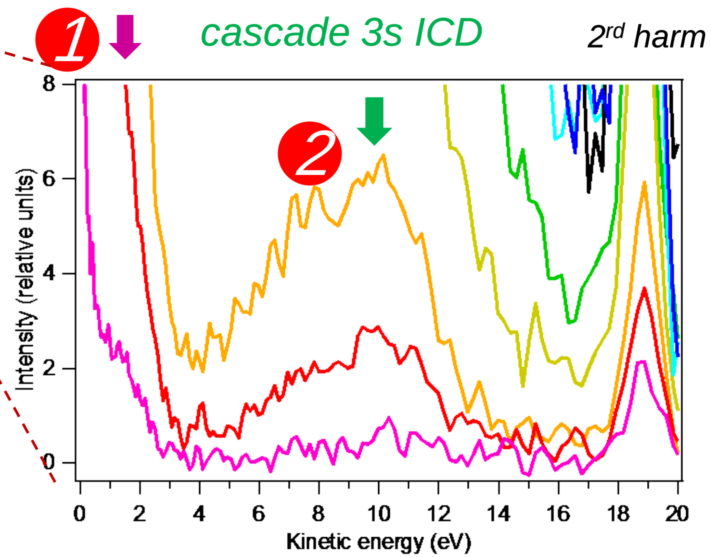

Summary of observed various ICDs

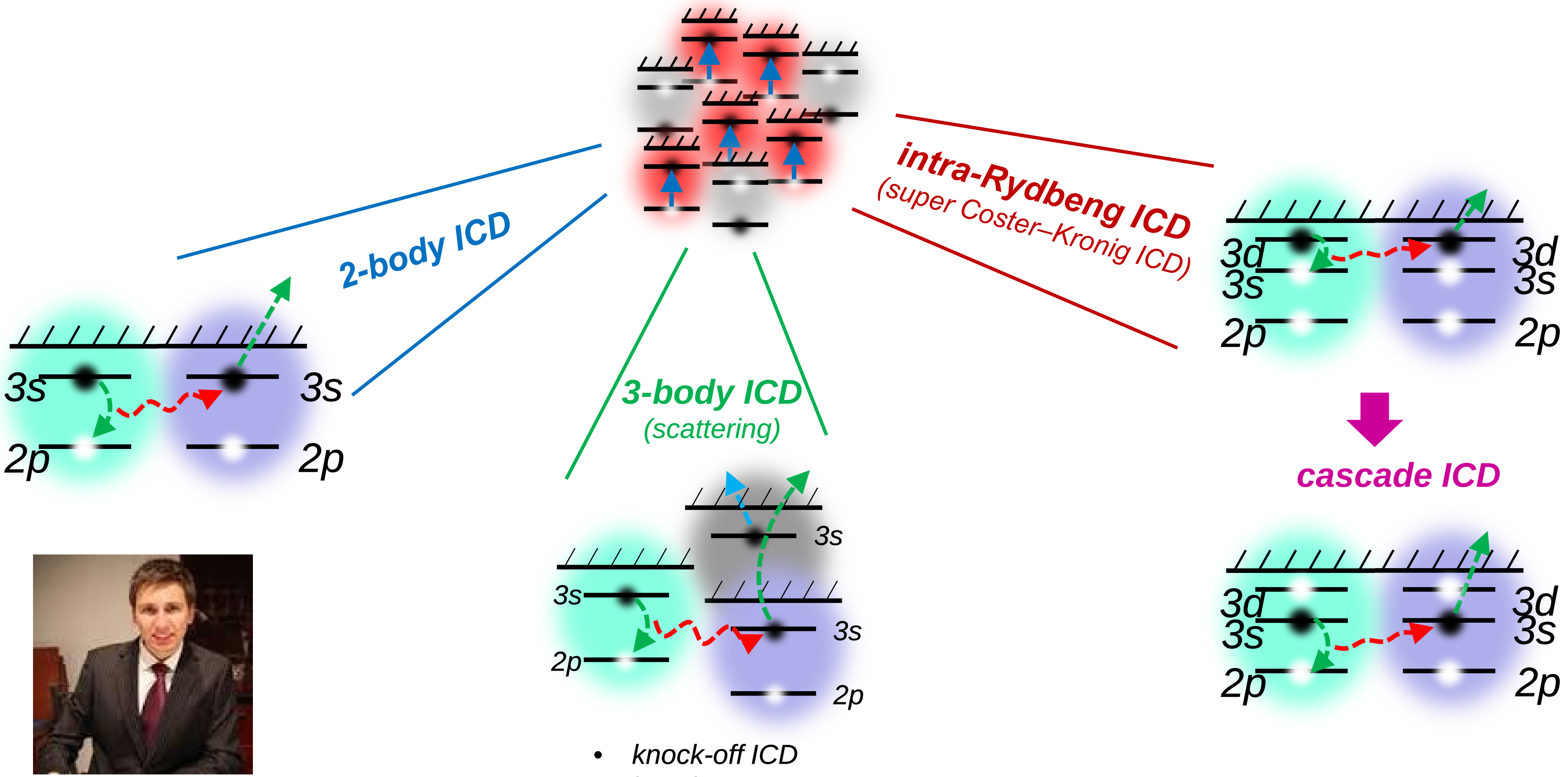

- *knock-off ICD*
- *knock-up ICD*

D. Iablonskyi, P. Johnsson, T. Takanashi, H. Fukuzawa, K. Motomura, Y. Kumagai, S. Mondal, T. Tachibana, T. Nishiyama, K. Nagaya, P. Piseri, G. Sansone, A. Dubrouil, M. Reduzzi, P. Carpeggiani, C. Vozzi, M. Devetta, M. Negro, D. Faccialà, F. Calegari, A. Trabattoni, M. Castrovilli, Y. Ovcharenko, T. Moeller, M. Mudrich, F. Stienkemeier, M. Coreno, M. Alagia, B. Schütte, N. Berrah, C. Callegari, O. Plekan, P. Finetti, K. C. Prince, L. Giannessi, C. Spezzani, E. Ferrari, E. Allaria, G. Penco, C. Serpico, G. De Ninno, B. Diviacco, S. Di Mitri, M. Yao, and K. Ueda (in preparation)

Two-photon excitation of ICD in neon dimers

Theoretical prediction

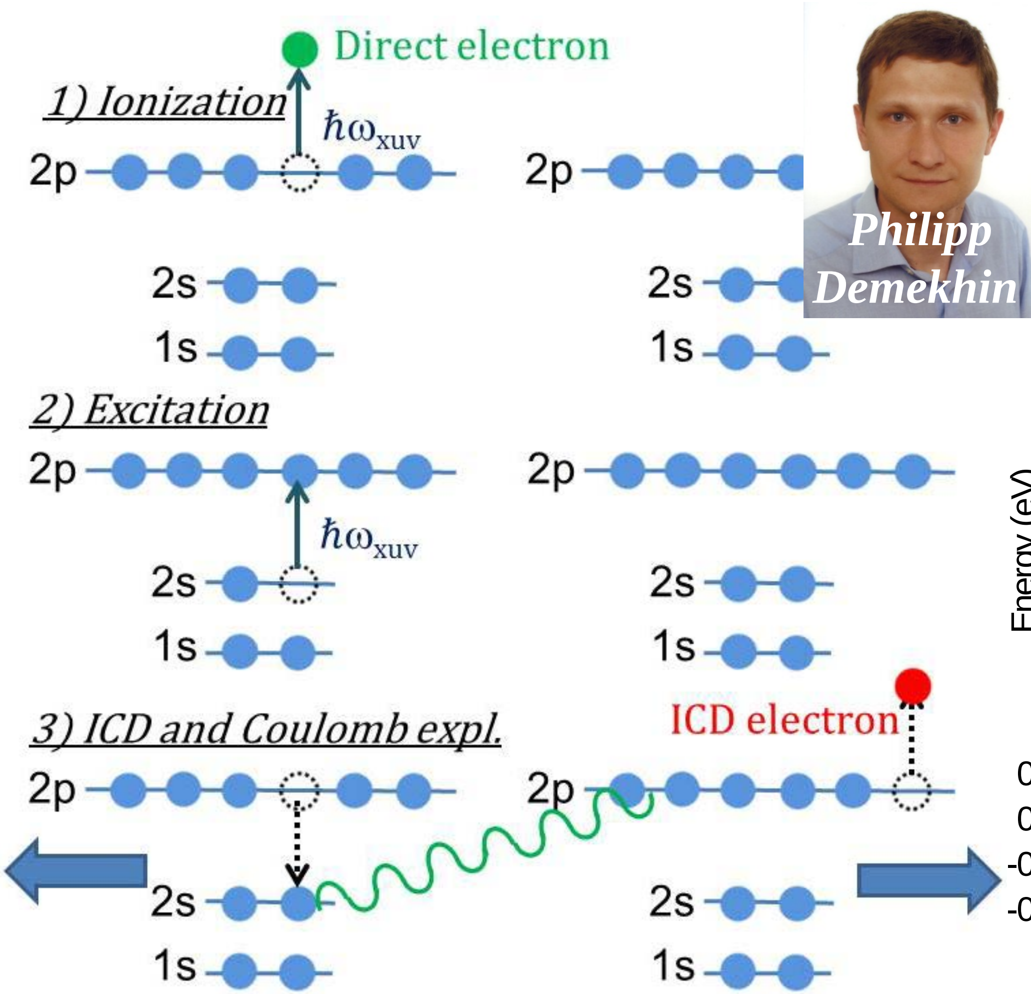

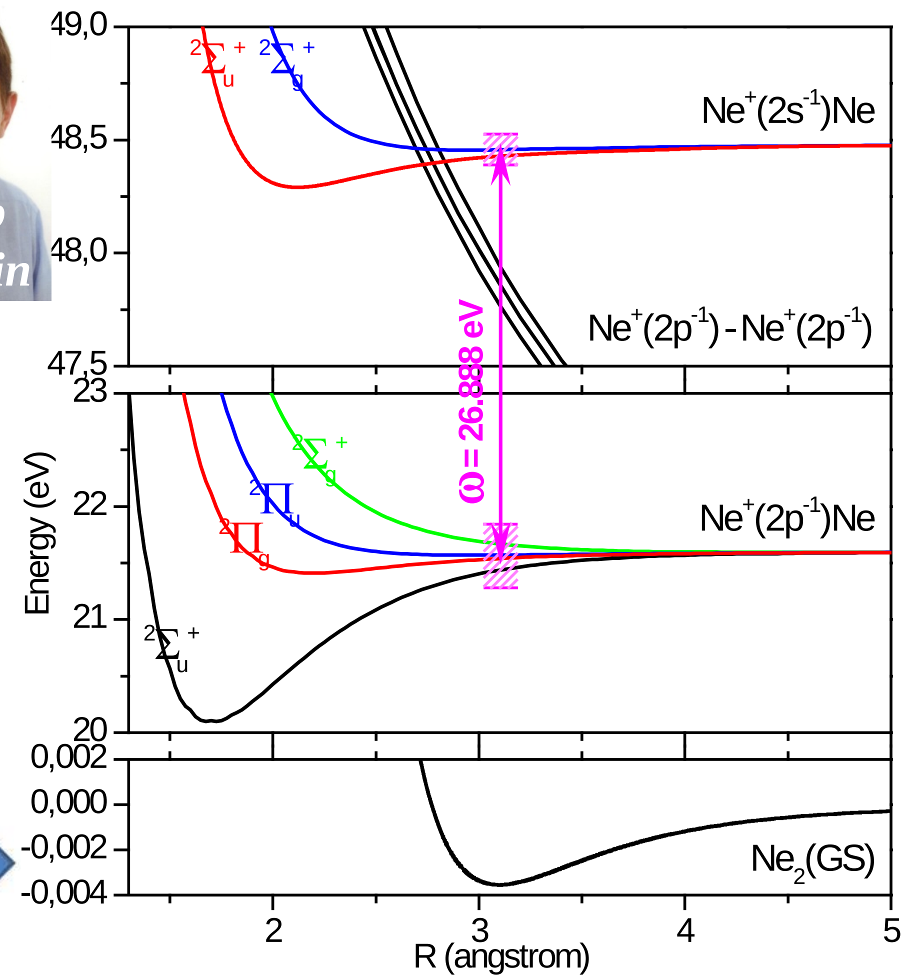

E_{2s}-E_{2p}=$\hbar\omega$ = 26.9 eV

…ekhin et al., PRL **107** (2011).

Two-photon-excitation-induced ICD in Ne_2

A Dubrouil, M Reduzzi, M Devetta, C Feng, J Hummert, P Finetti, O Plekan, C Grazioli, M Di Fraia, V Lyamayev, A La Forge, R Katzy, F Stienkemeier, Y Ovcharenko, M Coreno, N Berrah, K Motomura, S Mondal, K Ueda, K C Prince, C Callegari, A I Kuleff, Ph V Demekhin, G Sansone

(submitted)

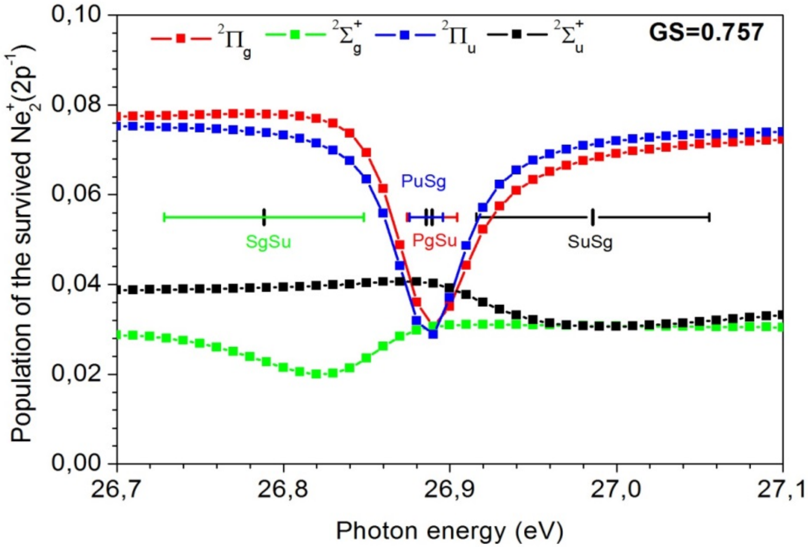

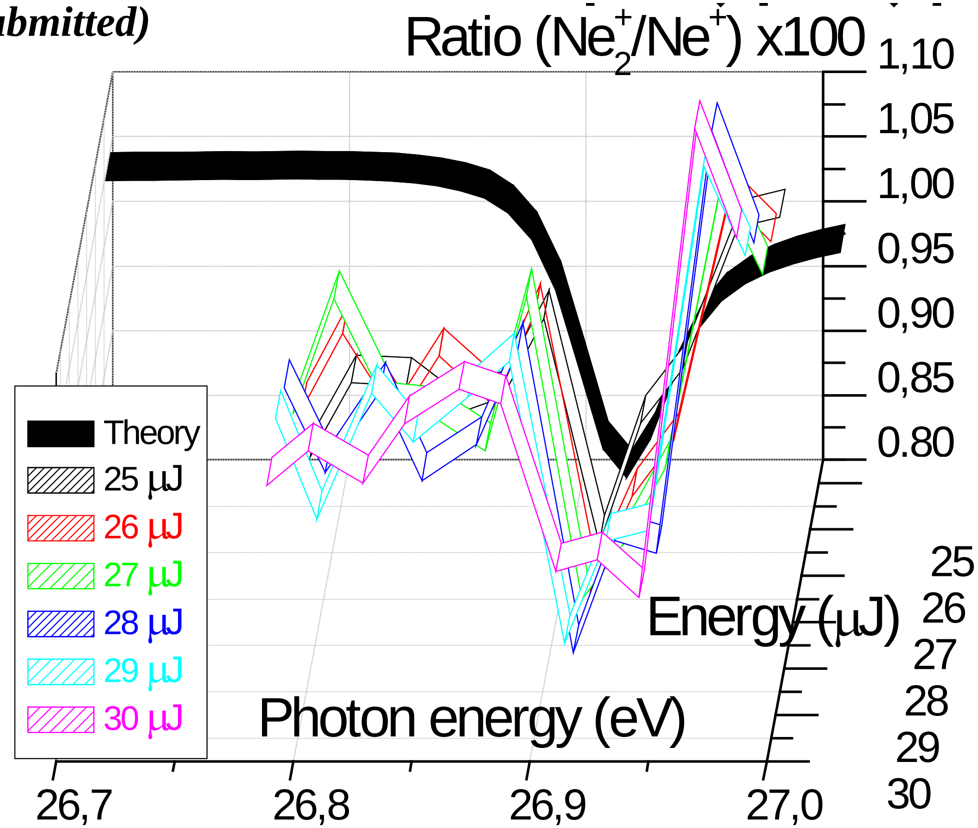

$$E_{2s}\text{-}E_{2p}=\hbar\omega = 26.9\ eV$$

We have experientally proved the depletion of ionized neon dimers Ne_2^+ through the resonance as predicted by theory!

Two-photon two-site excitation of ICD

ICD processes induced by two-photon double excitation in Ne_2

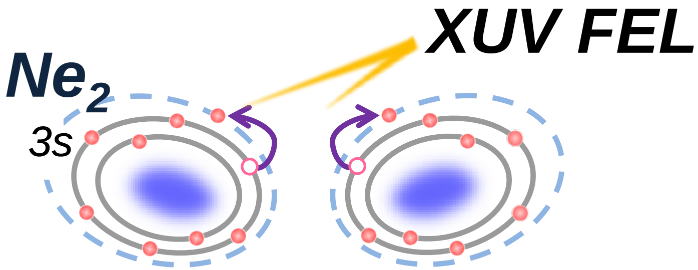

$Ne_2 + 2h\nu \rightarrow [Ne^*(2p^{-1}3s)]_2$

・・・two photon double excitation

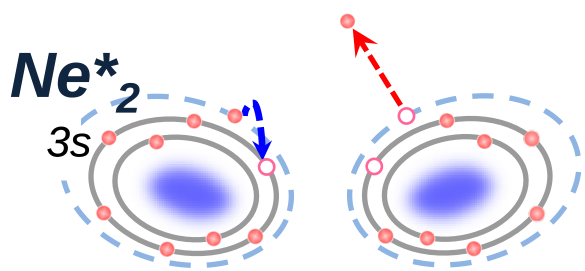

$[Ne^*(2p^{-1}3s)]_2 \xrightarrow{ICD} Ne^+(2p^{-1})\text{-}Ne + e_{ICD}^-$

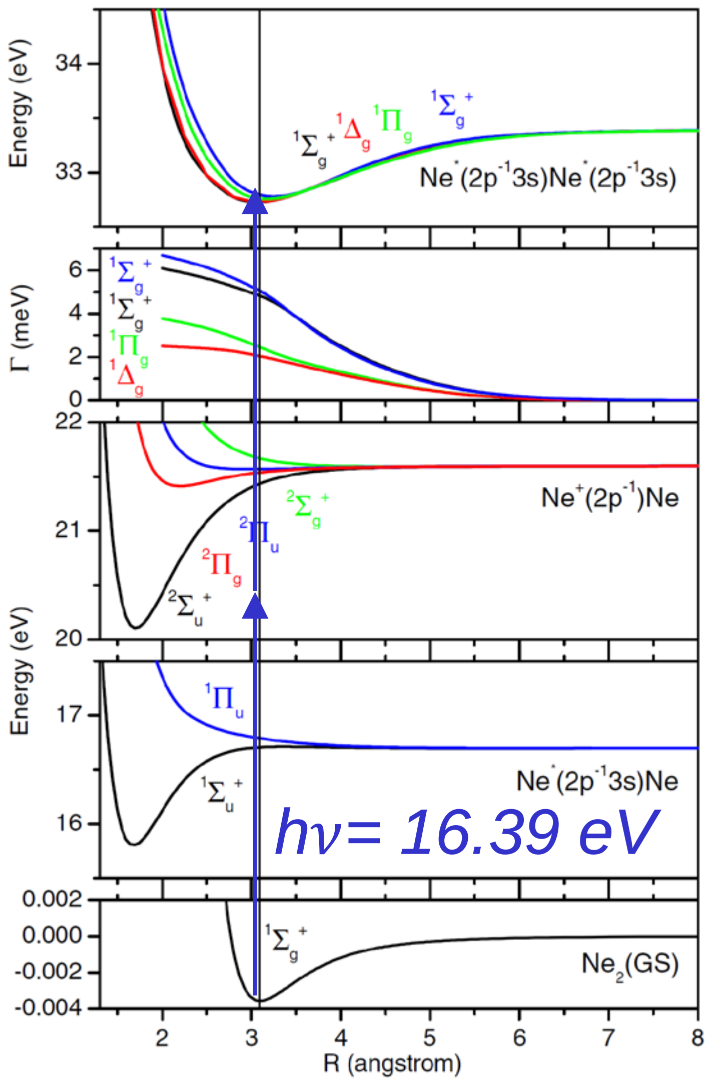

Ph. V. Demekhin et al., J. Phys. B: At. Mol. Opt. Phys. ***46****, 021001 (2013).*

Resonant energy to $[Ne^*(2p^{-1}3s)]_2$: prediction and measurement

To observe the doubly excited states, we have measured Ne_2^+ yield as a function of FEL photon energy.

Theoretical curve

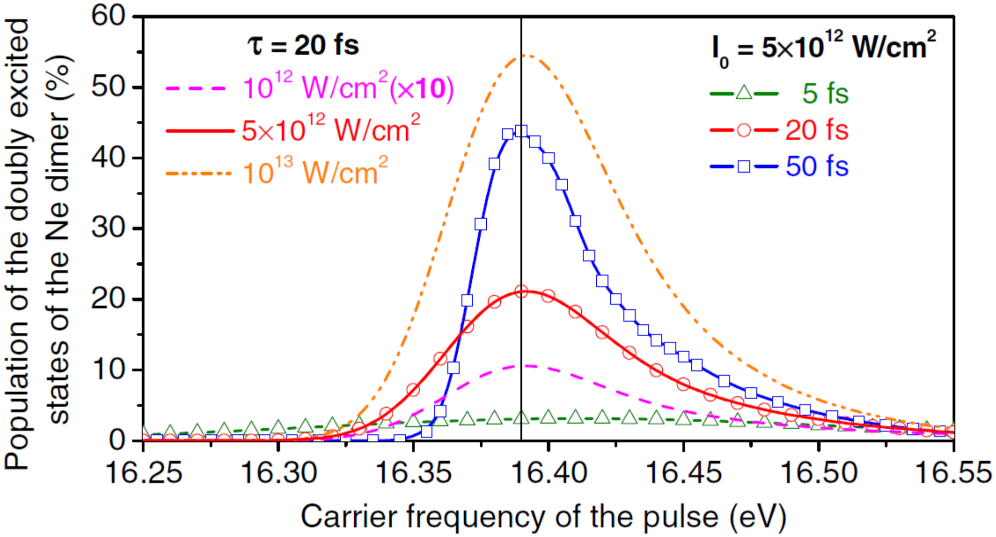

Ne_2^+ yield – photon energy plot

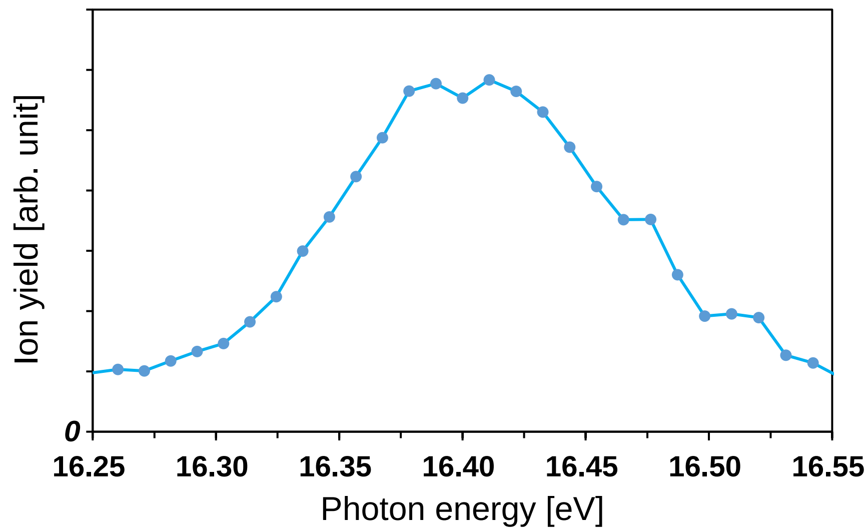

Two-photon absorption of Ne_2 leads to $[Ne^*(2p^{-1}3s)]_2$ that is subject to ICD.

Resonant energy: $h\nu$ =16.39 eV

Cf. Atomic resonant energy: 16.85 eV for $Ne \rightarrow Ne^*(2p^{-1}3s)$

Doubly excited state $[Ne^*(2p^{-1}3s)]_2$ was observed!

Resonant FEL energy was 16.4 eV

in agreement with the theoretical one!

Pump-probe scheme of the ICD process

➢ The target process

∗ Quenching the initial state of the ICD process

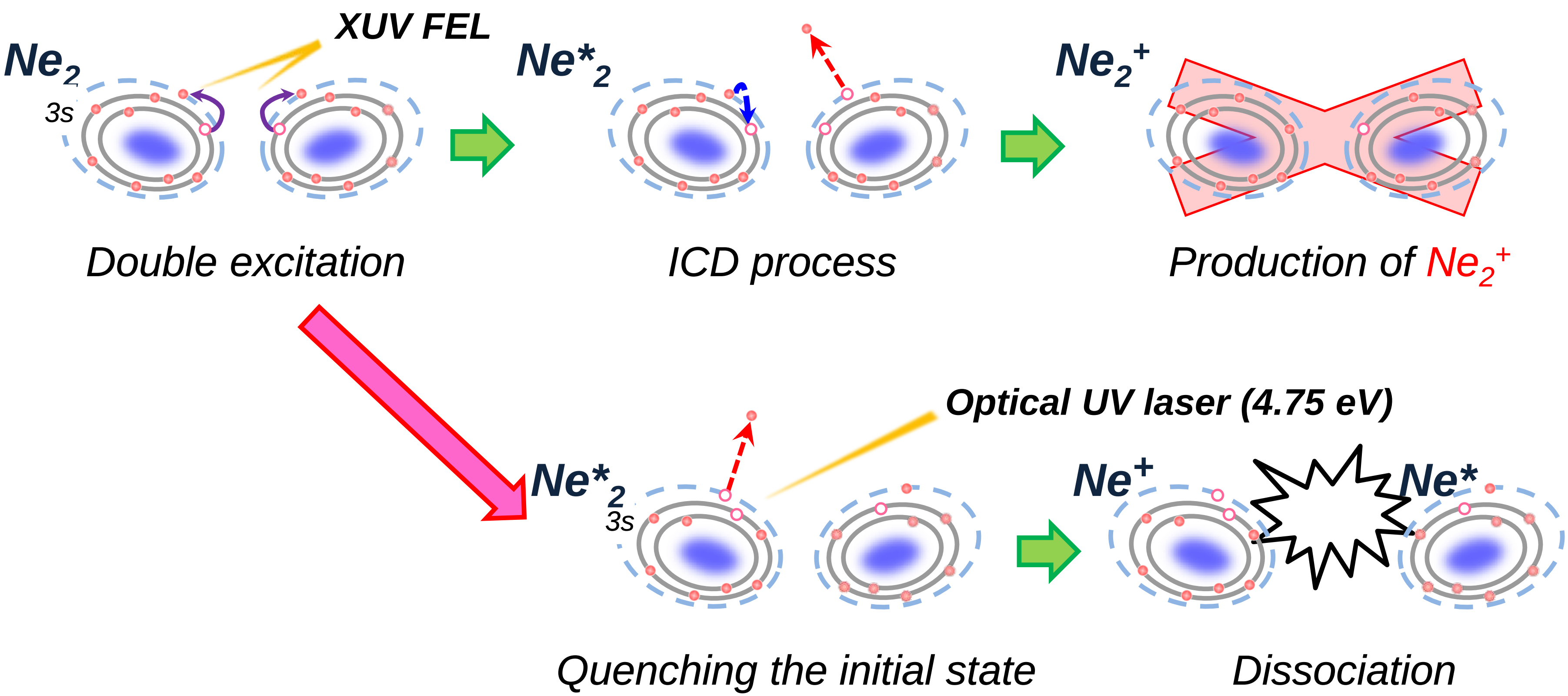

<u>→Measuring the time constant of ICD process by scanning UV delay time</u>

Time-resolved measurements of the ICD process

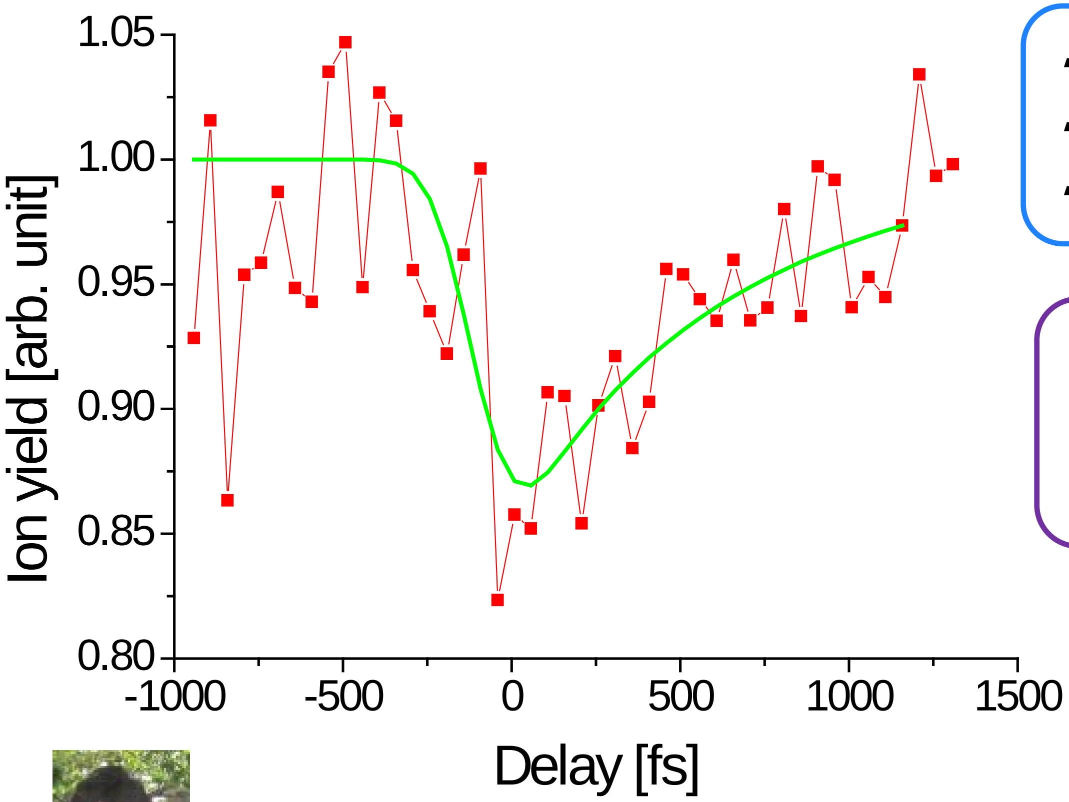

XUV-FEL pulse

- Photon energy: 16.40 eV
- Pulse duration (FWHM): ~70 fs
- Power density: ~1.2 $\times 10^{13}$ W/cm^2

UV laser pulse

- Photon energy: 4.75 eV
- Pulse duration (FWHM): ~230 fs
- Power density: ~0.8 $\times 10^{13}$ W/cm^2

ICD rates

- τ_1=~100 fs
- **τ_2=~340 fs (cf. 308 fs in theory)**

T. Takanashi, *H. Fukuzawa, K. Motomura, Y. Kumagai, S. Mondal, T. Tachibana, T. Nishiyama, K. Matsunami, K. Nagaya, P. Johnsson, P. Piseri, G. Sansone, A. Dubrouil, M. Reduzzi, P. Carpeggiani, C. Vozzi, M. Devetta, M. Negro, D. Faccialà, F. Calegari, A. Trabattoni, M. Castrovilli, Y. Ovcharenko, M. Mudrich,F. Stienkemeier, M. Coreno, M. Alagia, B. Schütte, N. Berrah, C. Callegari, O. Plekan, P. Finetti, K. C. Prince, L. Giannessi, C. Spezzani, E. Ferrari, E. Allaria, G. Penco, C. Serpico, G. De Ninno, B. Diviacco, S. Di Mitri, A. Kullef, N. Golubev, P. Demekhin, M. Yao, and K. Ueda (in preparation)*

Phase-controlled harmonics!

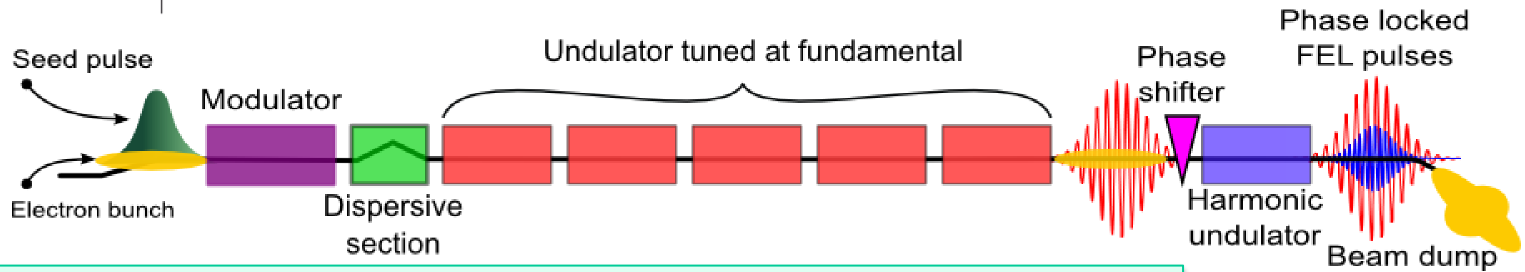

Tuning the last undulator at one harmonic gives the possibility to control the phase between two pulses with different wavelength.

schematic

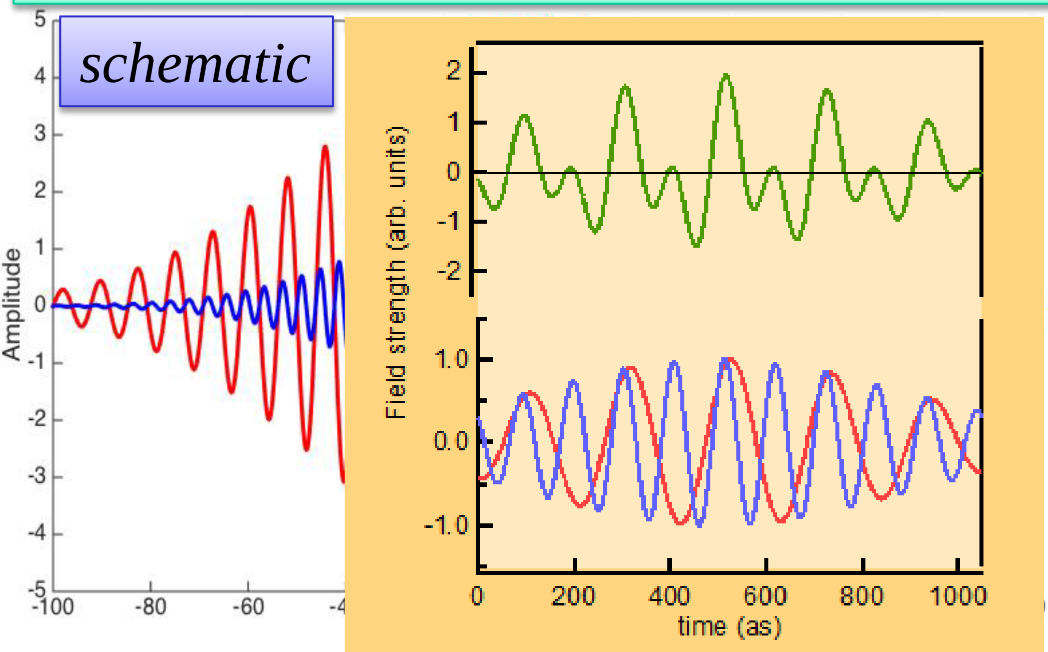

GINGER simulations

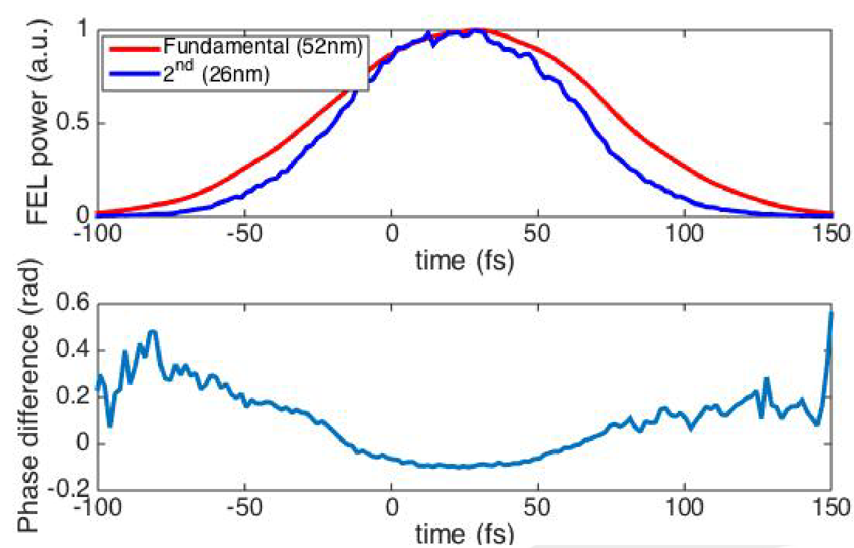

figures and data courtesy of Enrico Allaria

Atomic photoionization with phase control

$1^{st}+3^{rd}$ harmonic:
*Chen, Yin, Elliot, PRL **64,** 507 (1990)*

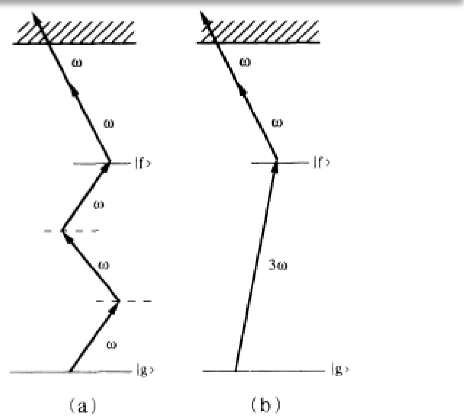

FIG. 1. The two processes which interfere in this observation. The transition $|g\rangle \rightarrow |f\rangle$ is three- and one-phonon allowed, as shown in (a) and (b).

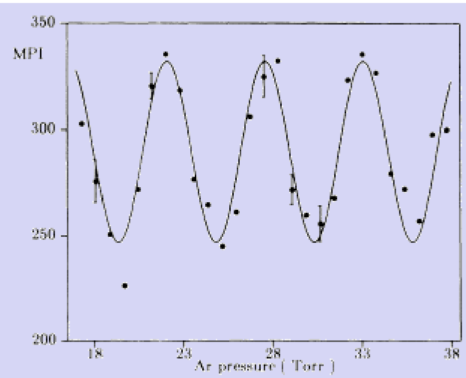

FIG. 3. Ionization signal measured as a function of argon pressure in chamber 2. Solid line indicates a best fit to the data. Error bars showing 1 standard deviation of the mean are shown for a few data points.

$1^{st}+2^{nd}$ harmonic:
*Yin et al., PRL **69,** 2352 (1992)*

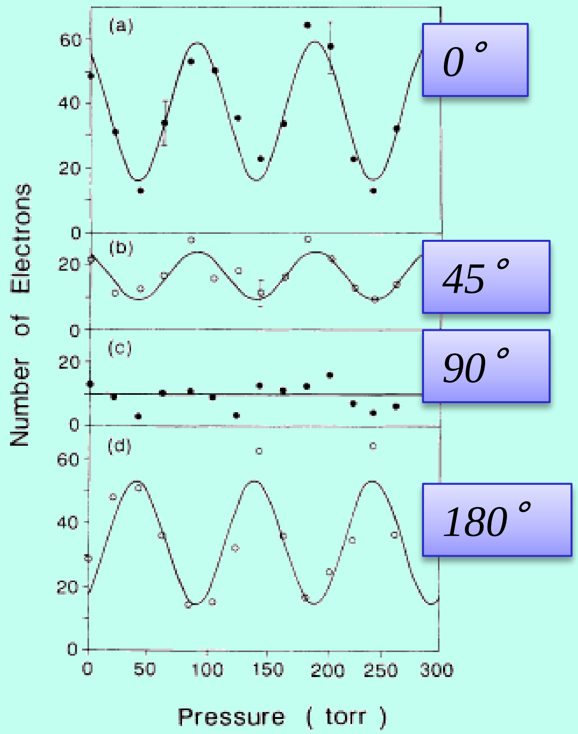

FIG. 3. Experimental data. The total electron count as a function of pressure of N_2 gas in the phase delay cell for the four detectors positioned at (a) 0°, (b) 45°, (c) 90°, and (d) 180°. The solid line is the result of a least-squares fit of a sinusoidally varying curve to the data.

Our scheme
Ne 2p->4s for 1^{st} harmonic

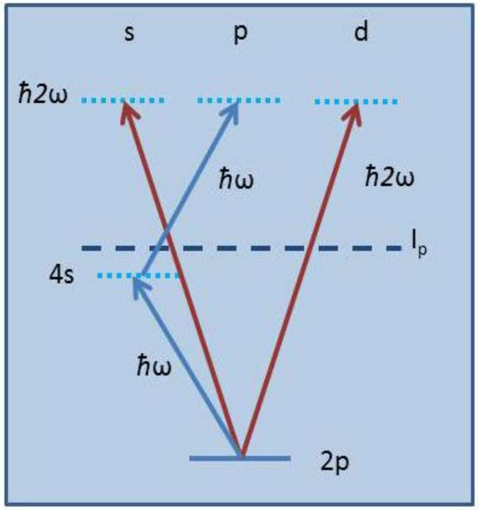

$$|M_1 + M_2(\phi)|^2 = |M_1|^2 + |M_2(\phi)|^2 + 2\,Re(M_1 M_2(\phi))$$

Two color coherent control at FERMI

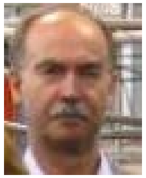

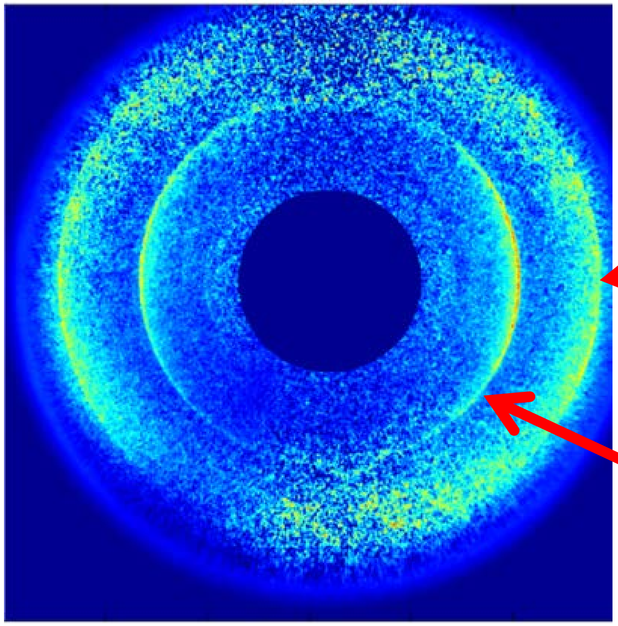

First harmonic plus second harmonic

VMI image at 62.974 nm (Ne $2p^5 4s$ resonance).

Outer ring: a sharp line due to third harmonic radiation, plus a broad distribution due to fluorescence (the fluorescence excites photoelectrons which then impinge on the detector).

Inner sharp ring: electrons ionized by two photons.

The center part of the image has been blanked

***K. C. Prince**, E. Allaria, C. Callegari, R. Cucini, G. De Ninno, S. Di Mitri, B. Diviacco, E. Ferrari, P. Finetti, D. Gauthier, L. Giannessi, N. Mahne, G. Penco, O. Plekan, L. Raimondi, P. Rebernik, E. Roussel, C. Svetina, M. Trovò, M. Zangrando, G. Sansone, M. Reduzzi, P. Carpeggiani, A. Grum-Grzhimailo, E.V. Gryzlova, S.I. Strakhova, K. Bartschat, D. Iablonskyi, Y. Kumagai, T. Takanashi, K. Ueda, A. Fischer, F. Stienkemeier, E. Ovcharenko, T. Mazza, M. Meyer (submitted)*

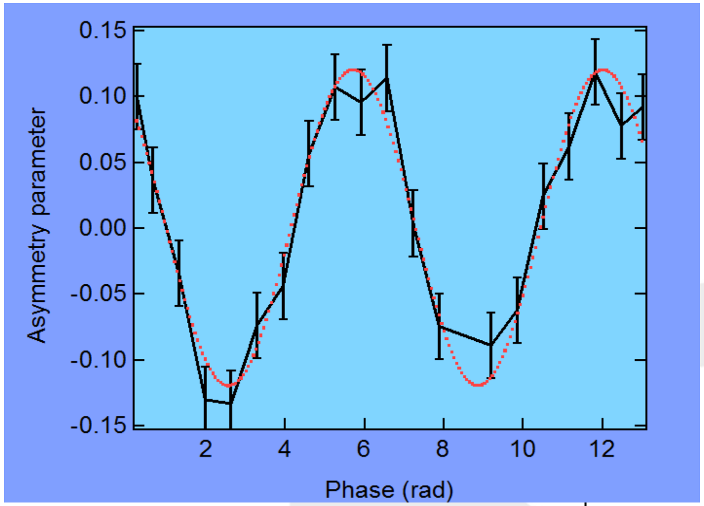

Coherent control at FERMI

Asymmetry emerges from non-linear process
*N. B. Baranova and B. Ya Zel'dovich, Sov. Phys. JETP **71**, 1043 (1990)*

FERMI can (potentially) generate up to 4 consecutive phase-locked harmonics

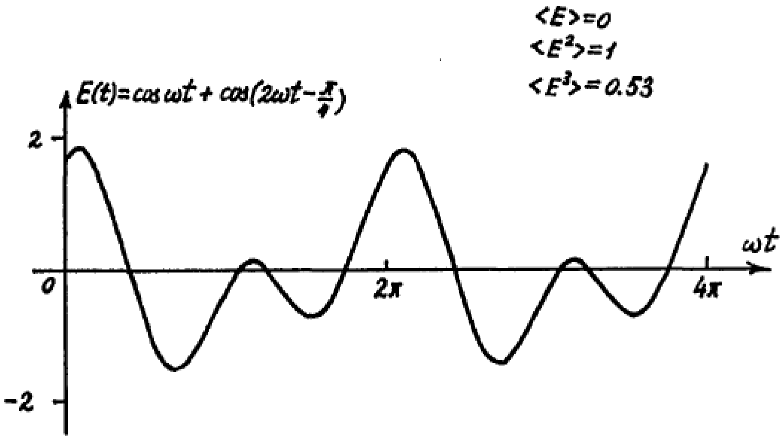

Fig. 1. Time dependence of the electrical field [Eq. (1)] at $E_1 = E_2 = 1$, $\Delta\varphi = \varphi_2 - 2\varphi_1 = 45°$. The time-averaged field is equal to zero, $\langle E \rangle = 0$, but the asymmetry in the upper direction is evident and is characterized by $\langle E^3 \rangle = 0.53 > 0$.

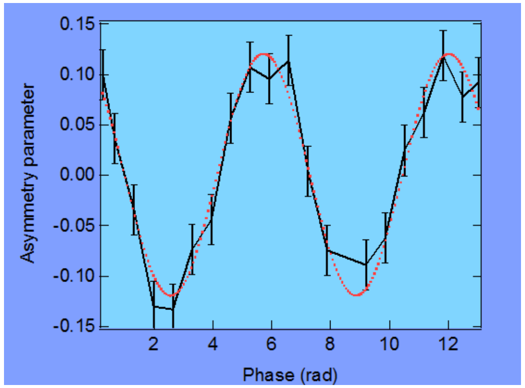

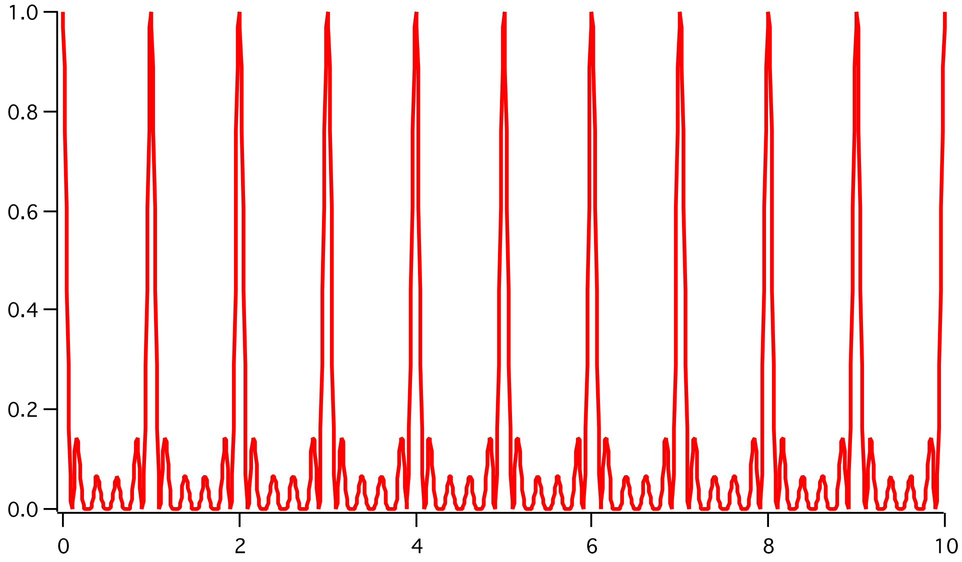

e.g. interval ~ 200 as at 63 nm (20 eV)

Summary

- ICD cascades and inelastic scattering of ICD electrons in neon clusters measured at SCSS and FERMI
- Time resolved study on two-photon excited ICD in neon clusters at FERMI
- Coherent control of photoionization with phase controlled harmonics at FERMI

Outlook

- Full characterization and control of photoionization and photo-dissociation with phase controlled harmonics at FERMI

SACLA XFEL (lased on 7 June 2011)

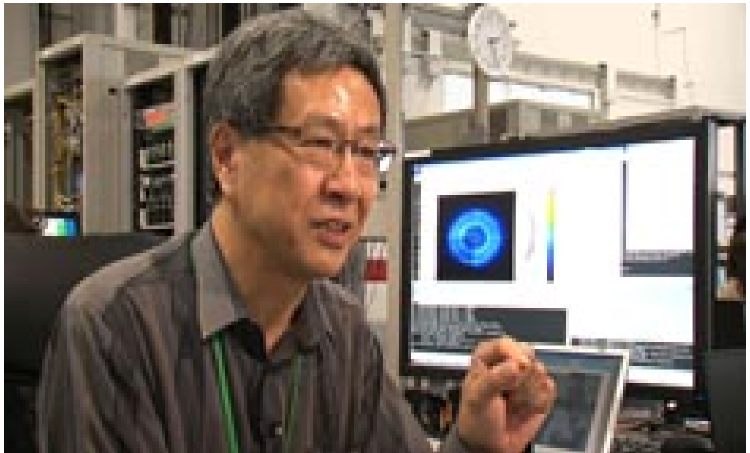

on air!

SACLA XFEL

Photon energy range: 4-20 keV

Photon numbers: ~10^{11} photons/pulse (5-15 keV)

Repetition rate: 10~60 Hz   Pulse width ~10 fs

Focusing optics: ~1 μm (1.5 m) → 50 nm (0.5 m)

Commissioning beam time: Nov. 2011-Feb. 2012

7-11 Nov. 2011: Detector test (no real FEL beam…)

20-24 Feb. 2012: Serial femtosecond crystallography

User beam time started in March 2012

First two beam times in 2012:

Atoms, molecules and atomic clusters

Third beam time in 2013: pump-probe, failed

Fourth beam time in 2014:

Single-short imaging of giant xenon clusters

Fifth and six beam time in 2014:

Pump-probe experiment on clusters

Novel structure determination

- ･phasing
- ･radiation damage

understanding dynamic behavior of heavy atoms!

Dynamic structure and light-induced reaction
―Femtosecond electronic and structure changes

Electron transfer

Structural change

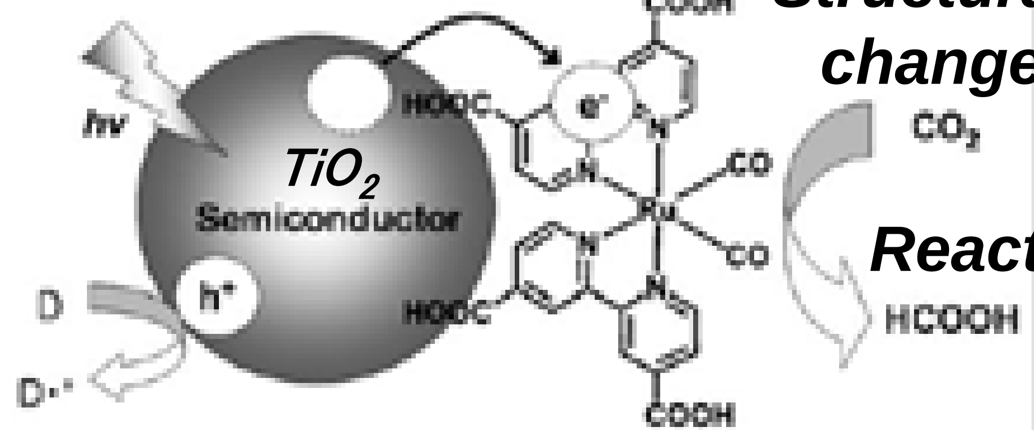

Reaction！

Dynamic behavior of metal atoms in strong XFEL fields

Sato et al. Angew. Chem. **49**, 5101 (2010) （Toyota）

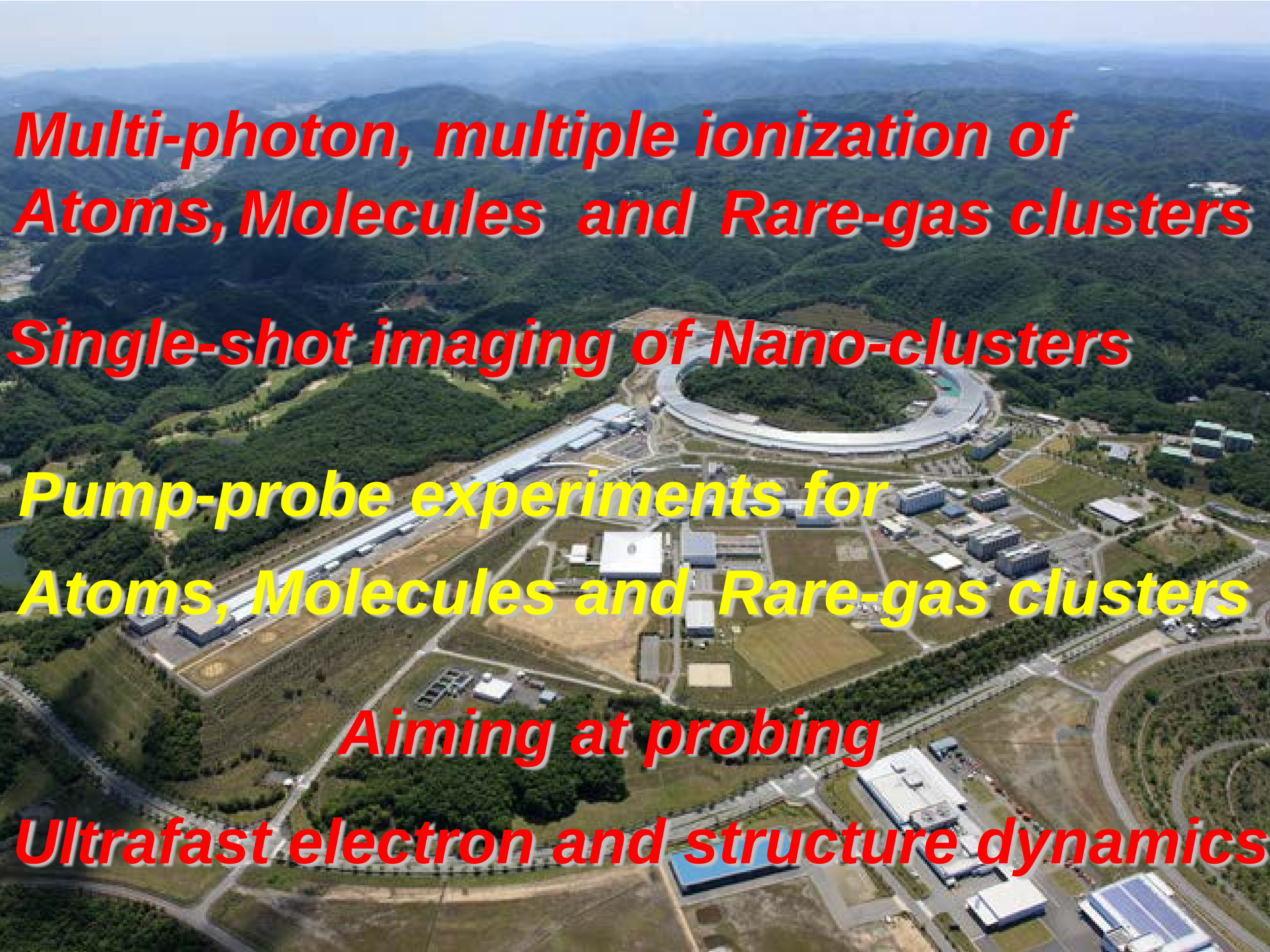

Multi-photon, multiple ionization of Atoms, Molecules and Rare-gas clusters

Single-shot imaging of Nano-clusters

Pump-probe experiments for Atoms, Molecules and Rare-gas clusters

Aiming at probing Ultrafast electron and structure dynamics

Experimental configuration @ SACLA BL3 EH3

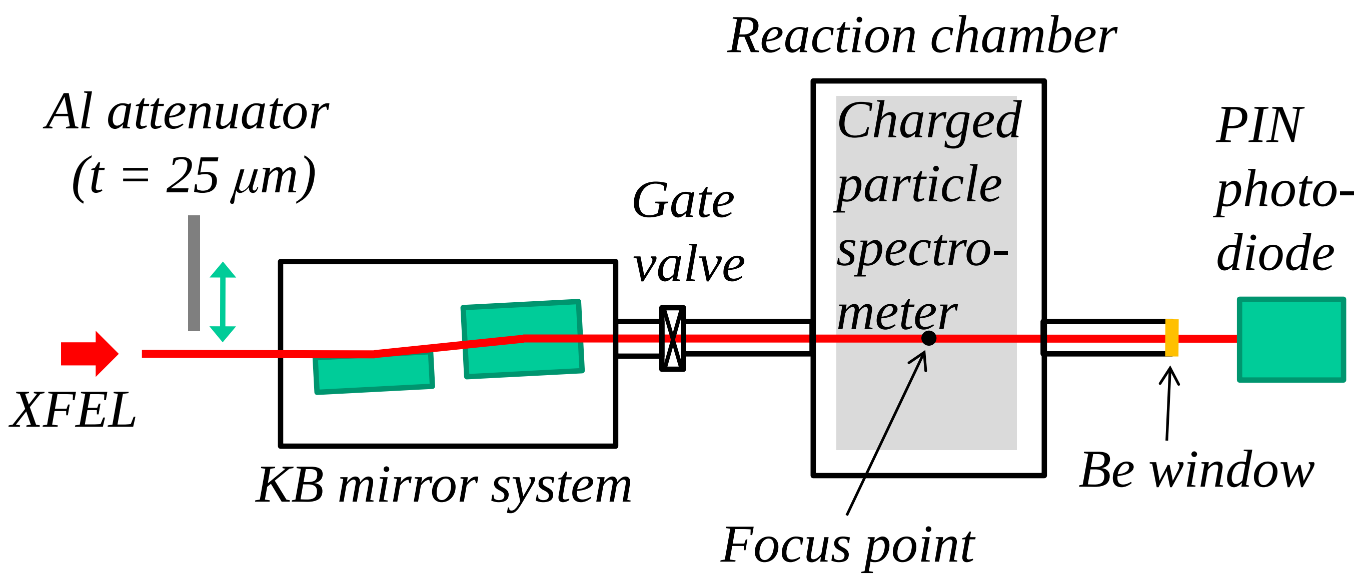

XFEL pulses

Photon energy: 5 and 5.5 keV
(Wavelength: 0.25 and 0.22 nm)
Band width: ~60 eV (FWHM)
Repetition: 10-30 Hz
Pulse energy before KB mirror:
~240 μJ (~3 ×10^{11} photons) @5.5keV
Fluctuation of pulse energy:
±25% (50% FWHM)

@Focus point
Focus size: ~1.5 μm (FWHM)
Peak fluence:
~47 μJ/μm^2 (atoms, clusters),
~26 μJ/μm^2 (molecules)

Sample gas was introduced as a pulsed super sonic gas jet to the focus point.

I. Deep inner-shell multiphoton absorption by intense x-ray free-electron laser pulses

H. Fukuzawa, S.-K. Son, K. Motomura, S. Mondal, K. Nagaya, S. Wada, X.-J. Liu, R. Feifel, T. Tachibana, Y. Ito, M. Kimura, T. Sakai, K. Matsunami, H. Hayashita, J. Kajikawa, P. Johnsson, M. Siano, E. Kukk, B. Rudek, B. Erk, L. Foucar, E. Robert, C. Miron, K. Tono, T. Togashi, Y. Inubushi, T. Sato, T. Katayama,T. Hatsui, T. Kameshima, M. Yabashi, M. Yao, R. Santra, and K. Ueda [PRL **110**, 173005 (2013) & JPB **46**, 164024 (2013)]

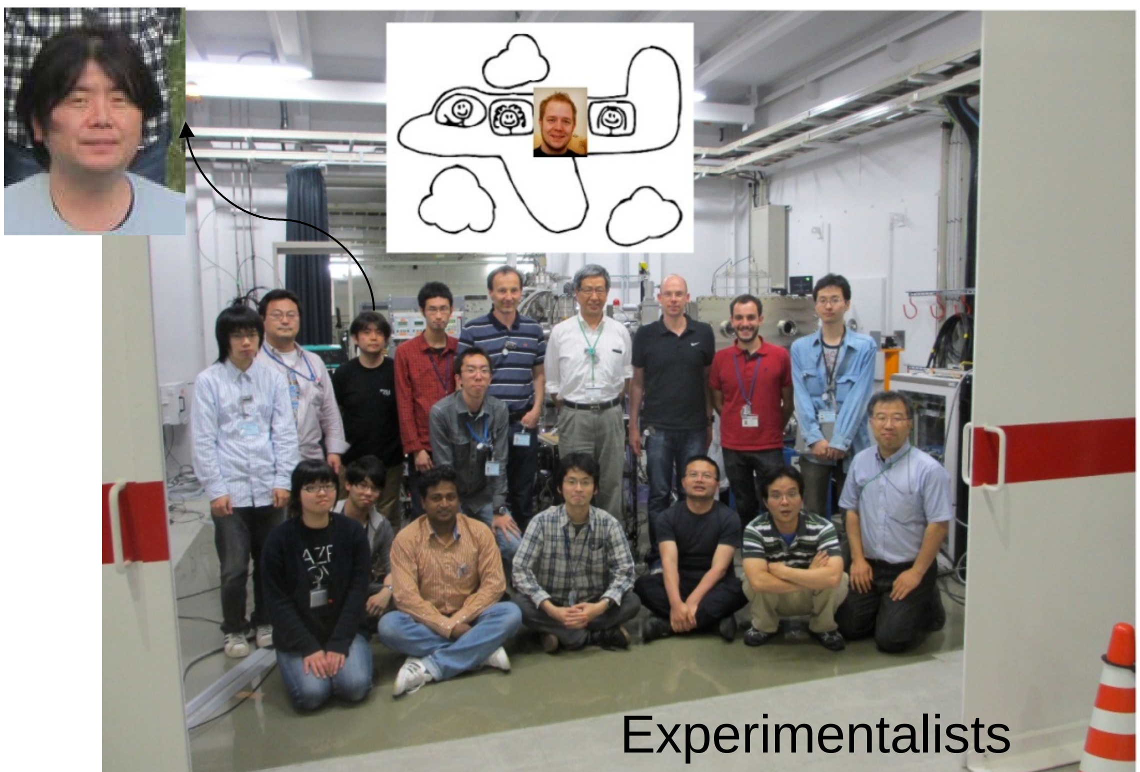

Experimentalists

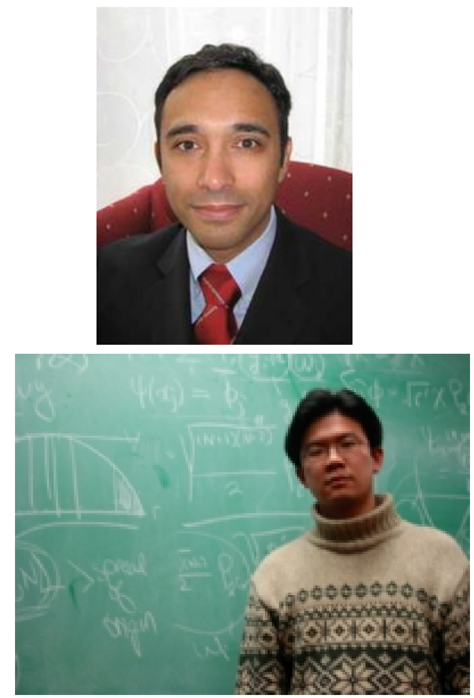

Theorists

Time of Flight spectrum of xenon ions

5.5 keV, 50 μJ/μm² at SACLA

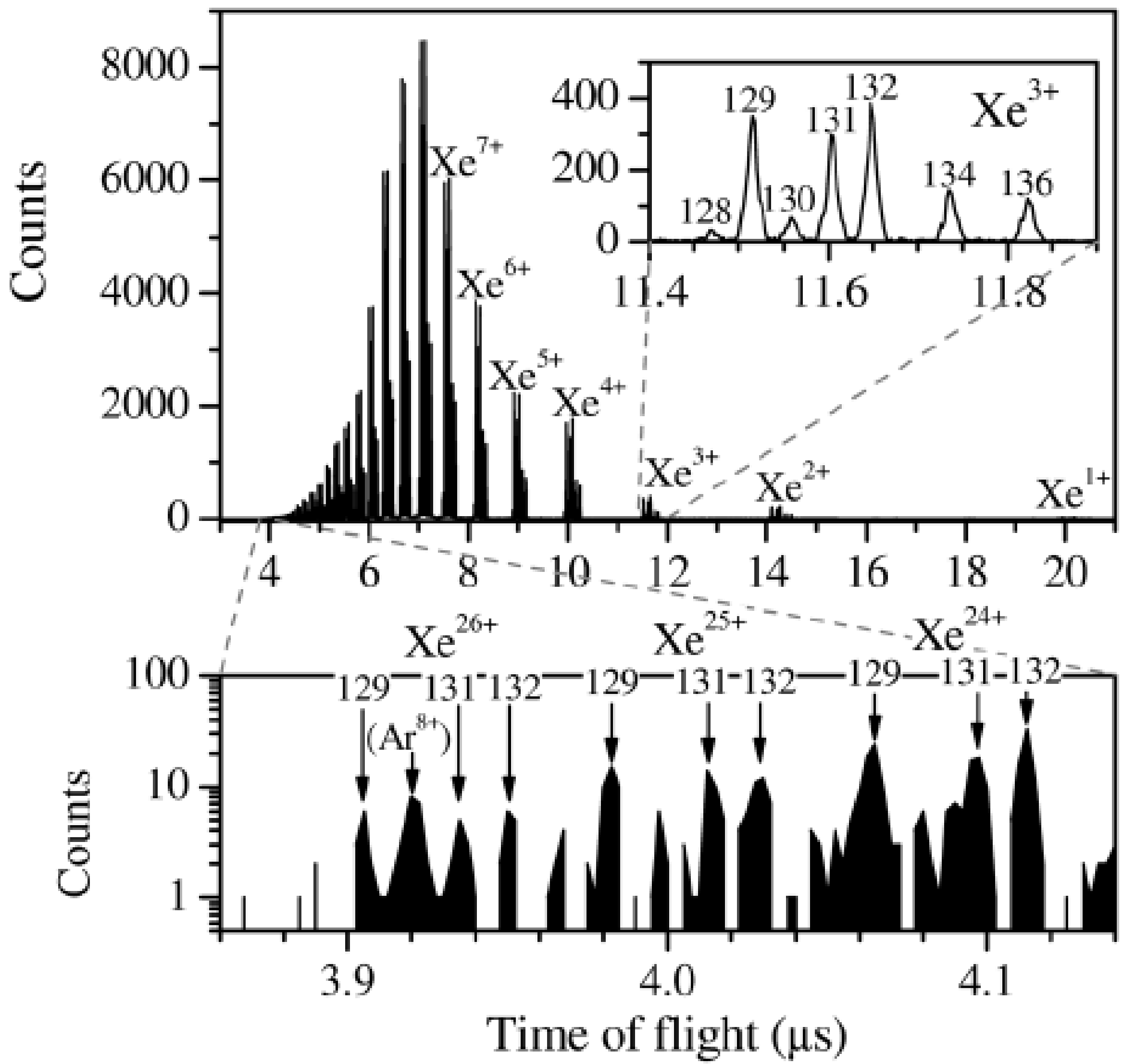

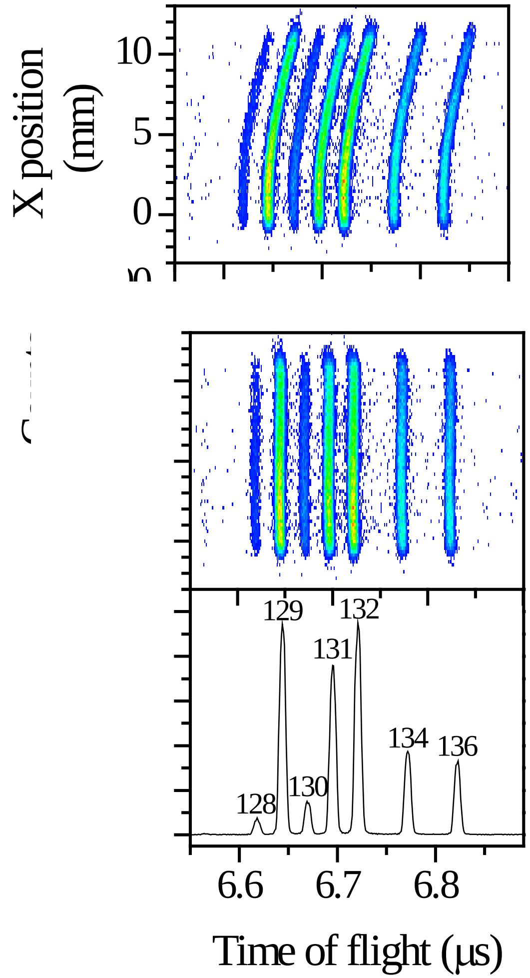

2D position resolved TOF improves the resolution!

High charge states Xe^{n+} with n up to 26 are produced!

XFEL fluence dependence for Xe^{n+} yields

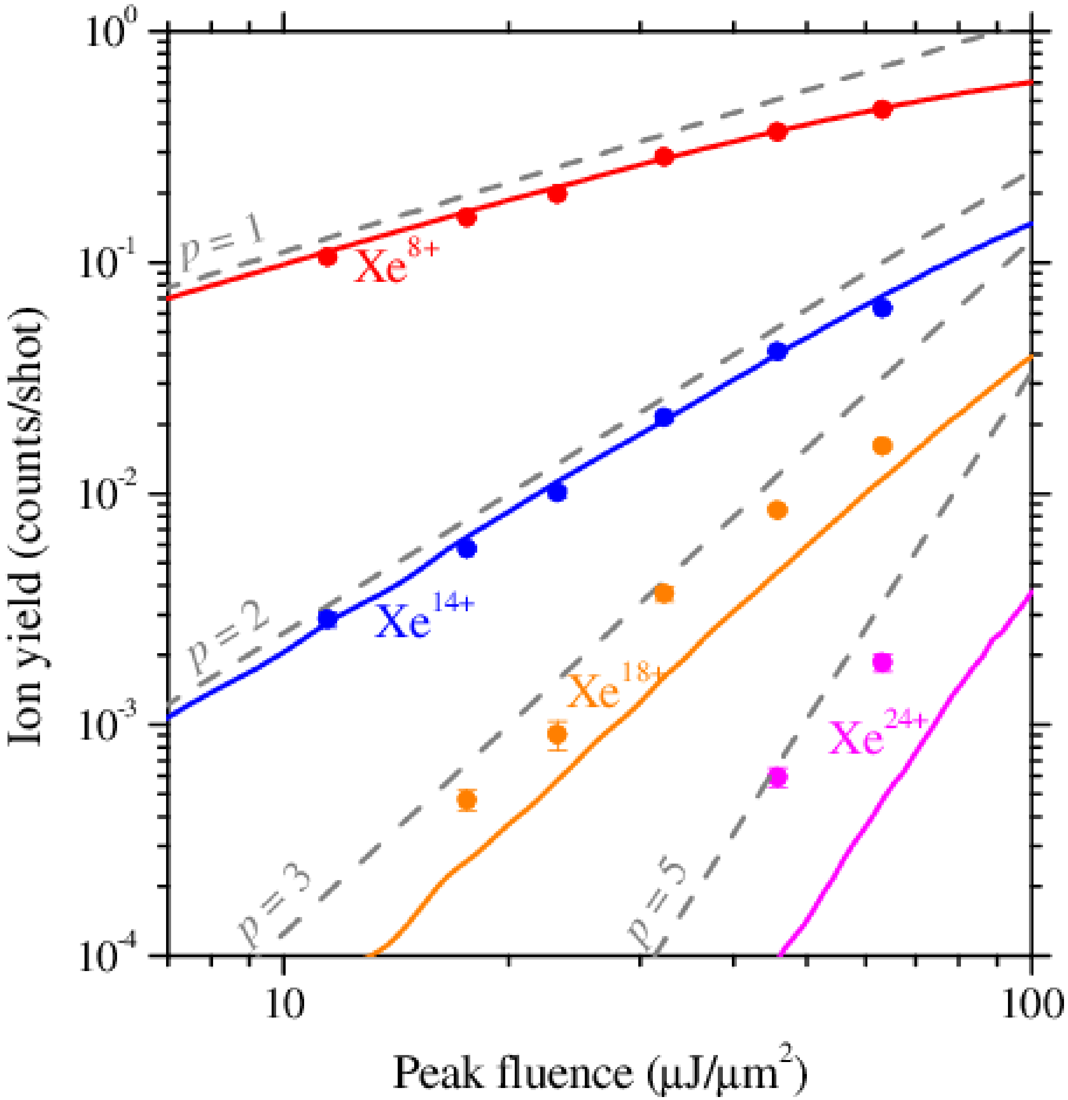

With help of ab initio calculations, we find that the observed high charge states ($n \geq 24$) are produced via five-photon absorption, evidencing the occurrence of multiphoton absorption involving deep inner shells.

Xenon ion charge distributions (exper. vs theory)

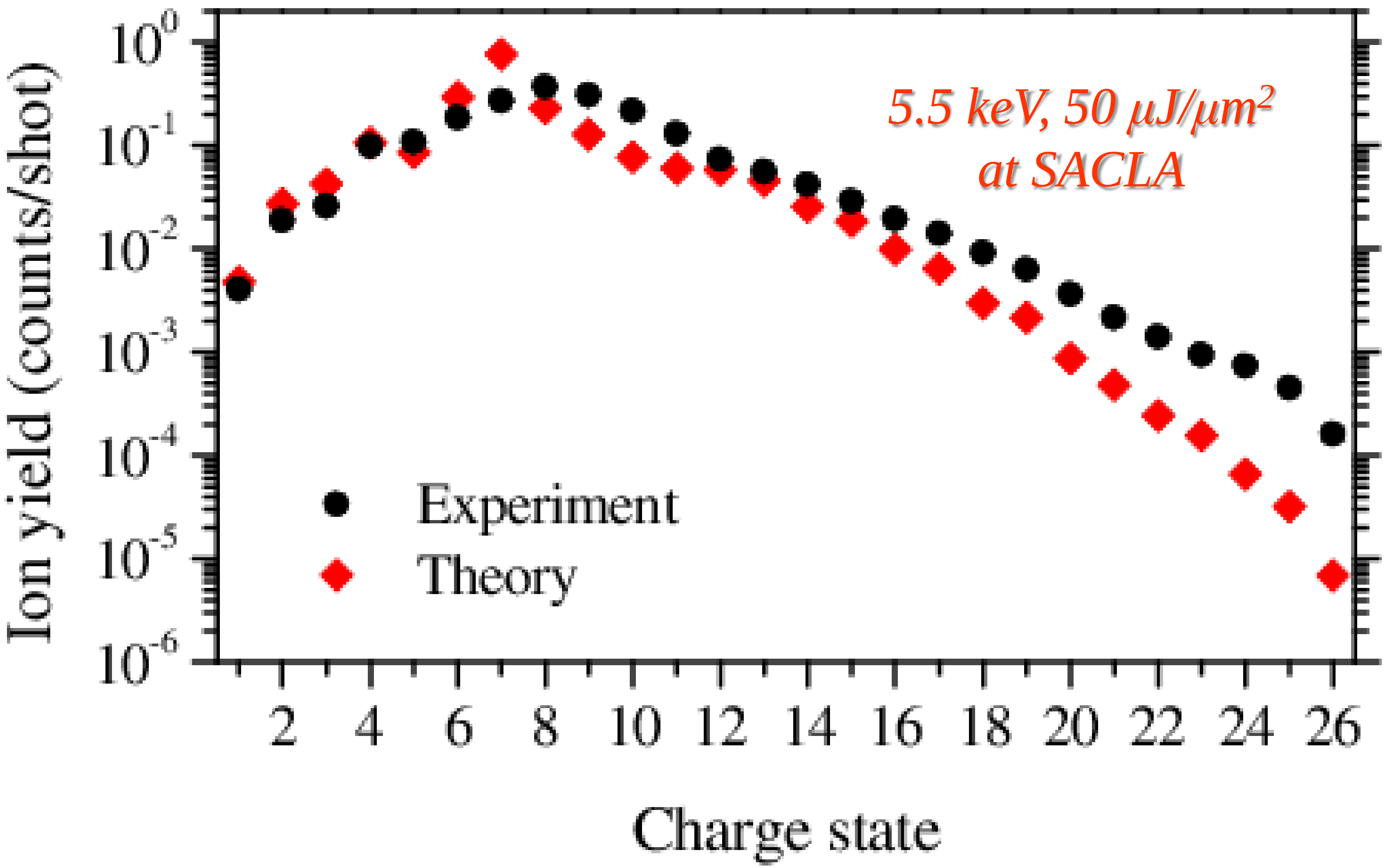

A newly developed theoretical model shows good agreement with the experiment!

An exemplary pathway of multiphoton multiple ionization

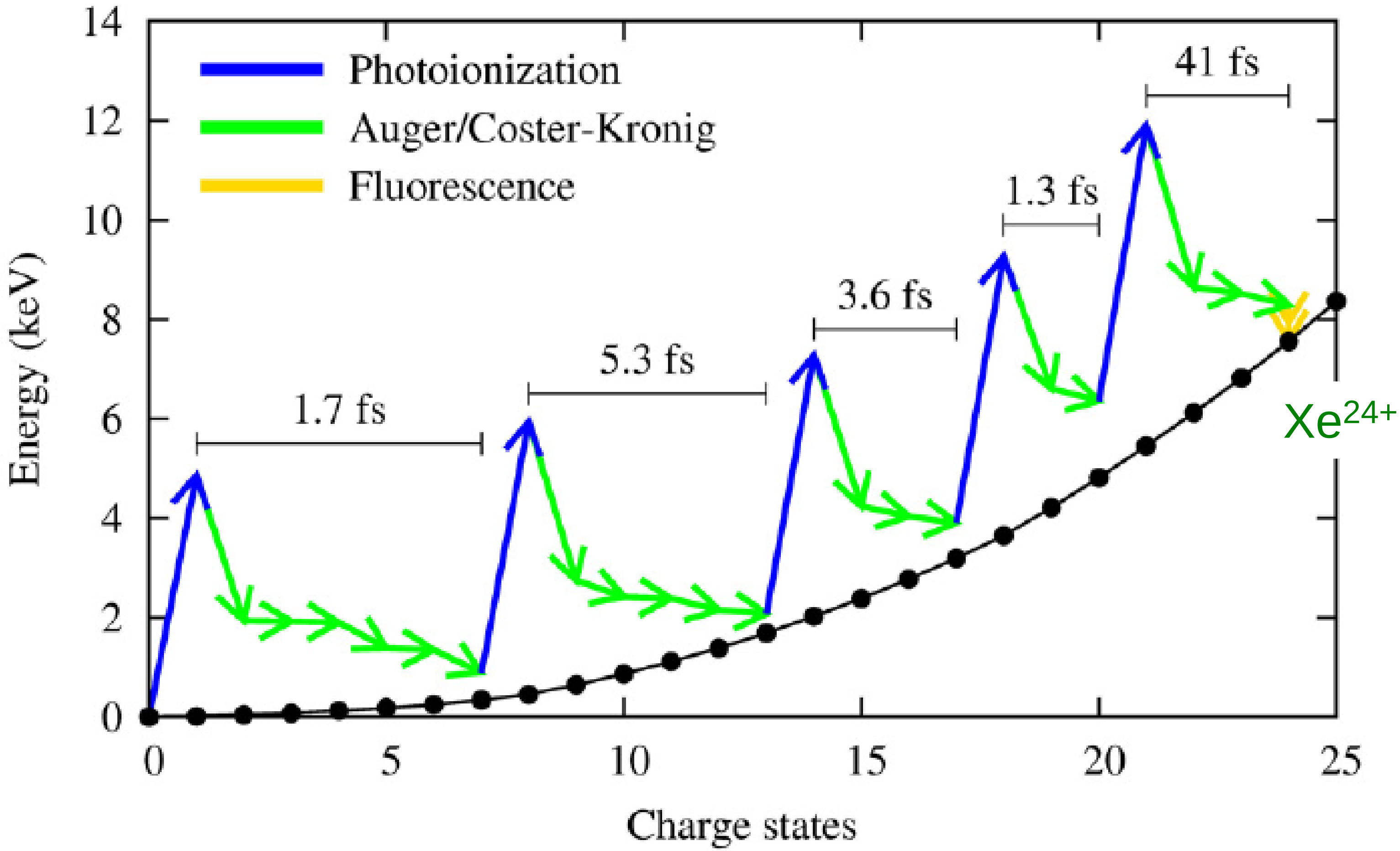

A newly developed theoretical model elucidates the complex pathways of sequential electronic decay cascades accessible in heavy atoms, *revealing that L shell ionization and sequential electronic decay cycles are repeated multiple times within the XFEL pulse duration of ~10 fs.*

*Fukuzawa, Son et al. PRL **110**, 173005 (2013)*

II. Charge transfer and molecular dissociation following deep inner-shell multi-photon multiple ionization of CH_3I and 5-Uracil molecules by intense x-ray free-electron laser pulses from SACLA


K. Motomura, E. Kukk, H. Fukuzawa, K. Nagaya, S. Omura, S. Wada**,** S. Mondal, T. Tachibana, Y. Ito, T. Sakai, K. Matsunami, A. Rudenko, C. Nicolas, X.-J. Liu, C. Miron, Y. Zhang, Y.H. Jiang, J. Chen, A. Milam, D. Kim, K. Tono, T. Hatsui, Y. Inubushi, M. Yabashi, H. Kono, M. Yao and K. Ueda (submitted).

iodomethane

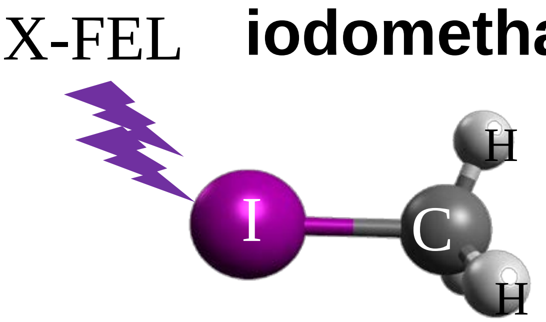

5-iodouracil

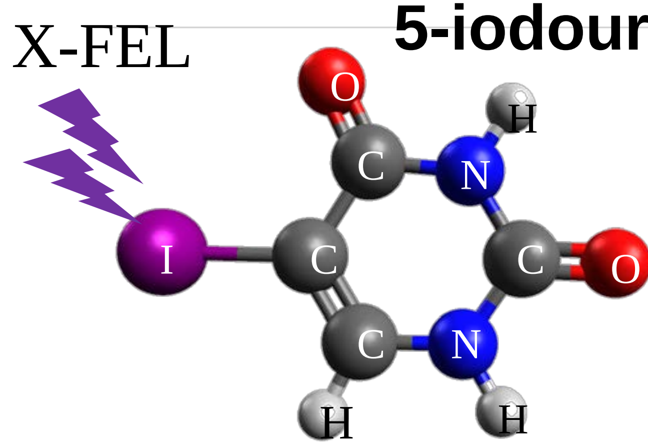

Ionization of iodomethane

We expect that the ionization proceeds with this sequence.

Selective ionization of iodine L-shell

Production of highly charged iodine ion by Auger cascades

Charge transfer from iodine

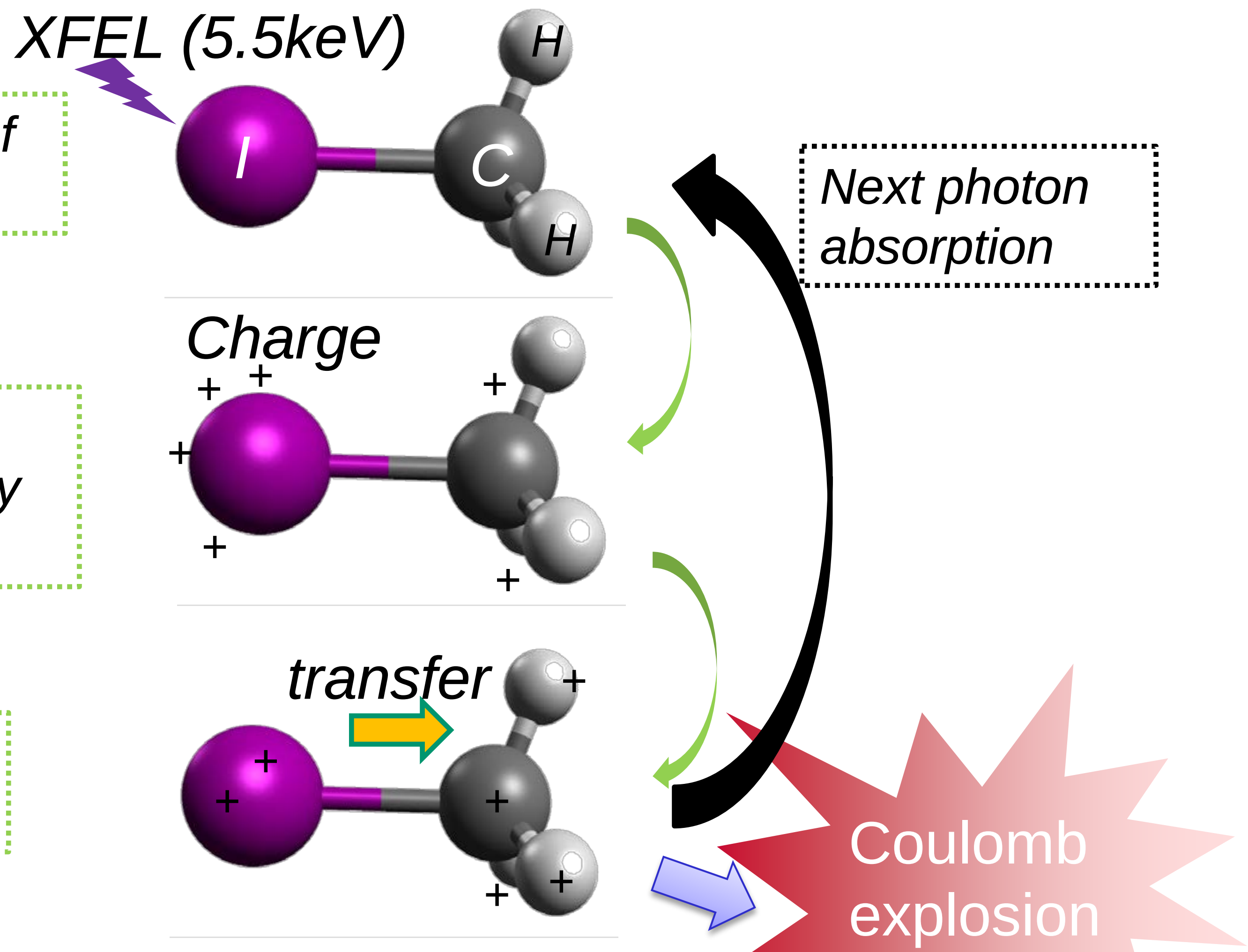

We tried to understand these processes by measuring momentum of ion fragments.

Iodomethane: Charge distribution

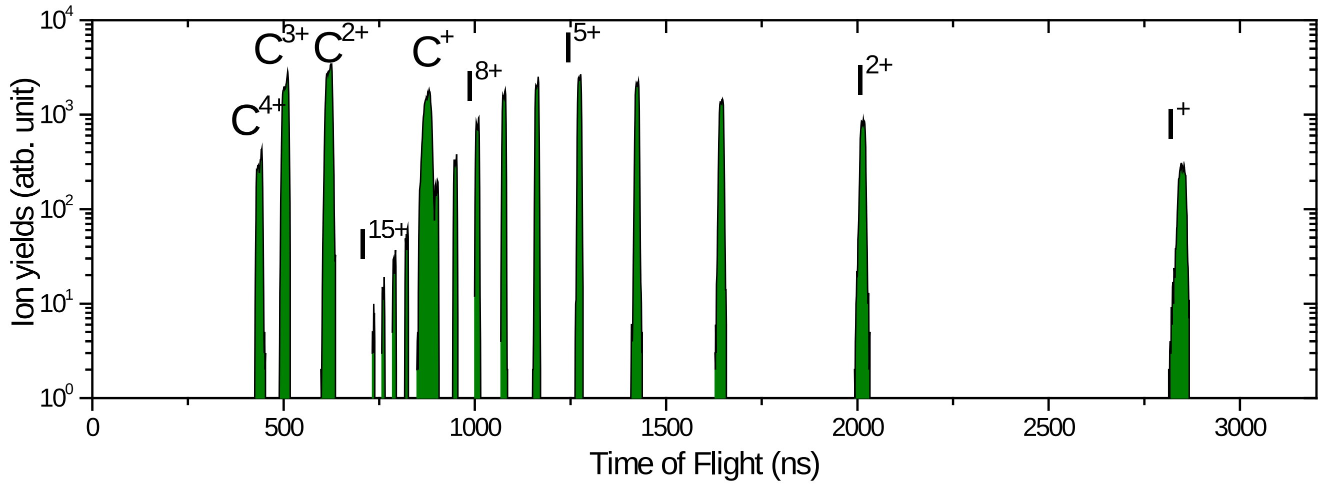

Momentum conservation: $\boldsymbol{P}(\mathrm{H1})+\boldsymbol{P}(\mathrm{H2})+\boldsymbol{P}(\mathrm{H3})+\boldsymbol{P}(\mathrm{C})+\boldsymbol{P}(\mathrm{I}) = \mathbf{0}$

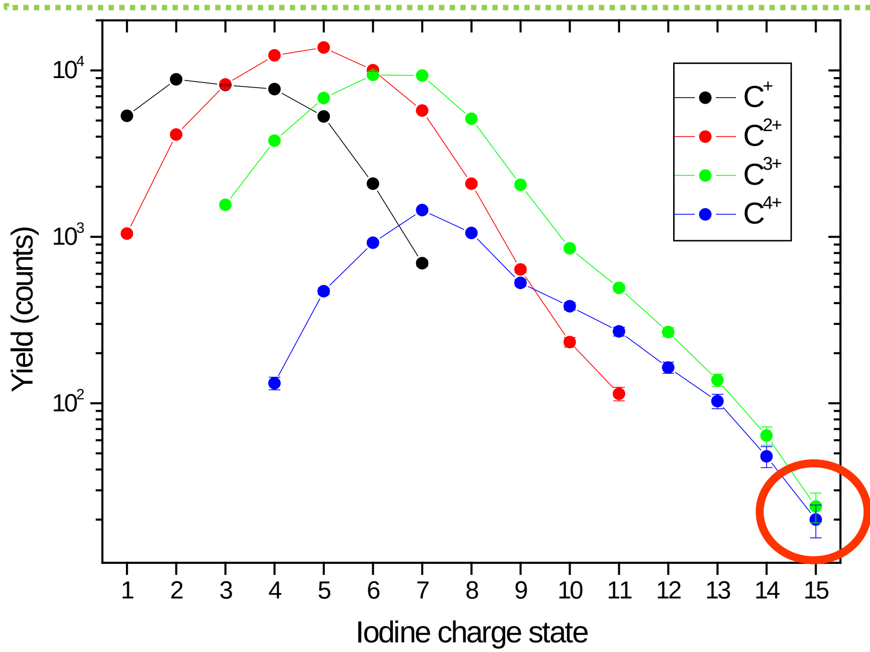

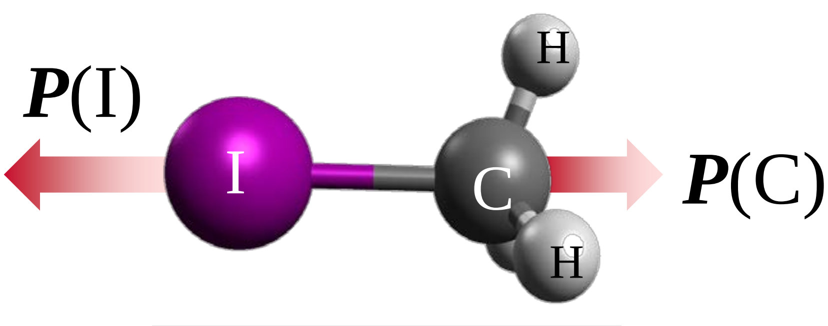

$I^{15+} + C^{4+} + 3H^{+} \rightarrow (CH_3I)^{22+}$

Charge state dependence of ion momentum

Charge state dependence for the momentum of carbon ions

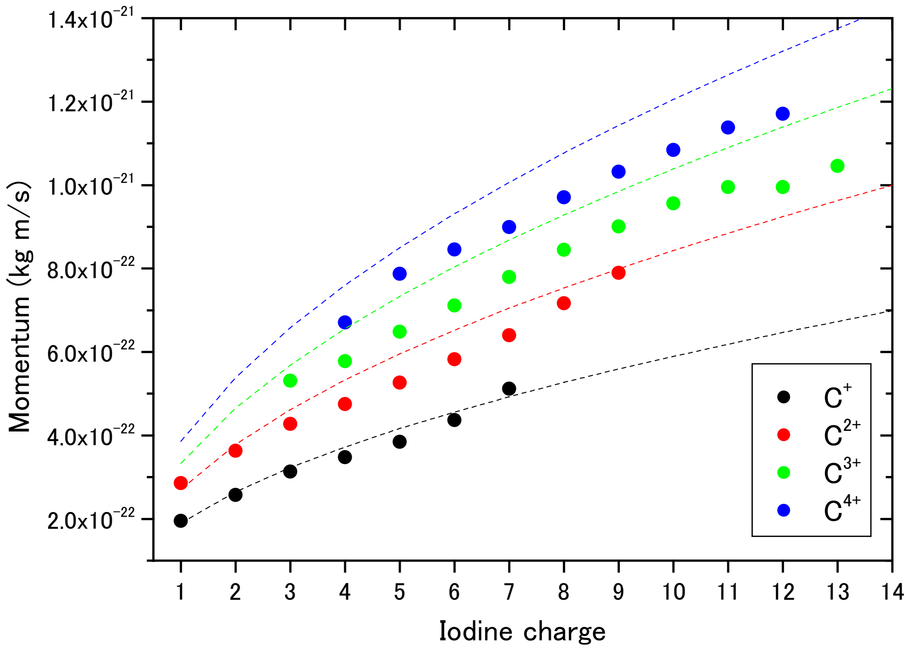

Ratio of the momentum of carbon ions and iodine ions

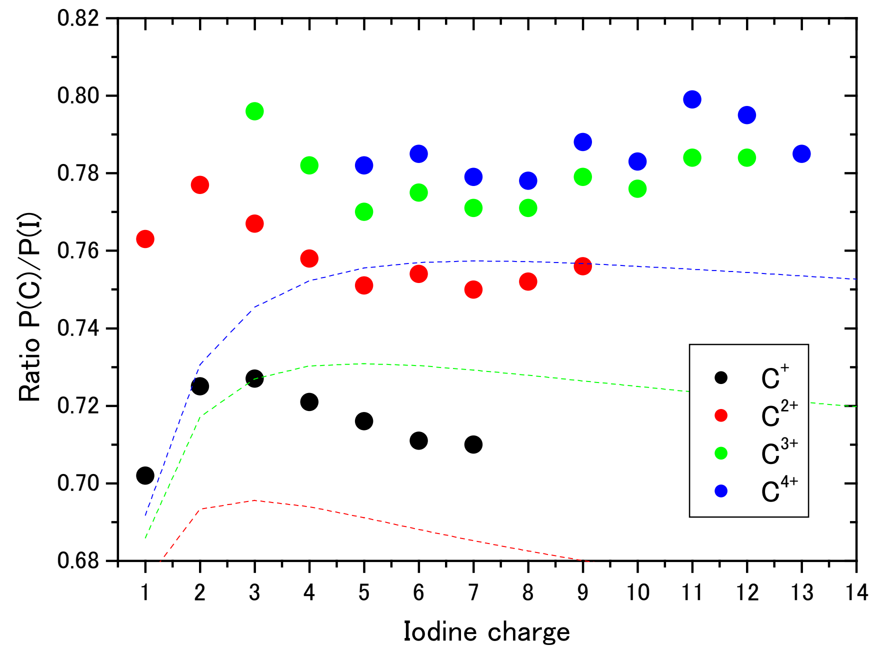

***Dashed line:** Simulation with instant charge build up and transfer within the intact molecule; the charges are arranged before the Coulomb explosion starts.*

The results of the simulation do not agree with the experimental results. Dissociation may compete with the charge buildup and transfer.

Charge build up and transfer model

*We introduced two parameters "**τ**" and "**R**".*

XFEL ionizes iodine L-shell

Charge build up in a molecule.

$$Q_{total}(t) = Q\left(1 - e^{-\frac{t}{\tau}}\right)$$

Charge transfer from iodine

$$\frac{dQ_{CH3}(t)}{dt} = R \times Q_I(t)$$

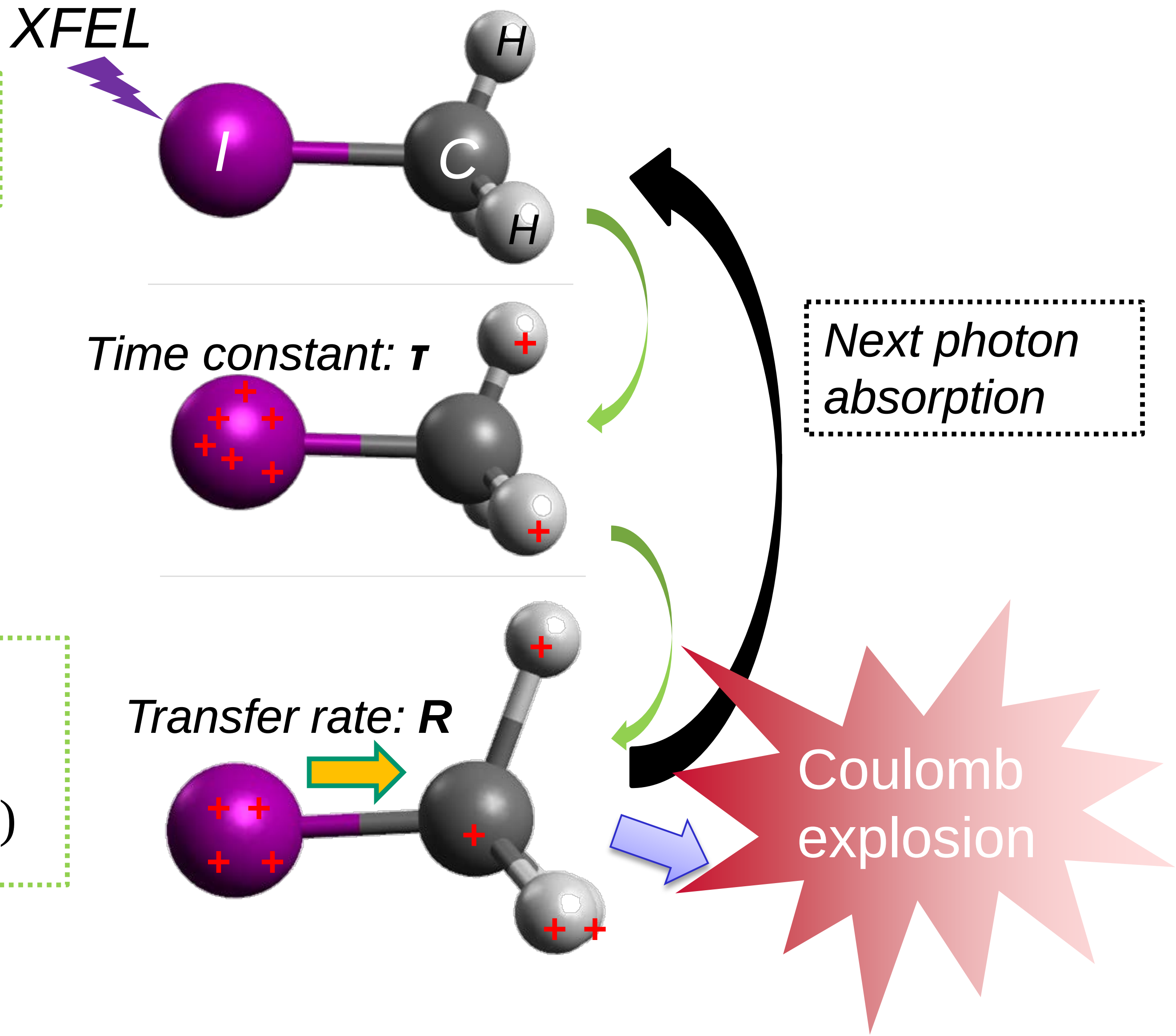

Comparison with charge build up and transfer model

Charge state dependence for the momentum of carbon ions

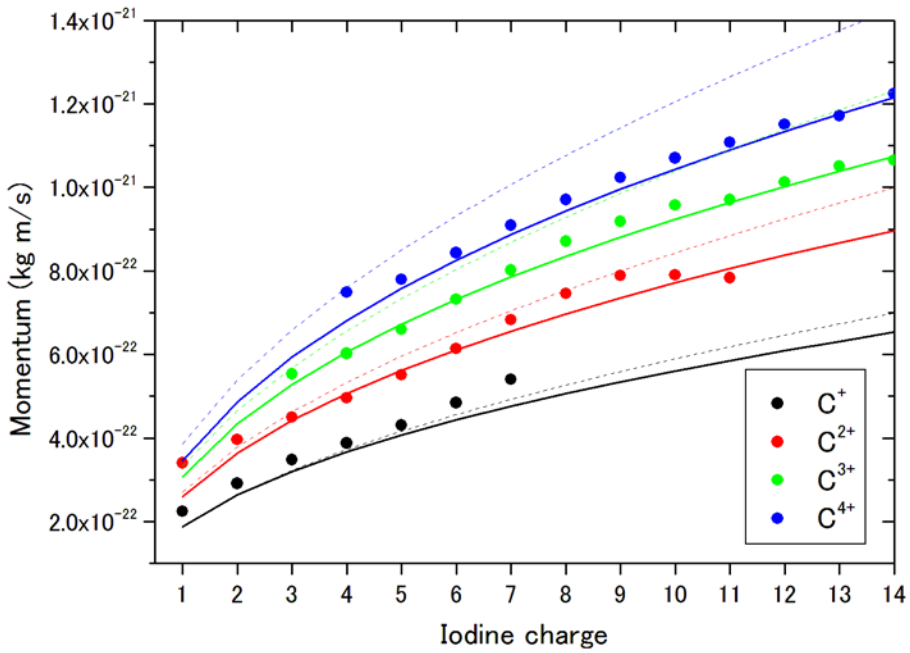

Ratio of the momentum of carbon ions and iodine ions

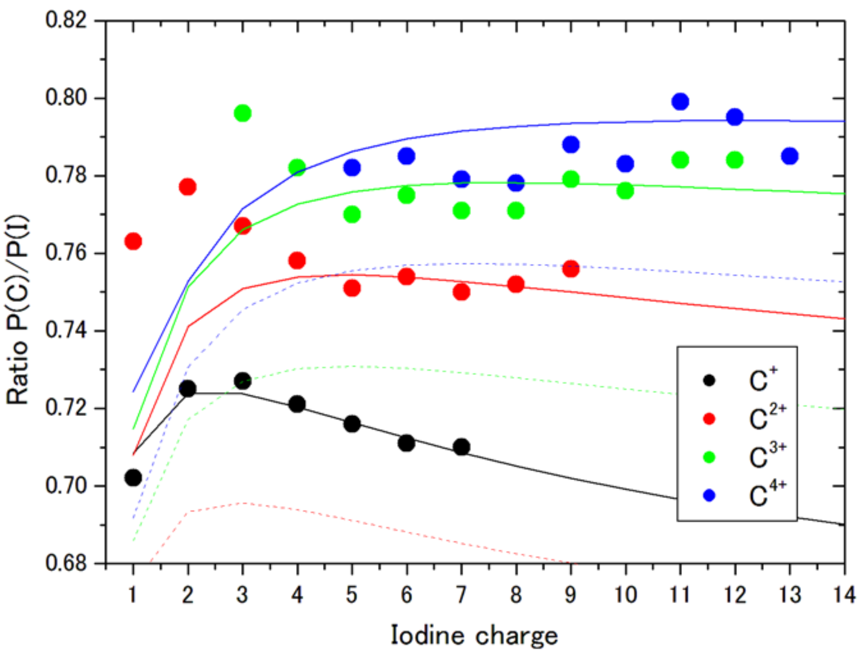

Solid line: *Simulation with charge build up and transfer*
Dashed line: *Simulation with Instant charge buildup and transfer*

Using the parameters ***τ = 9 fs*** *and* ***R = 0.37 fs⁻¹****, the simulations agree with experimental results.*
τ of 9 fs is consistent with the results of atomic xenon results and roughly the same as the XFEL pulse width (~10 fs).

5-iodouracil ($C_4H_3IN_2O_2$)

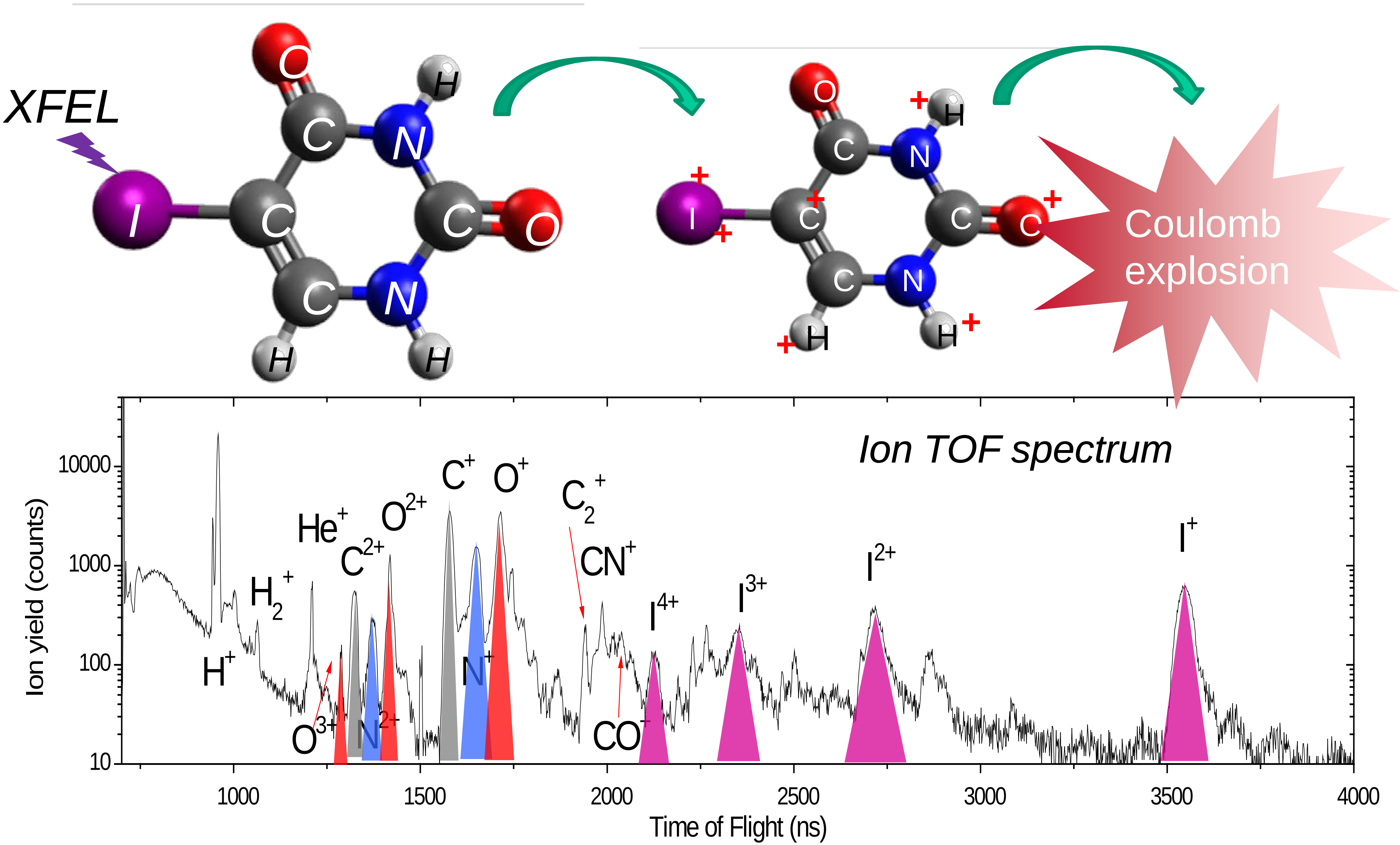

We observed iodine ions with the charge up to +4 and many more ions

Ion trajectory tracing by classical MD

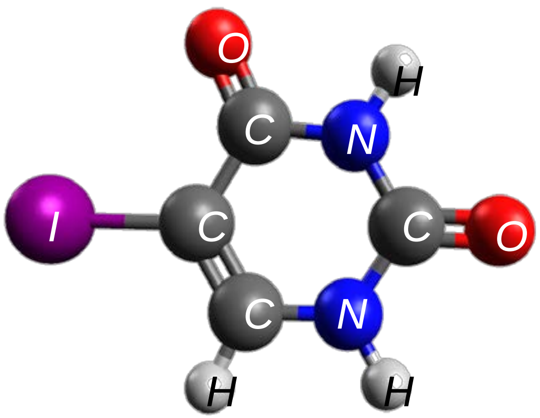

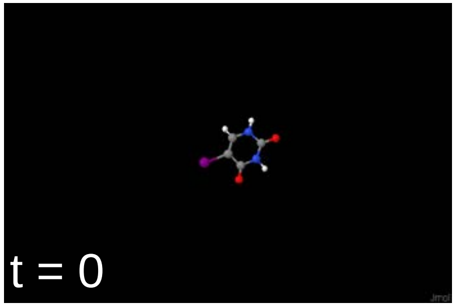

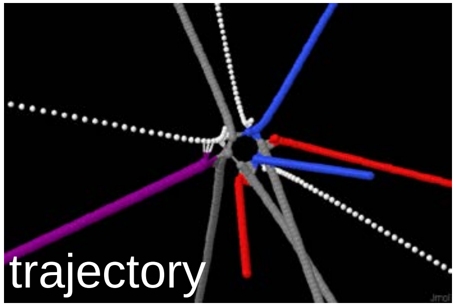

Trajectories of emitted ion are traced by classical MD.

MD conditions

- Coulombic repulsive force between ions is considered.
- Time step is 0.2 fs, total MD time is 10 ps.
- Calculate 1,000 ensembles for each condition.

Charge distribution

- We adopt the charge distribution of CH_3I molecule for ion distribution of parent 5-I-Uracil molecule.
- One charge is fixed to iodine (absorber). Rest of charges are randomly distributed within constituent at t=0 of MD.
- Charges in ion are increased according to **(1 - exp(- t/τ))** with a charge build-up time constant τ .

Initial structure of MD calculations

- Initial molecular structures of MD are prepared by B3LYP/3-21Gd level calculations by GAMESS package
- Thermally randomized structure and velocity distribution is estimated by GAMESS using Nose/Hoover method.

MD with T = 300 K and t = 10 fs reproduces experimental results well.

Influence of charge-build up time for KED in MD

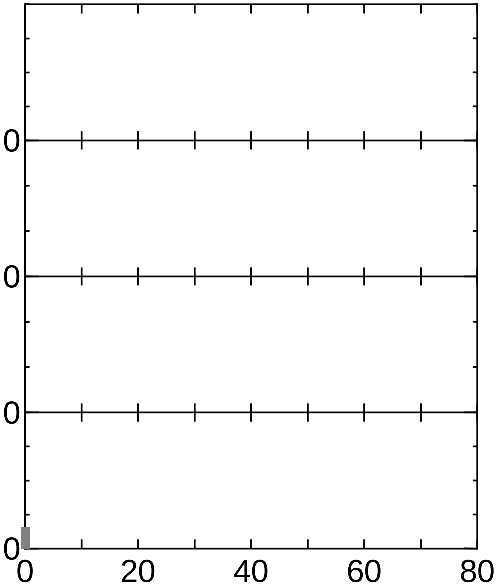

Solid bars: experiment

MD @ 300K
Dotted lines: τ = 0fs
Solid lines: τ = 10fs

2-body angular correlation

Black: I^+, Red: I^{2+}, Blue: I^{3+}, Green: I^{4+}

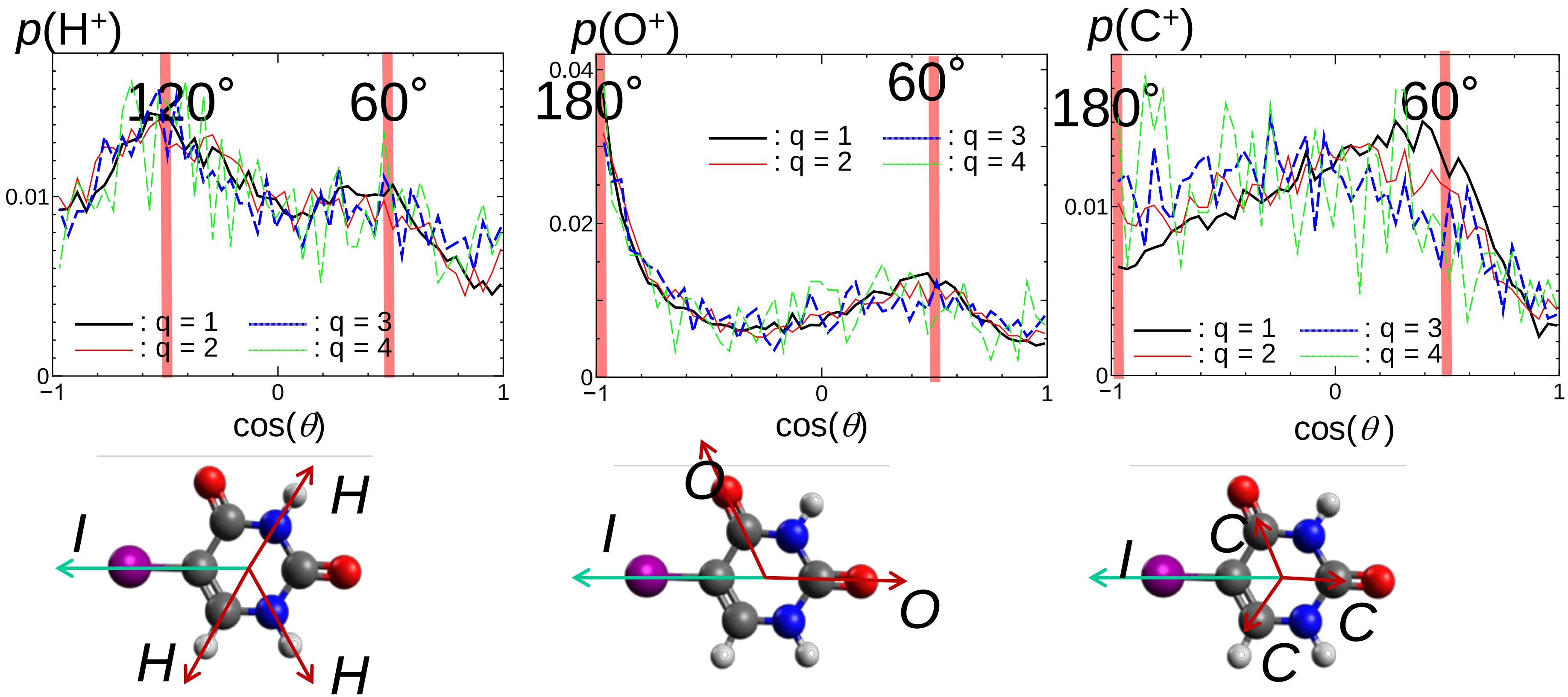

Red lines indicate angle between I direction and H, O, or C directions from the center of the aromatic ring in the neutral molecule.

Angular correlations of fragment ions (except carbon ions) reflect the shape of parent molecule.

Comparison between Experiment and MD
2-body angular correlation

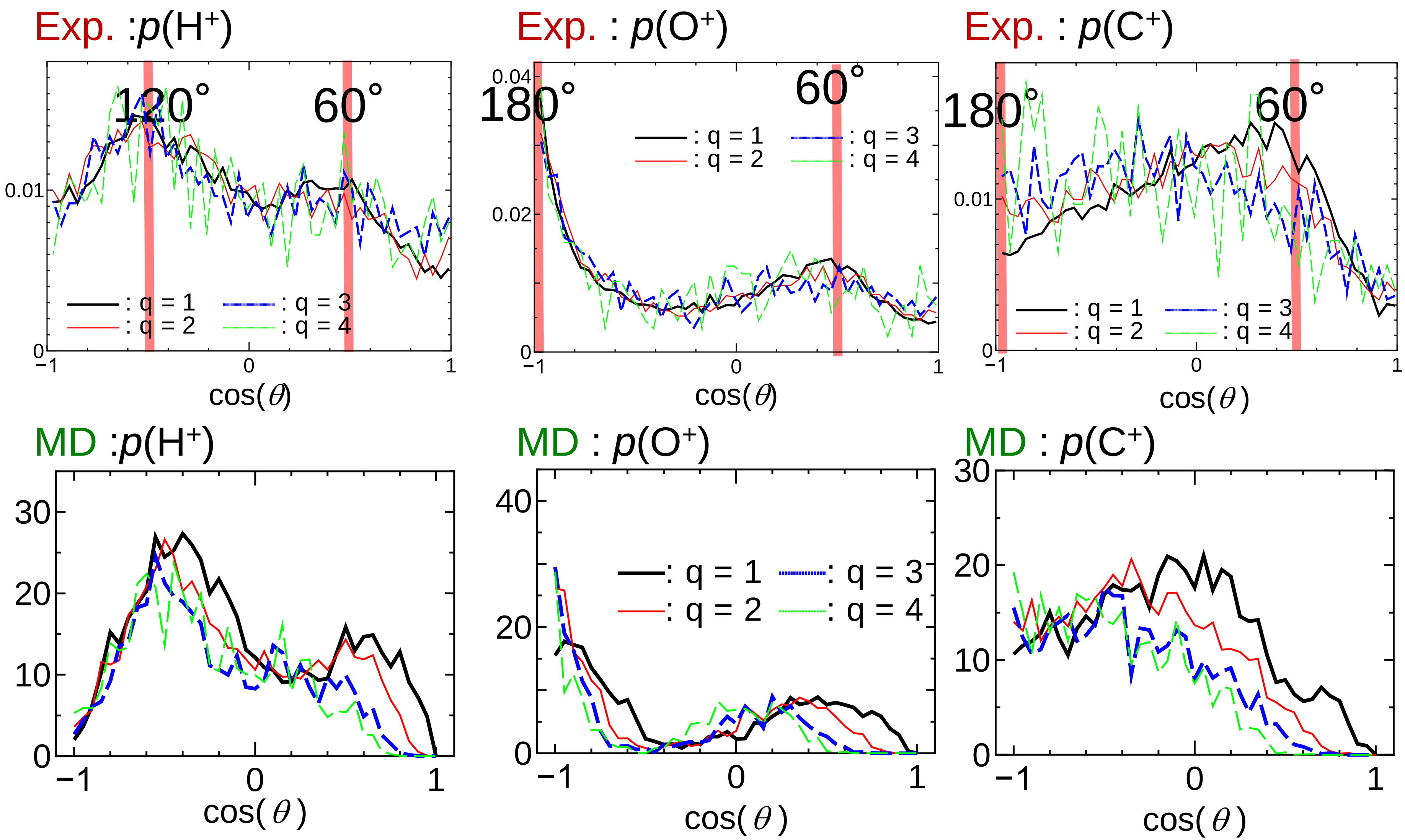

Black: I^{+}, *Red*: I^{2+}, *Blue*: I^{3+}, *Green*: I^{4+}

3-body angular correlation

I^+-H^+-H^+

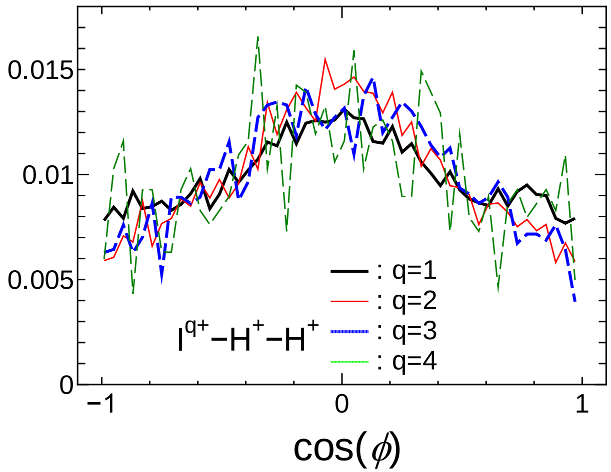

I^+-H^+-O^+

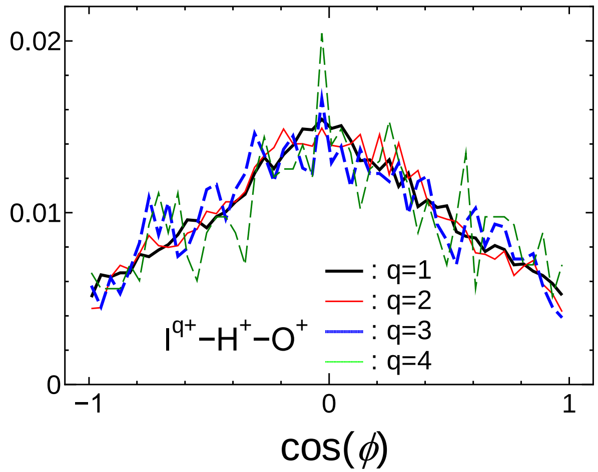

I^+-H^+-C^+

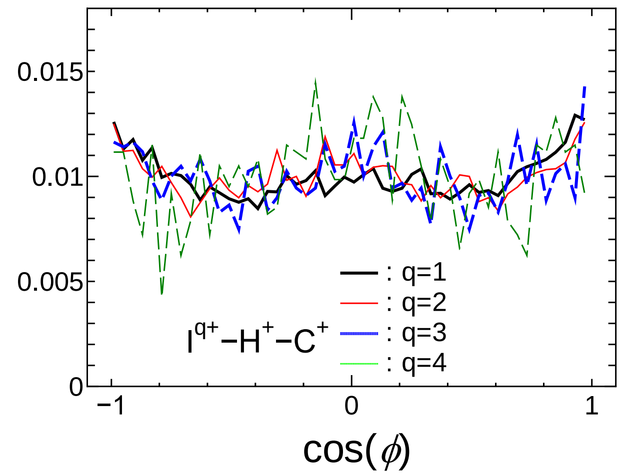

Black: I^+, Red: I^{2+}, Blue: I^{3+}, Green: I^{4+}

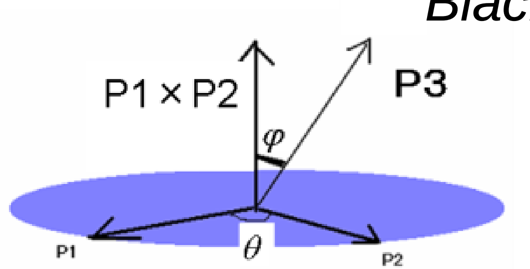

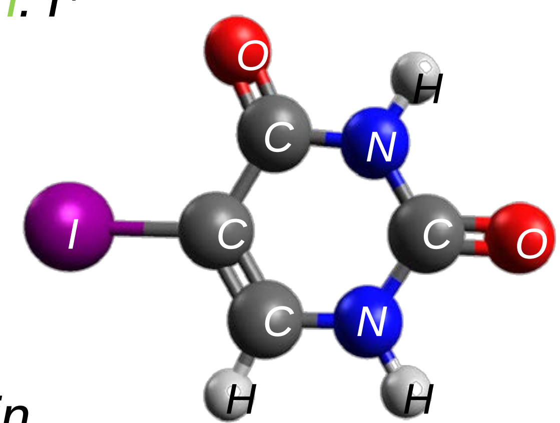

$$\cos(\varphi) = (\mathbf{P}_1 \times \mathbf{P}_2) \cdot \mathbf{P}_3 / (|\mathbf{P}_1||\mathbf{P}_2||\mathbf{P}_3| \sin(\theta)).$$

***P_1*, *P_2* and *P_3* are momentum of ions.**

$\cos(\varphi) = 0$ means that three momentum vectors are in the same plane.

These results suggest that carbon ions are released to off-planar direction.

Comparison between Experiment and MD
3-body angular correlation

Exp. : I^{q+}-H^{+}-H^{+}

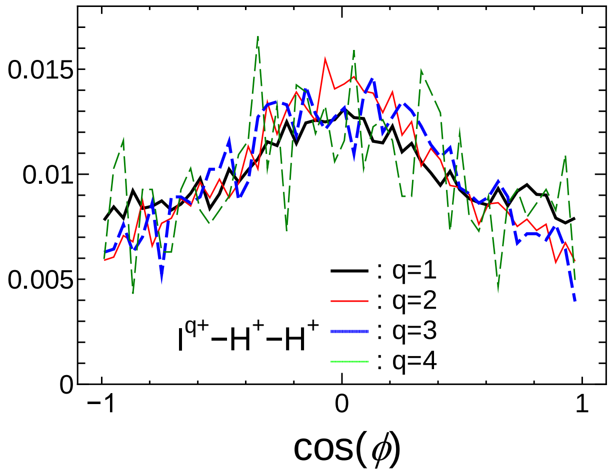

Exp. : I^{q+}-H^{+}-O^{+}

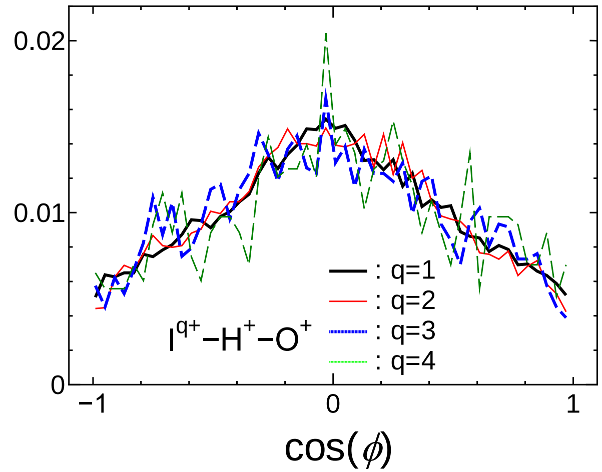

Exp. : I^{q+}-H^{+}-C^{+}

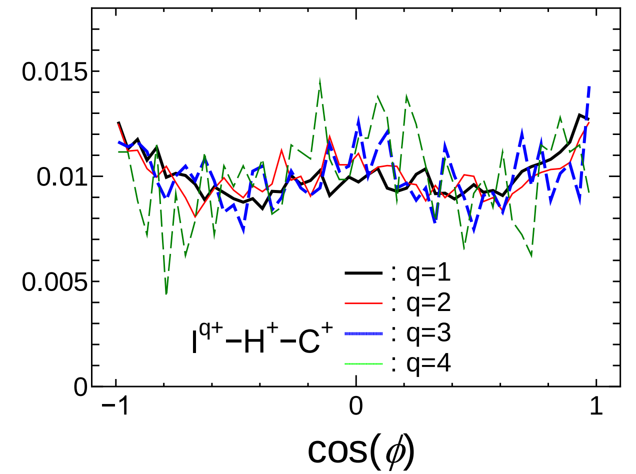

MD : I^{q+}-H^{+}-H^{+}

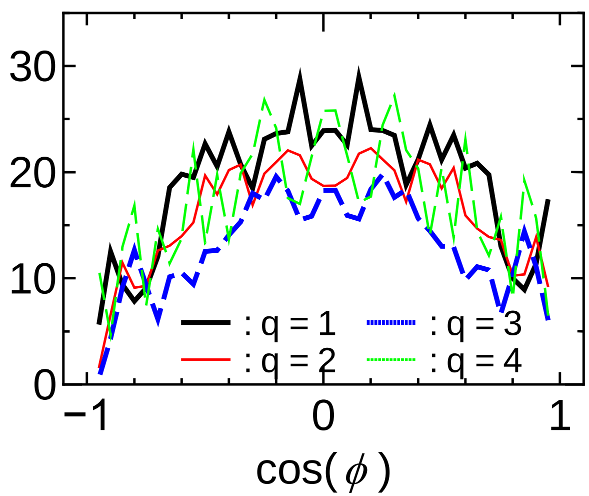

MD : I^{q+}-H^{+}-O^{+}

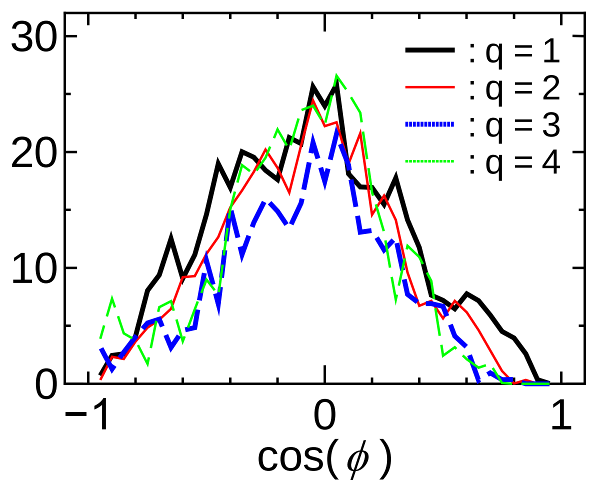

MD : I^{q+}-H^{+}-C^{+}

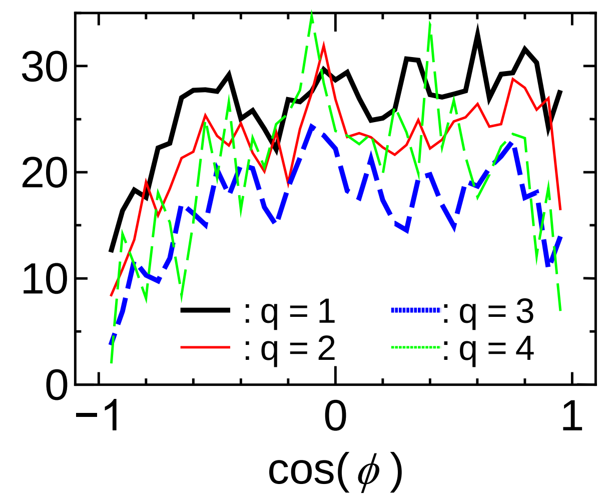

Black: I^{+}, Red: I^{2+}, Blue: I^{3+}, Green: I^{4+}

III. Efficient Nanoplasma Formation from Argon Clusters Irradiated by the Hard X-ray Free Electron Laser

T. Tachibana, Z. Jurek, H. Fukuzawa, K. Motomura, K. Nagaya, S. Wada, P. Johnsson, M. Siano, S. Mondal, Y. Ito, M. Kimura, T. Sakai, K. Matsunami, H. Hayashita, J. Kajikawa, , X.-J. Liu, E. Robert, C. Miron, R. Feifel, , J. Marangos, K. Tono, T. Togashi, Y. Inubushi, T. Hatsui, M. Yabashi, B. Ziata, S. Son, M. Yao, R. Santra, and K. Ueda (*Scientific Reports; in press).*

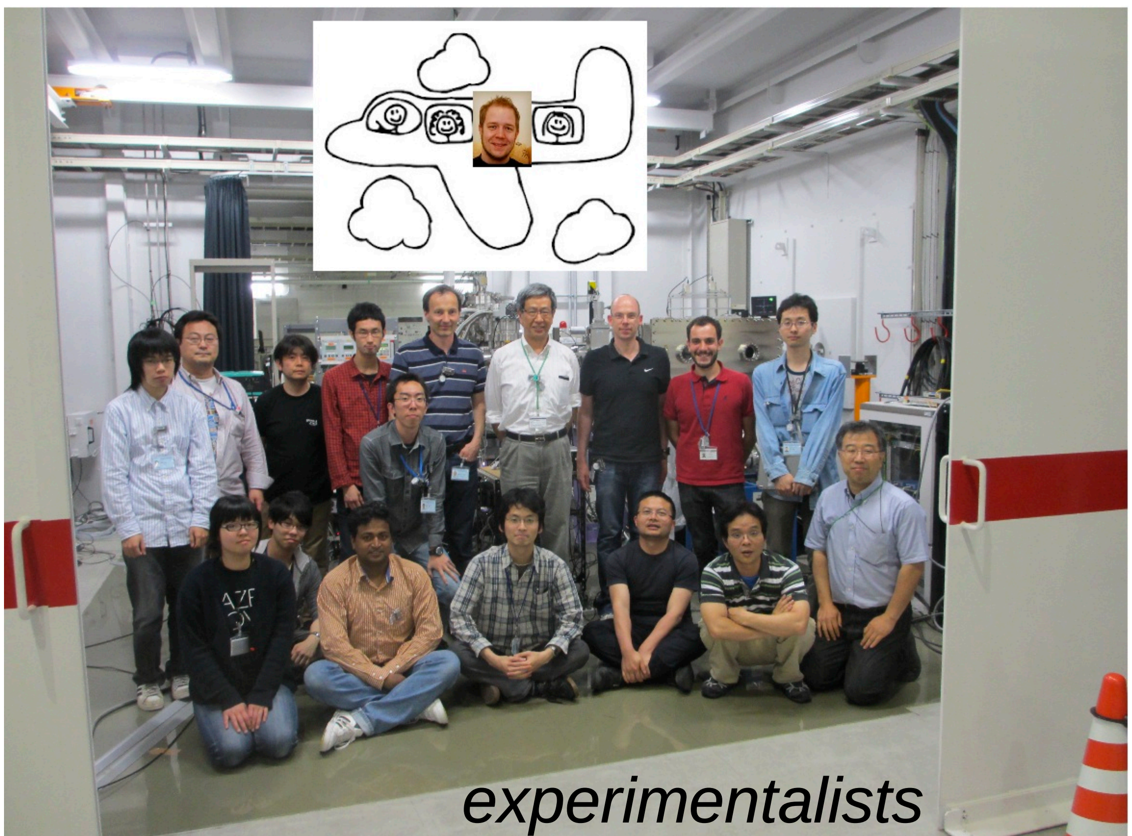

experimentalists

theorists

Nanoplasma formation by intense laser irradiation

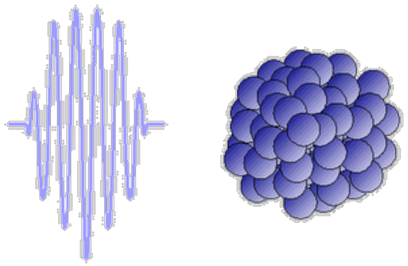

Laser irradiation into cluster

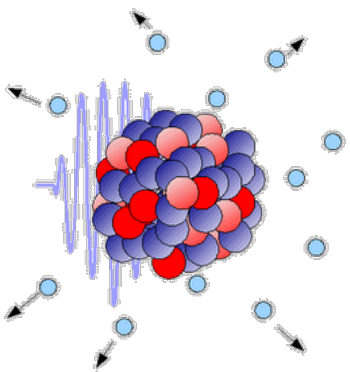

Many atoms in the cluster are ionized

Nanoplasma is formed when the electrons ejected from atoms trapped by the Coulomb potential of the multiply charged cluster ion.

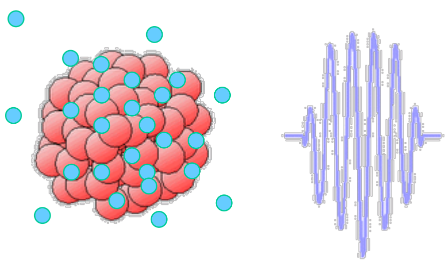

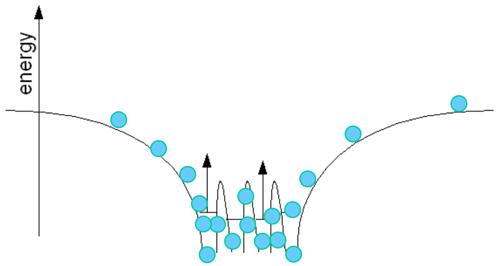

Is nanoplasma also formed by intense hard x-ray pulse irradiation?

How is nanoplasma formed?

Experimental & theoretical electron spectra of Ar clusters

Photon energy: 5 keV
Ar K edge: 3.2 keV

Dashed blue: Experiment,
Solid red: Theory

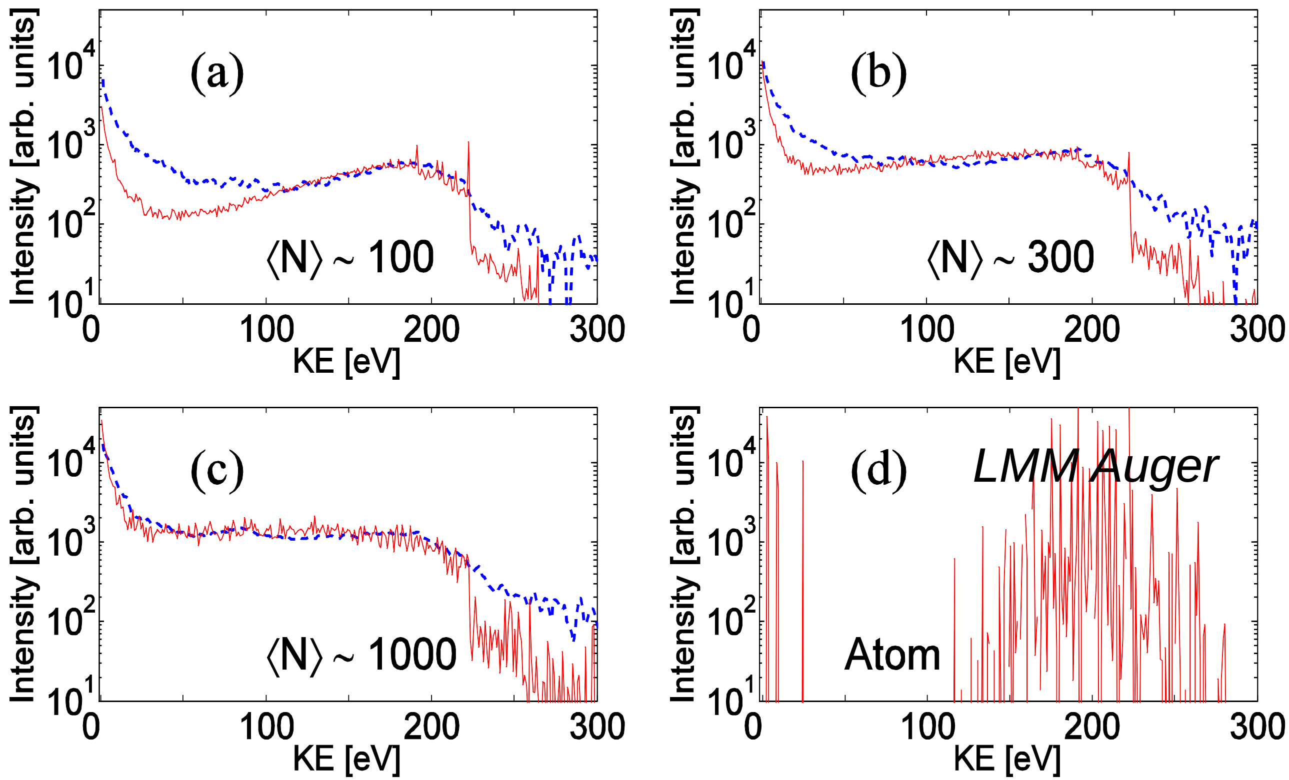

A plateau in the spectra is produced by the deceleration of the electrons. With the increase of the cluster size, a stronger potential builds up, decelerating the emitted electrons more.

The strong peak at zero kinetic energy is due to the thermal emission from nanoplasma.

T. Tachibana, Z. Jurek, H. Fukuzawa et al., Scientific Reports (in press).

Time evolution for the theoretical electron spectrum

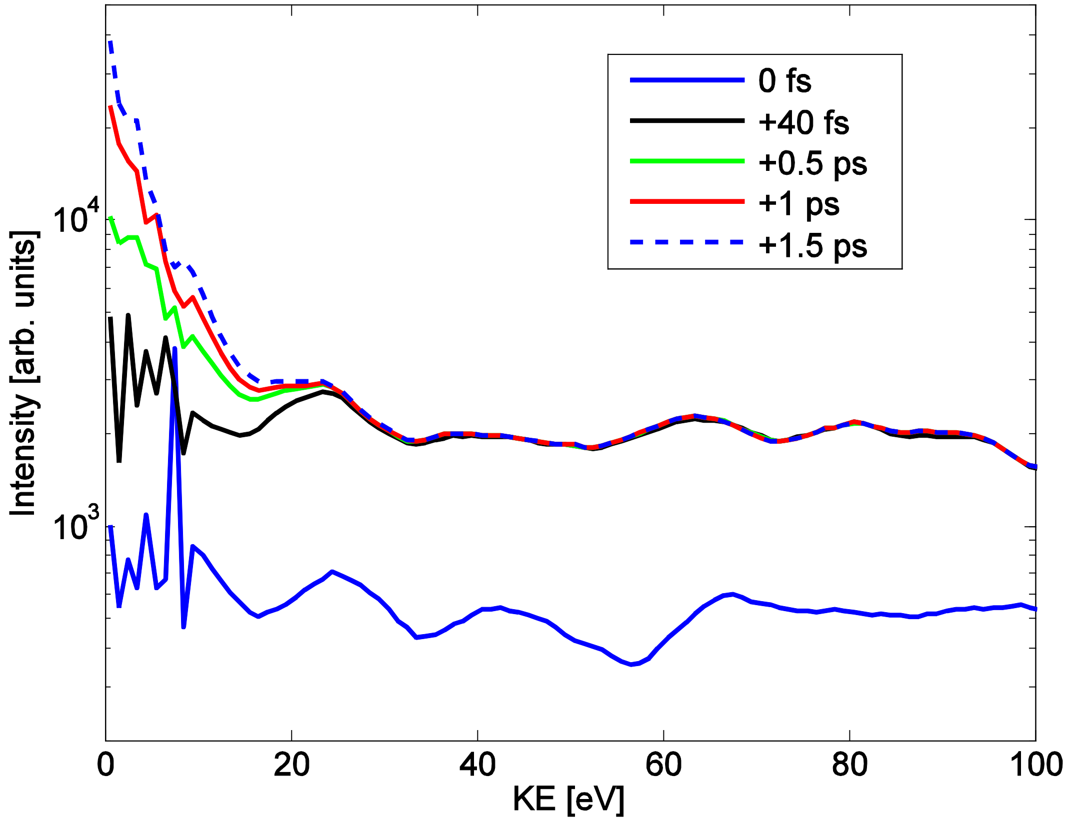

During the XFEL pulse, only the plateau is formed. The main peak at 0 eV develops after the XFEL pulse when the ionic system has started to expand and let some of trapped electrons escape from nanoplasma.

T. Tachibana, Z. Jurek, H. Fukuzawa et al., Scientific Reports (in press).

Electron spectra of Ar_{1000} in the whole region

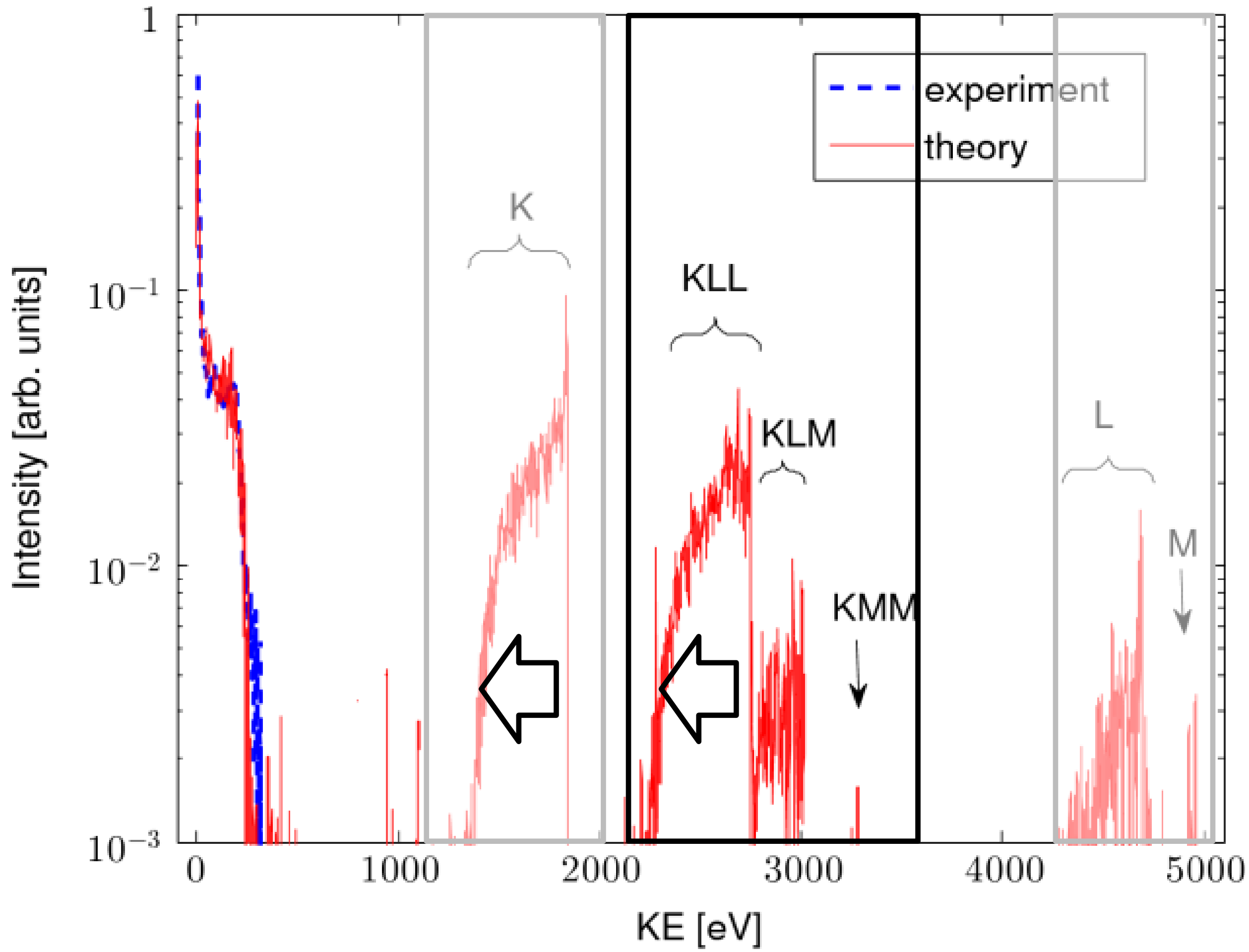

Photon energy : 5 keV
Ar K edge : 3.2 keV

Photo electron
Auger electron

Emitted electrons are decelerated ~500 eV

T. Tachibana, Z. Jurek, H. Fukuzawa et al., Scientific Reports (in press).

Origin of the slow electrons that can be trapped

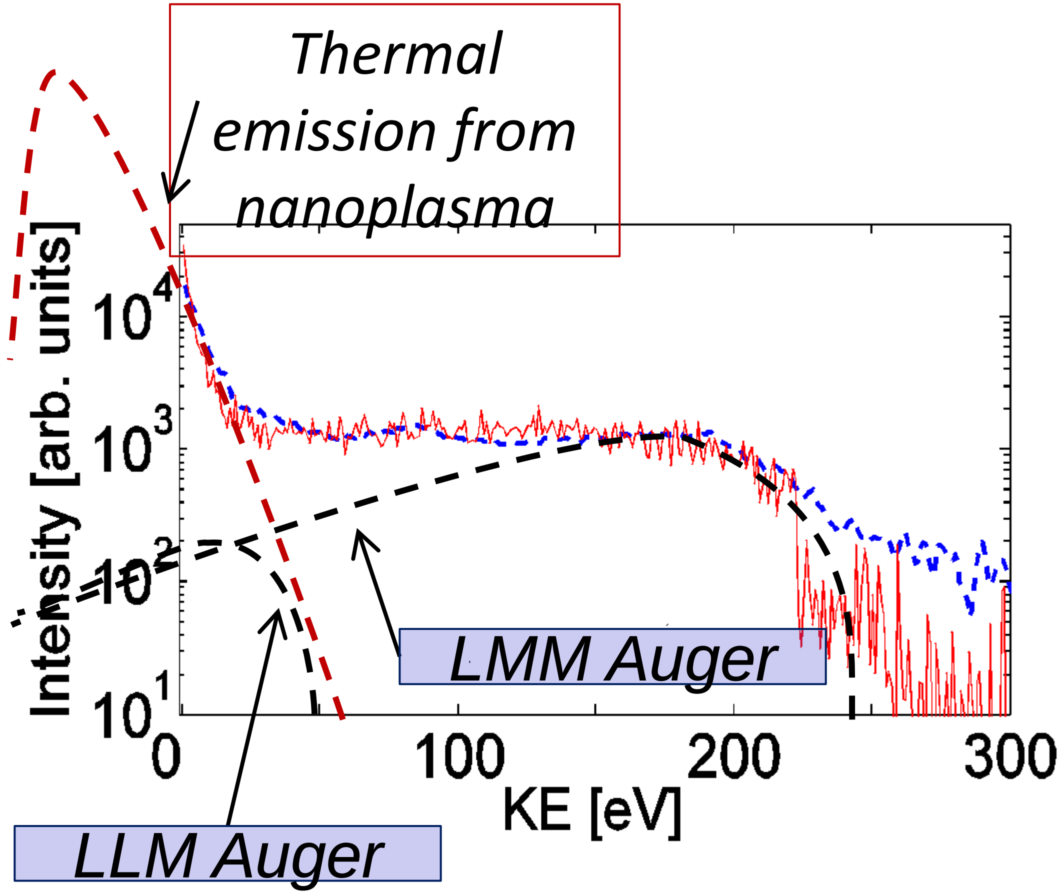

The majority of trapped electrons are created by impact ionizations caused by low-energy Auger and secondary electrons.

T. Tachibana, Z. Jurek, H. Fukuzawa et al., Scientific Reports (in press).

IV. Single-shot imaging of giant Xe clusters with X-ray free-electron laser (5.5 keV)

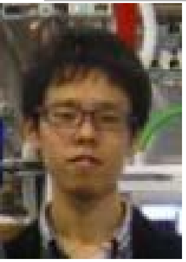

***T. Nishiyama, C. Bostedt, K. Nagaya**, K. R. Ferguson, C. Hutchison, H. Fukuzawa, K. Motomura, S. Wada, T. Sakai, K. Matsuami, T. Tachibana, Y. Ito, W. Q. Xu, S. Mondal, T. Umemoto, C. Nicolas, C. Miron, K. Kameshima, Y. Jochi, K. Tono, H. Hatsui, M. Yabashi, M. Yao, and K. Ueda* (in preparation).

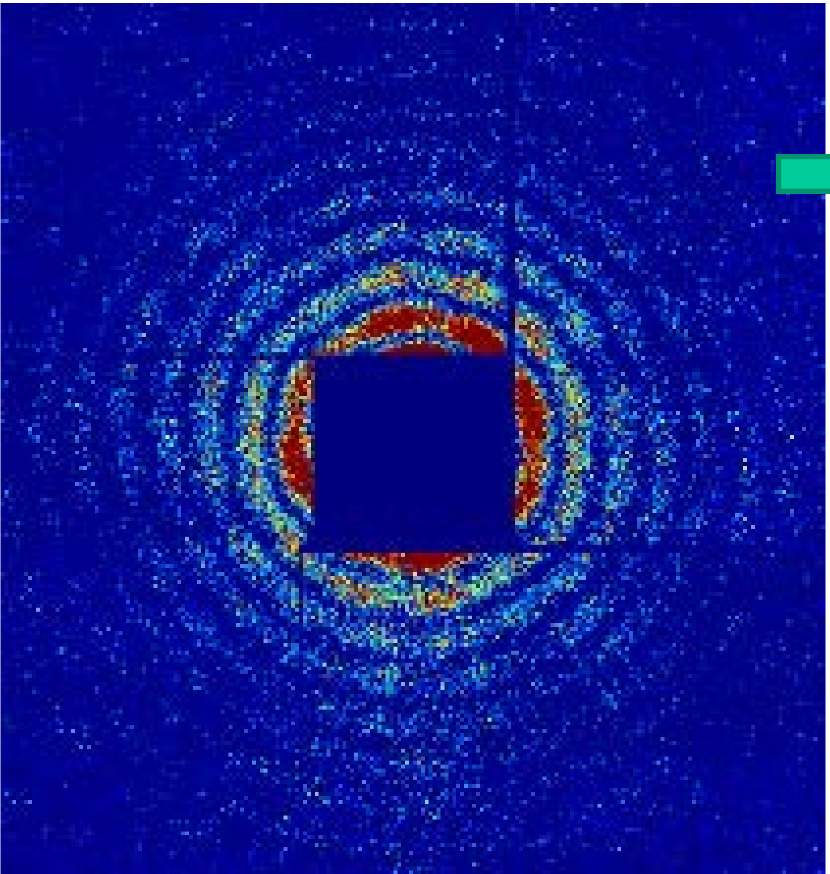

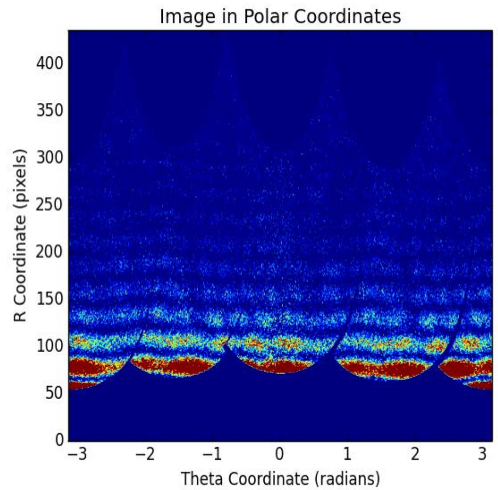

Diameter: 250nm

~1.1 × 10^8 atoms

FEL fluence:

~10 μJ/μm^2

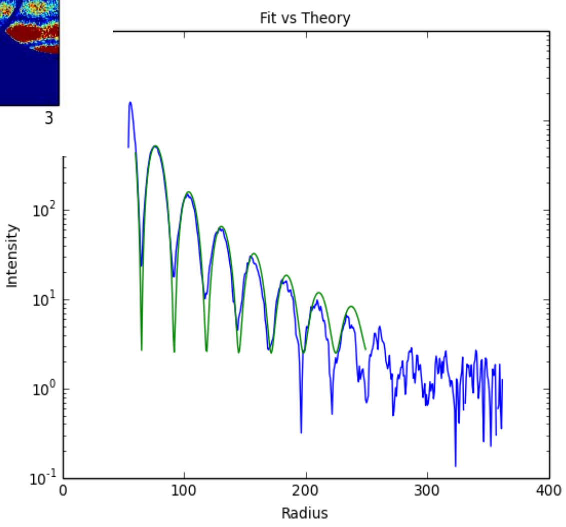

IV. Single-shot imaging of Xe clusters with XFEL

5.5 keV with fluence of ~ 10 μJ/μm²

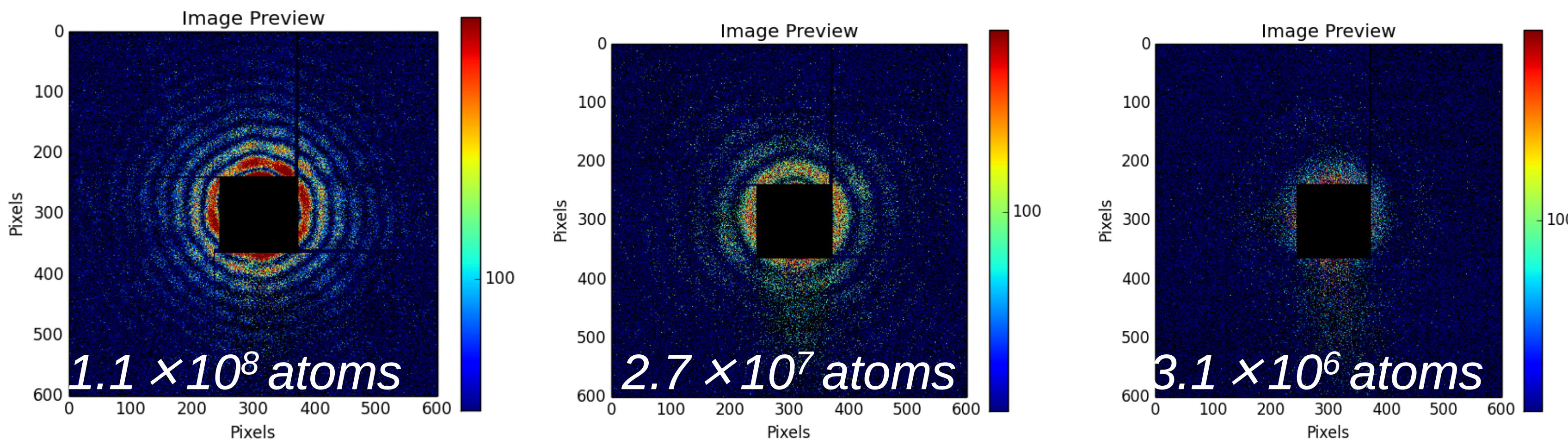

Ion Time of Flights

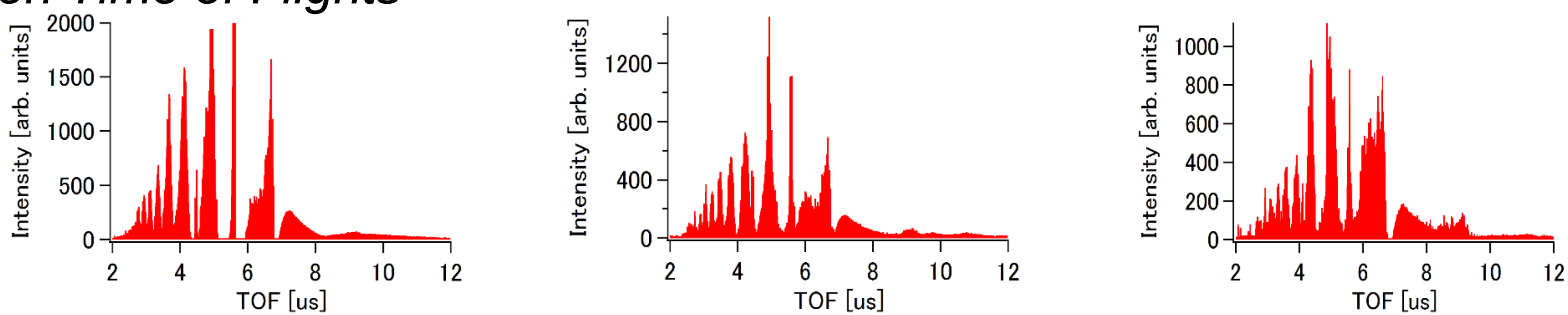

Fluorescence

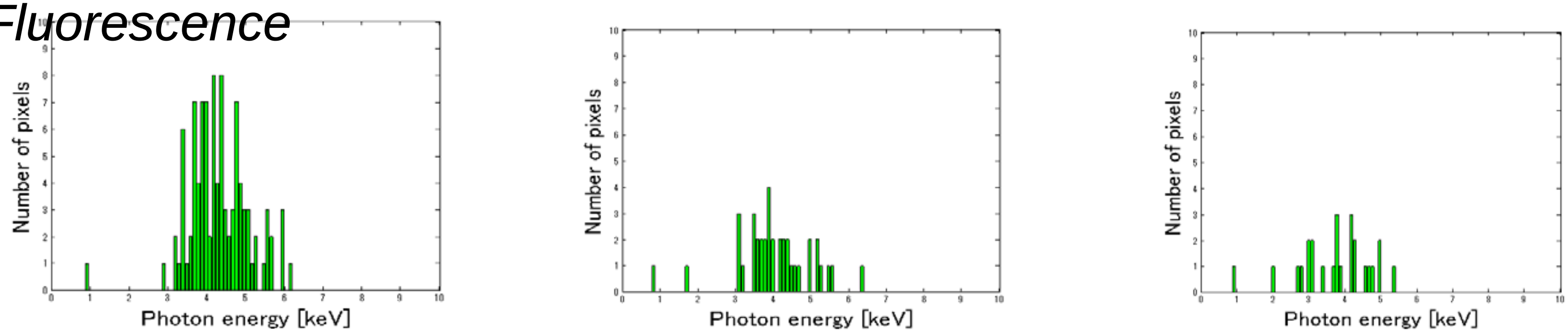

IV. Single-shot imaging of Xe clusters with XFEL

5.5 keV with the cluster size of ~ 120 nm

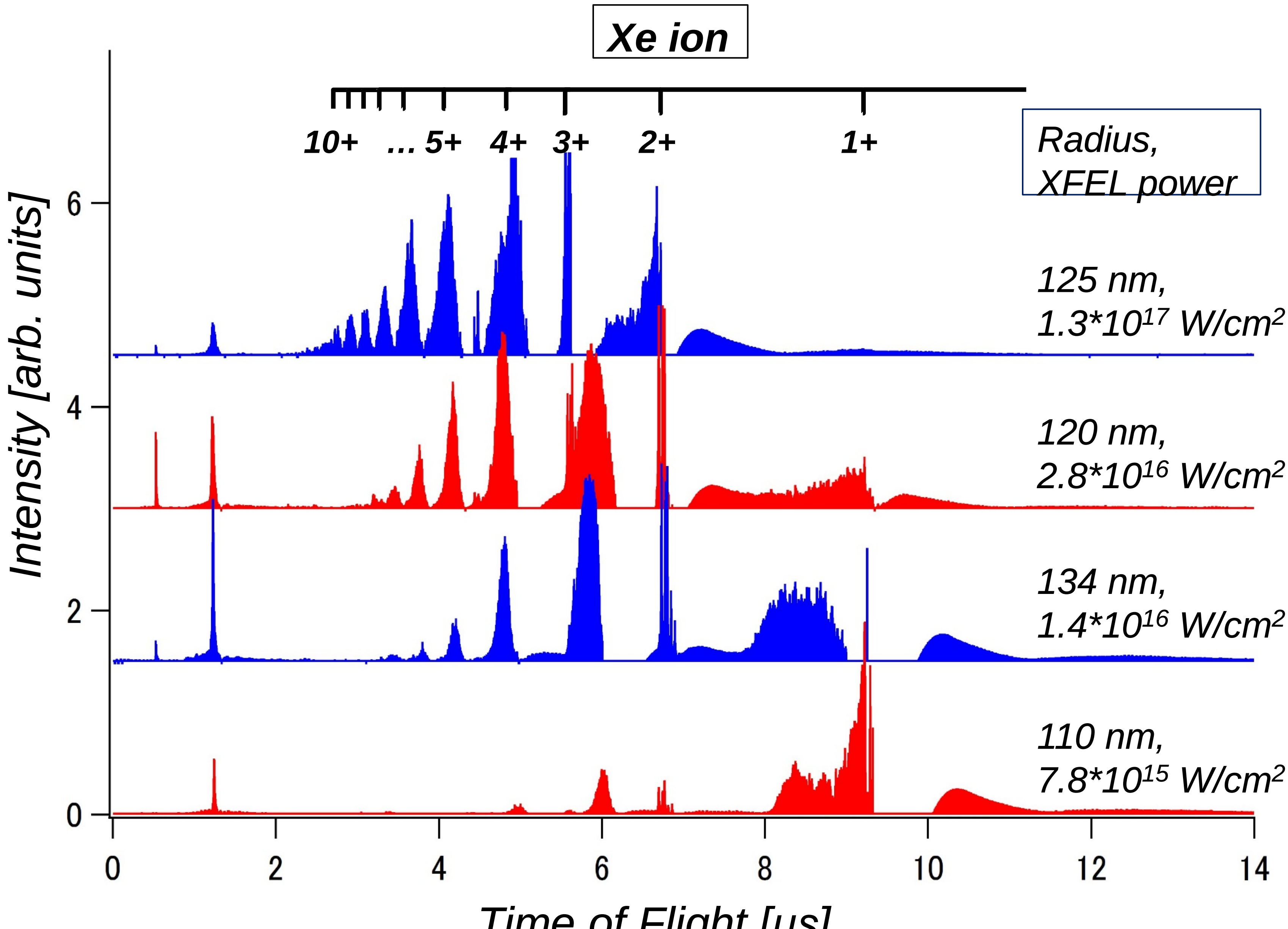

V. Real-time study on the ultrafast plasmon resonance heating of nanoplasma produced by the XFEL irradiation to rare gas clusters at SACLA

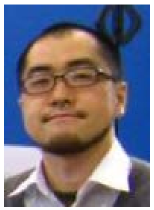  

Y. Kumagai, W. Xu, Z. Jurik, H. Fukuzawa, K. Motomura, S. Mondal, T. Tachibana, Y. Ito, K. Nagaya, T. Sakai, K. Matsunami, T. Nishiyama, M. Yao, S. Wada, T. Umemoto,C. Nicolas, C. Miron, T. Togashi, K. Tono, Ogawa, S. Owada, M. Yabashi, B. Ziata, S. Son, R. Santra, and K. Ueda

(in preparation)

Dynamics of nanoplasma produced by XFEL

- ***Photoionization Auger cascades***
- ***Nanoplasma formation***

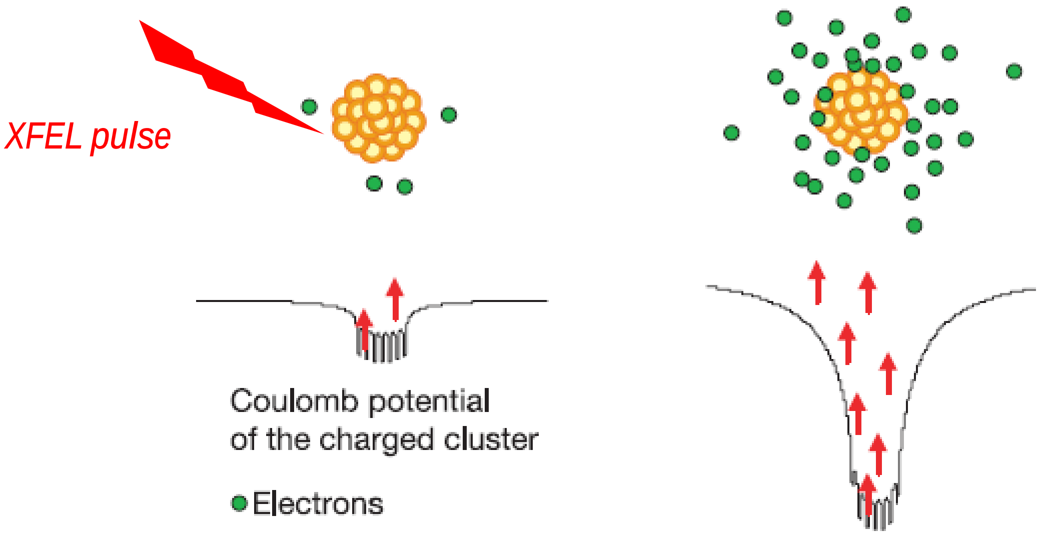

Dynamics of nanoplasma produced by XFEL

- ***Photoionization Auger cascades***
- ***Nanoplasma formation***

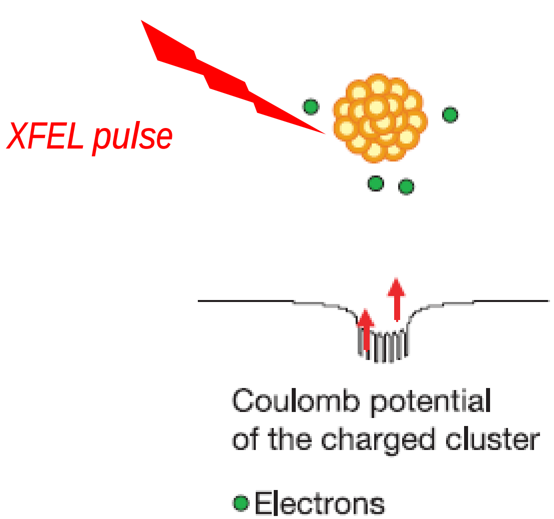

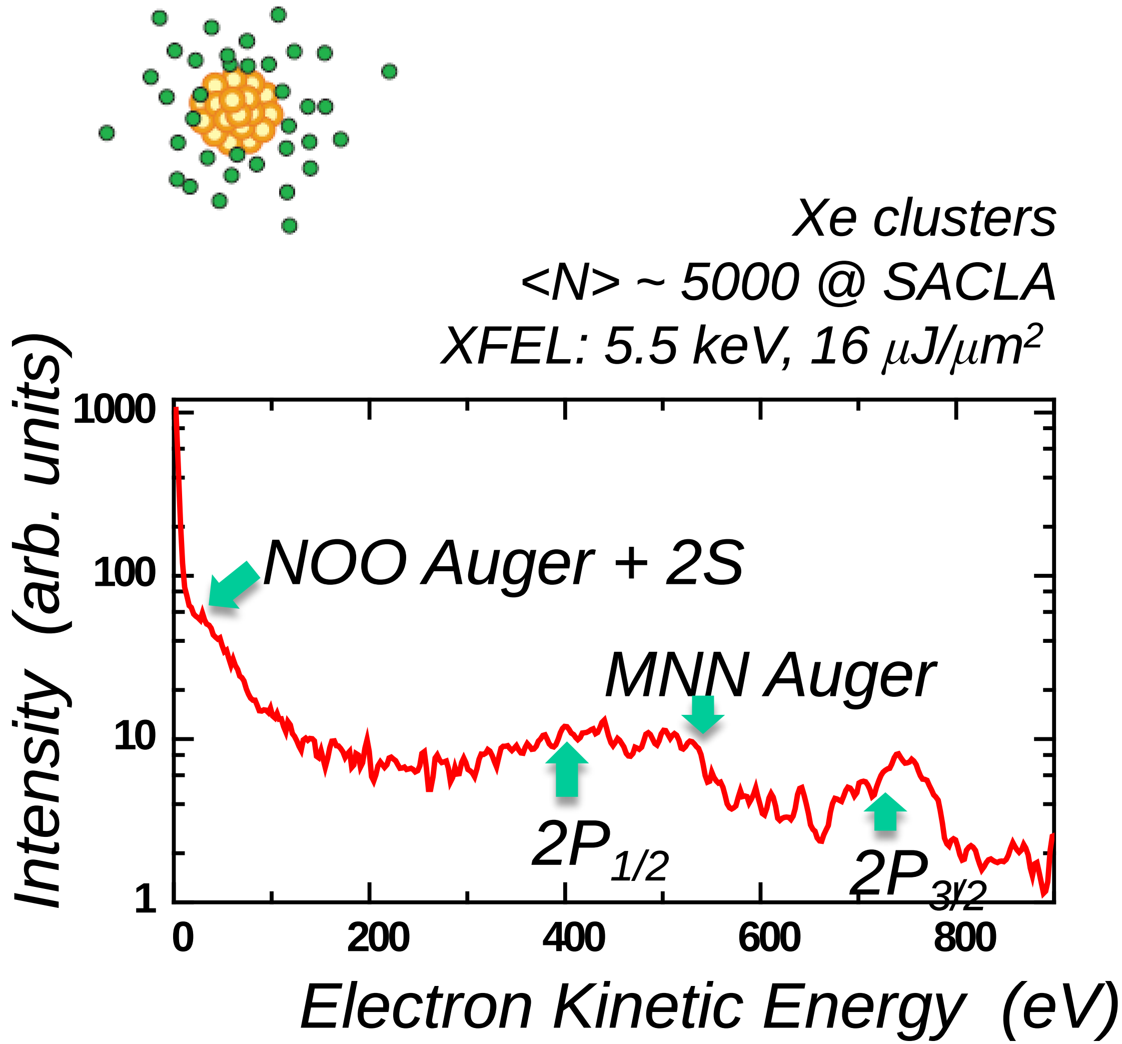

Dynamics of nanoplasma produced by XFEL

- ***Photoionization Auger cascades***
- ***Nanoplasma formation***

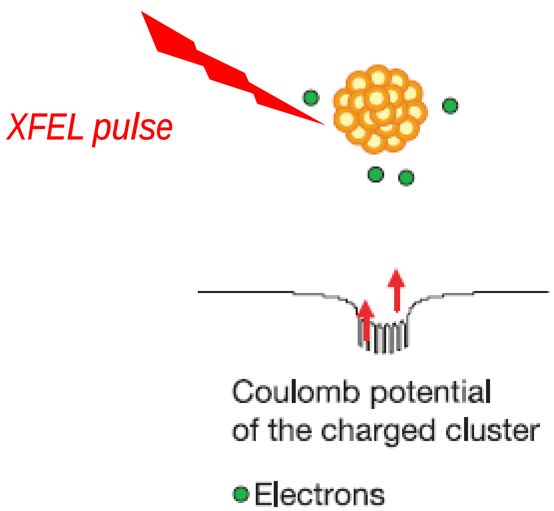

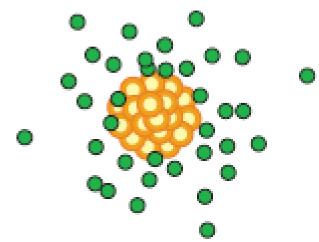

Xe clusters
<N> ~ 5000 @ SACLA
XFEL: 5.5 keV, 16 $\mu J/\mu m^2$

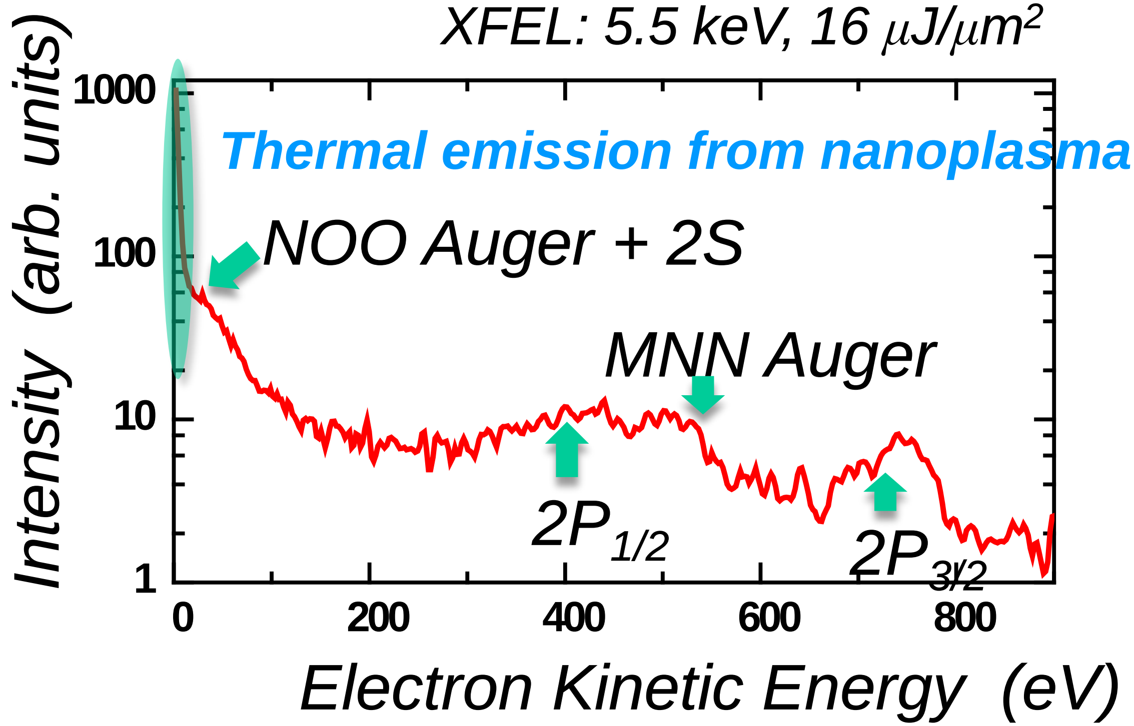

Dynamics of nanoplasma produced by XFEL

- **Photoionization Auger cascades**
- **Nanoplasma formation**
- **Coulomb explosion**

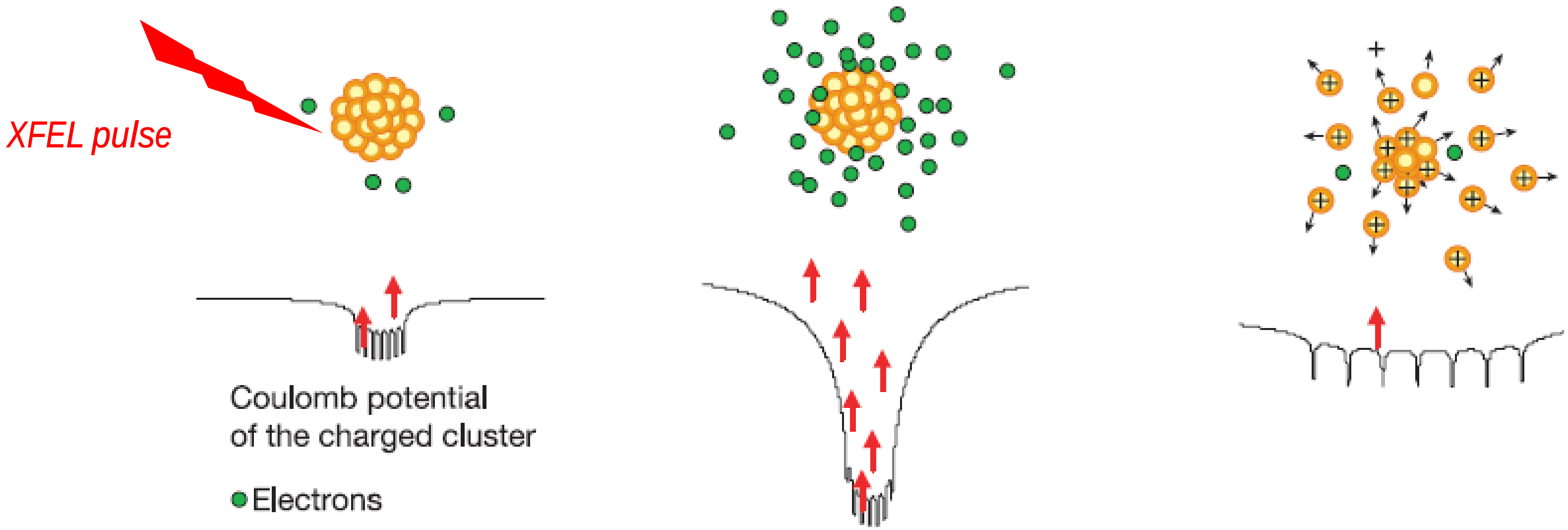

• • • To probe nanoplasma formation and to investigate its dynamics
we employ pump-probe technique

To search the plasmon resonance heating

- *Photoionization Auger cascades*
- *Nanoplasma formation*
- *Coulomb explosion*

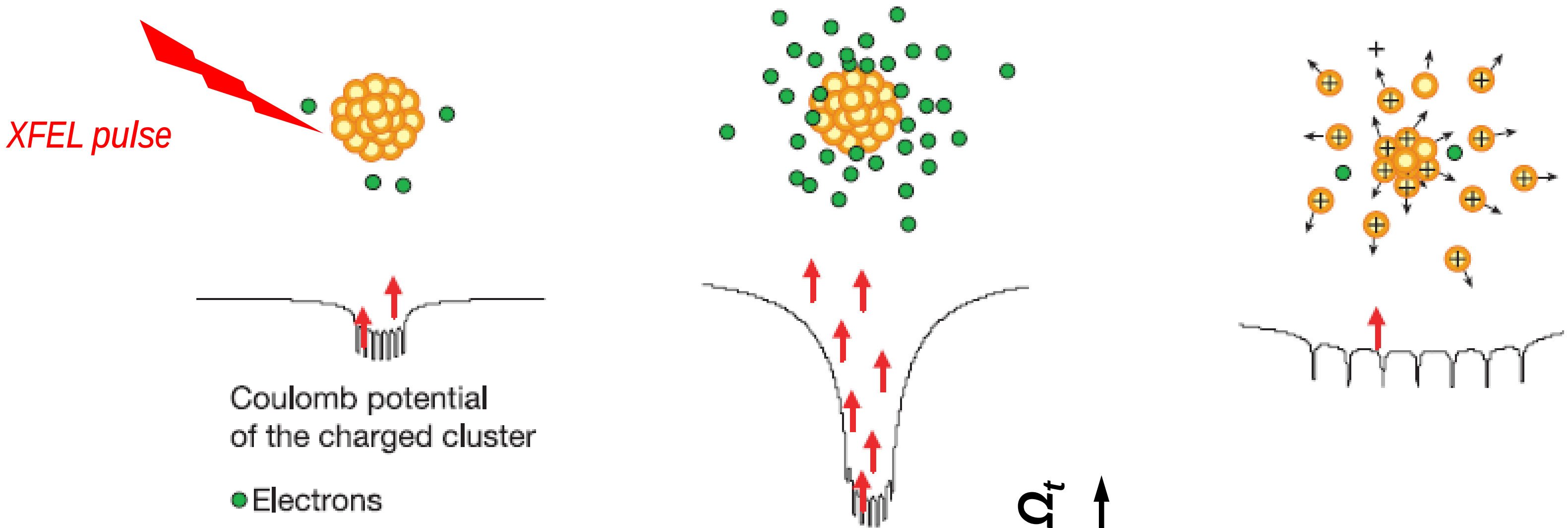

Surface-plasma frequency

$$\Omega_t = \sqrt{\frac{N_t Z_t}{R_t^3}} = \frac{\omega_{pl}}{\sqrt{3}}$$

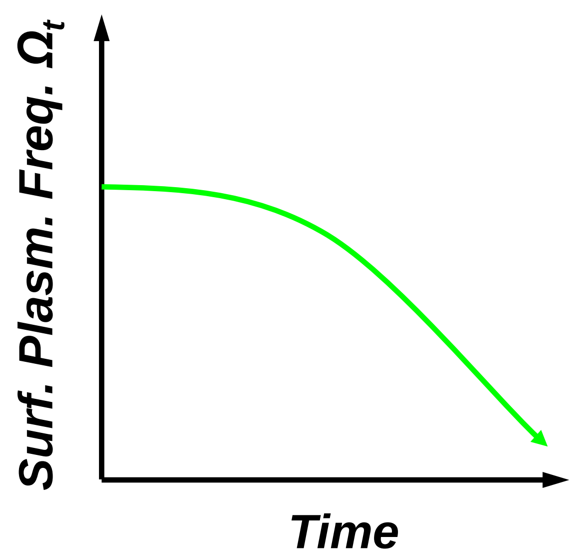

To search the plasmon resonance heating

Photoionization
Auger cascades

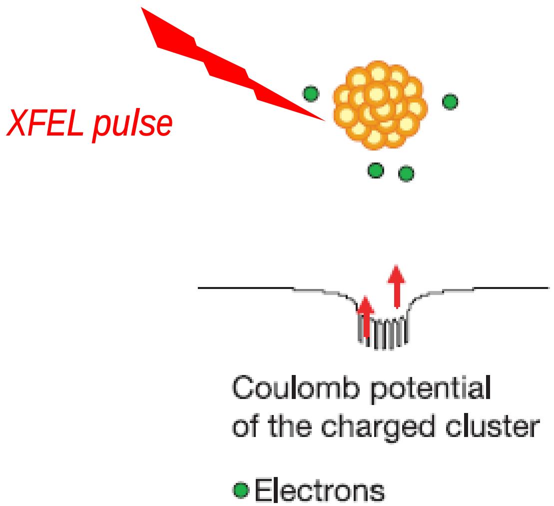

Nanoplasma formation

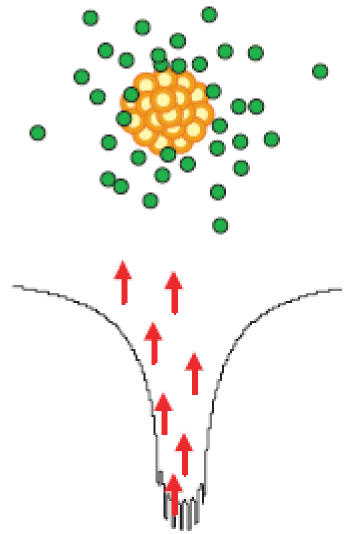

Coulomb explosion

$$\Omega_t \propto \sqrt{\frac{N_t Z_t}{R_t^3}} = \frac{\omega_{pl}}{\sqrt{3}}$$

Surface-plasma frequency

$$\Omega_t \propto \sqrt{\frac{N_t Z_t}{R_t^3}} = \frac{\omega_{pl}}{\sqrt{3}}$$

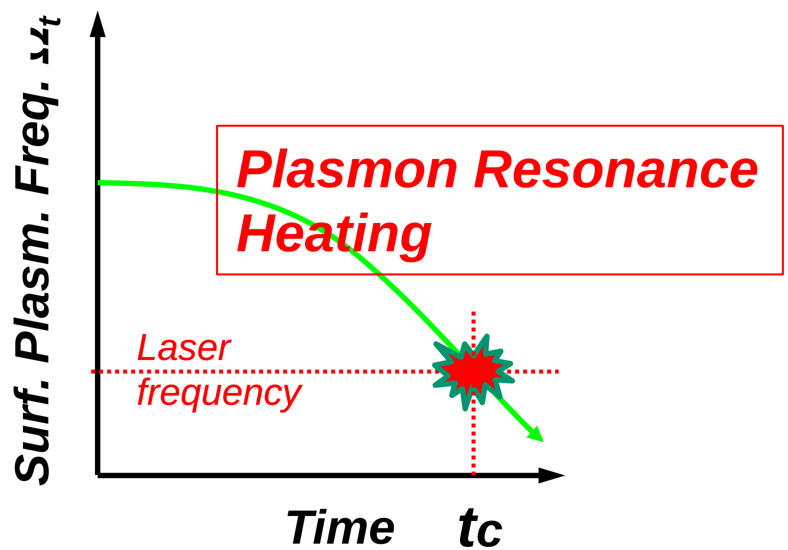

Experimental setups

■ XFEL @ SACLA

Photon energy: 5.5 keV
Spectral width: ~33 eV (FWHM)
Repetition rate: 30 Hz
Pulse duration: <10 fs
Focused beam size: ~1 μm
Peak intensity: ~3.28 / 3.38 x 10^{16} W/cm^2

■ NIR laser

Wavelength: 800 nm
Repetition rate : 30 Hz
Pulse duration : 80 fs
Focused beam size: ~200 μm
Intensity: ~2.7 / 5.1 x 10^{12} W/cm^2

■ Clusters

Size of Xe clusters: ~5000 atoms
Nozzle diameter: ~250 μm

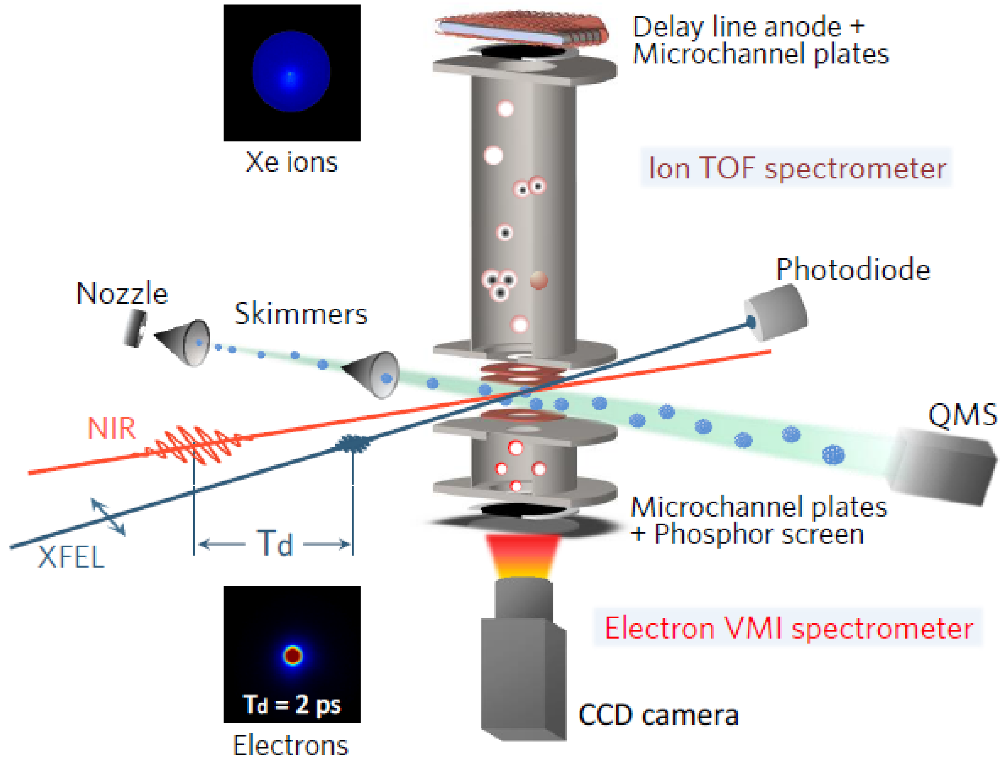

K. Tono *et al.*, New J. Phys. **15**, 083035 (2013);
A. T. J. B. Eppink and D. H. Parker, Rev. Sci. Instrum. **68**, 3477 (1997); K. Motomura *et al.*, J. Phys. B. **46**, 164024 (2003)

Time-resolved TOF spectra of Xe clusters

XFEL: 16 μJ/μm²; NIR: 4.1 nJ/μm²

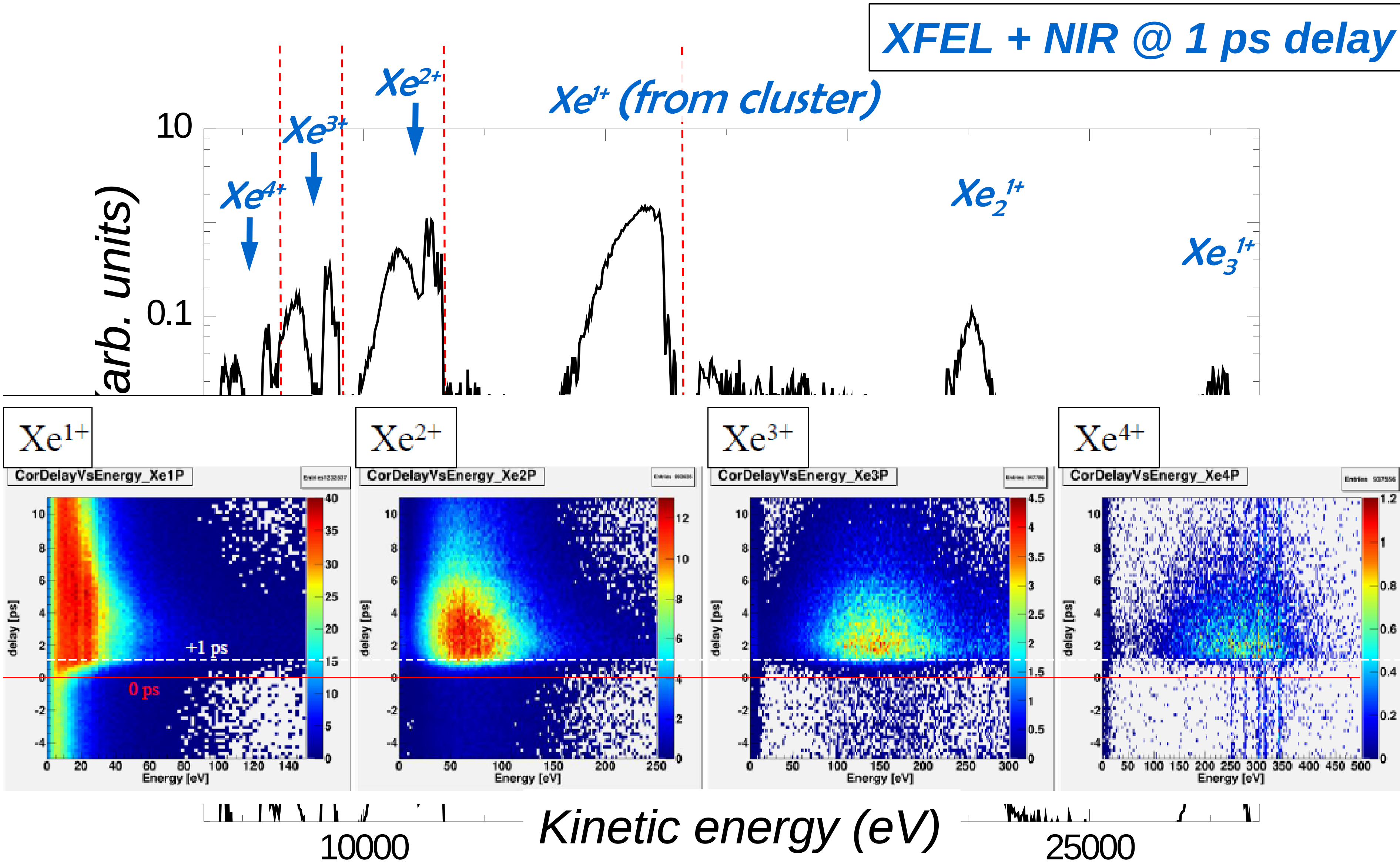

Plasmon heating in time-resolved PES

XFEL: 16 μJ/μm^2; NIR: 4.1 nJ/μm^2

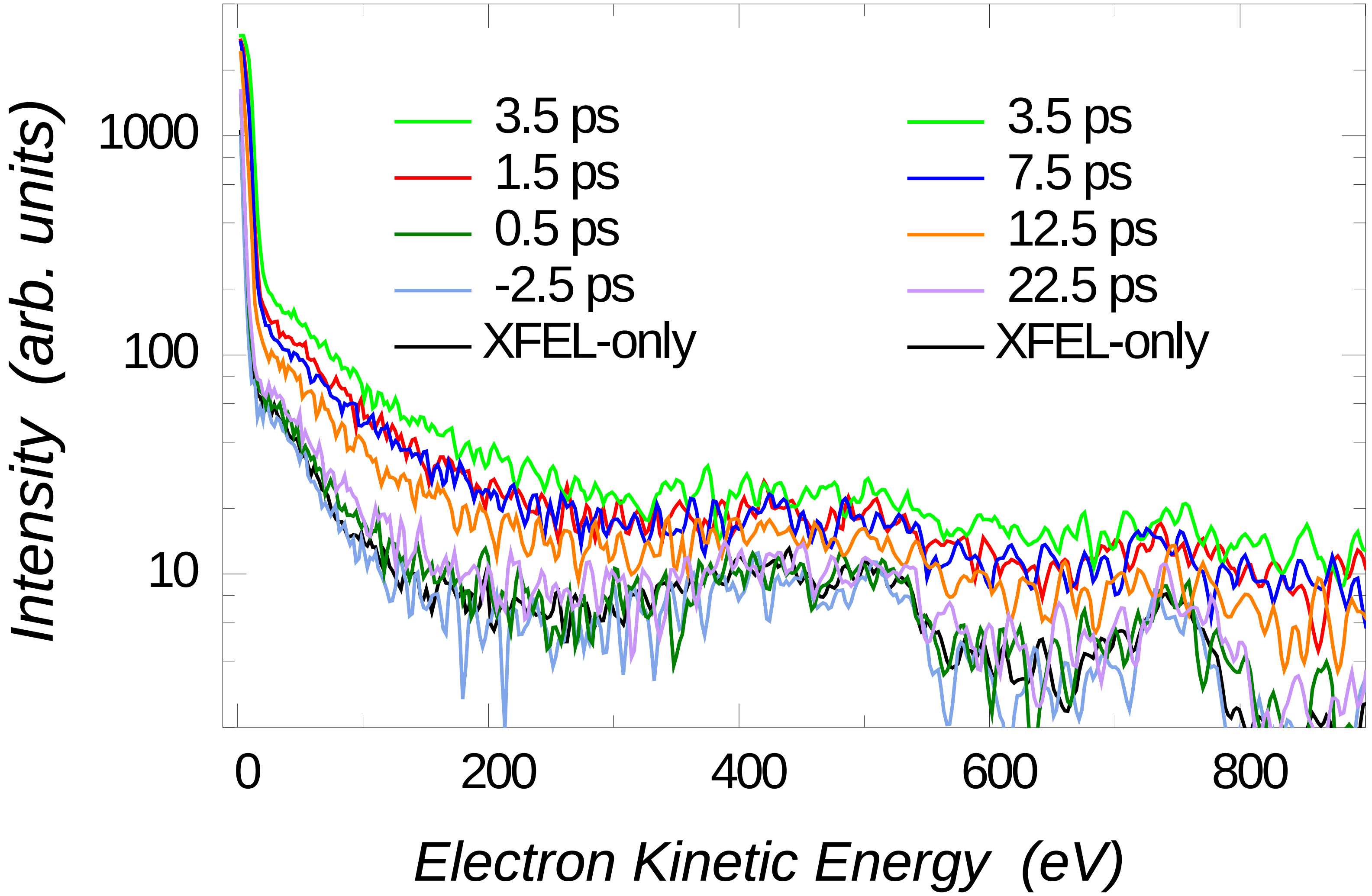

Plasmon heating in time-resolved PES

XFEL: 16 μJ/μm²; NIR: 4.1 nJ/μm²

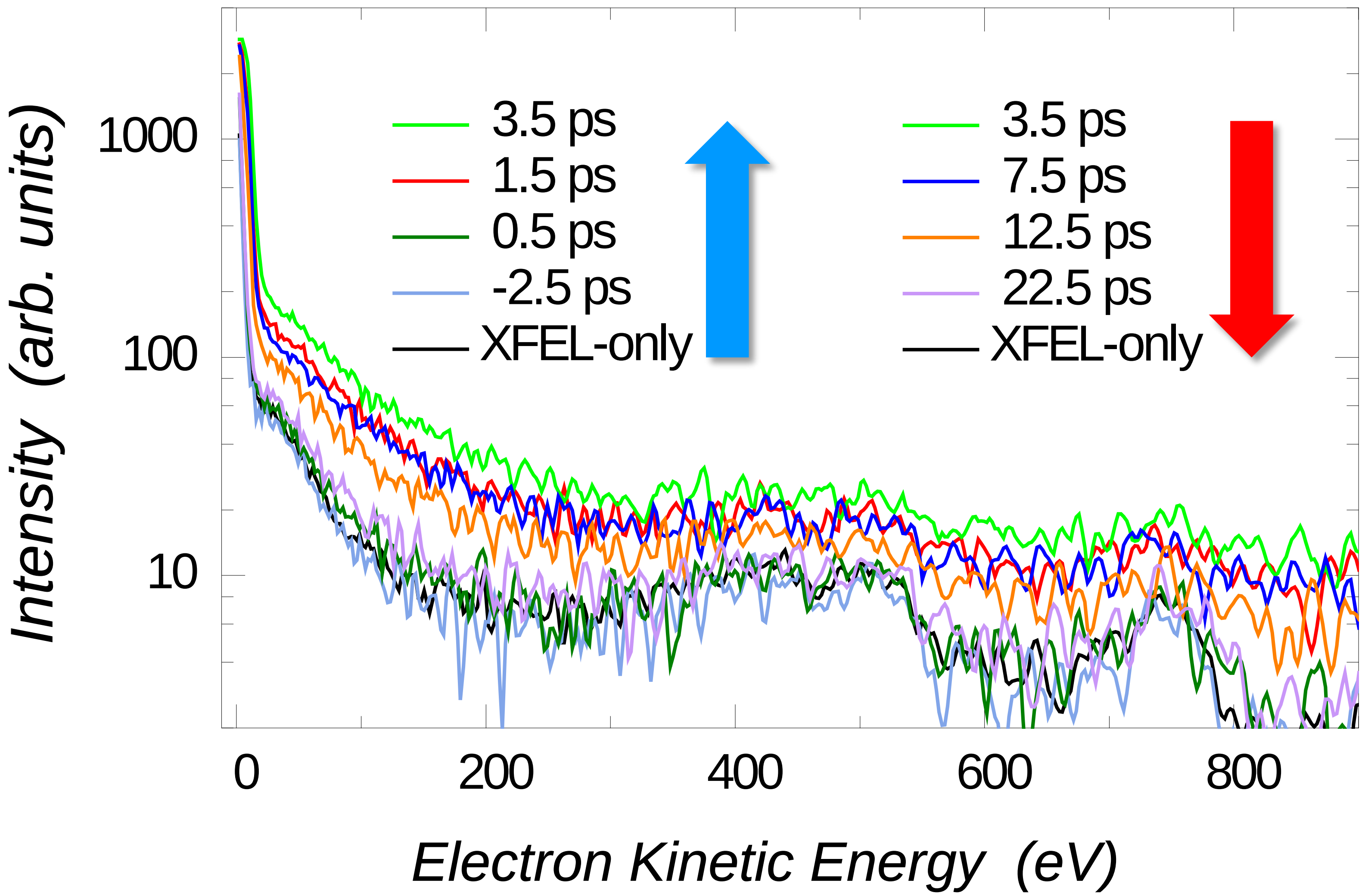

Summary

- Deep inner-shell multi-photon absorption of Ar and Xe atoms by **SACLA** XFEL pulses – Electronic damage

- Photoion-photoion coincidence imaging following deep inner-shell multi-photon absorption by **SACLA** XFEL pulses (CH_3I, 5I-uracil) – Radiation damage in the atomic level

- Electron spectroscopy of argon and xenon clusters heated by **SACLA** XFEL pulses – Nanoplasma formation

- Single-shot imaging of xenon nano-clusters – Influence of the electronic damage to the imaging

- IR-probe experiment of XFEL induced nanoplasma formation – Nanoplasma dynamics

What's next…

- UV/XFEL pump – XFEL probe for I-contained molecules
  Intra-molecular charge transfer via ionic fragmentation
- X-ray imaging for UV/XFEL induced nanoplasma from giant clusters
  Influence of nanoplasma formation to X-ray imaging….
- UV pump – XFEL probe for photocatalytic molecules
  Intra-molecular charge transfer via TR X-ray spectroscopy
- Serial femtosecond X-ray crystallography
  Phasing vs radiation damage


The end


Thank you very much for your attention!

Characteristic properties of FEL pulses

Coherent, intense, and ultra-short pulses at short wavelengths (EUV to X –rays)

Coherent X-ray imaging of non-crystalized samples

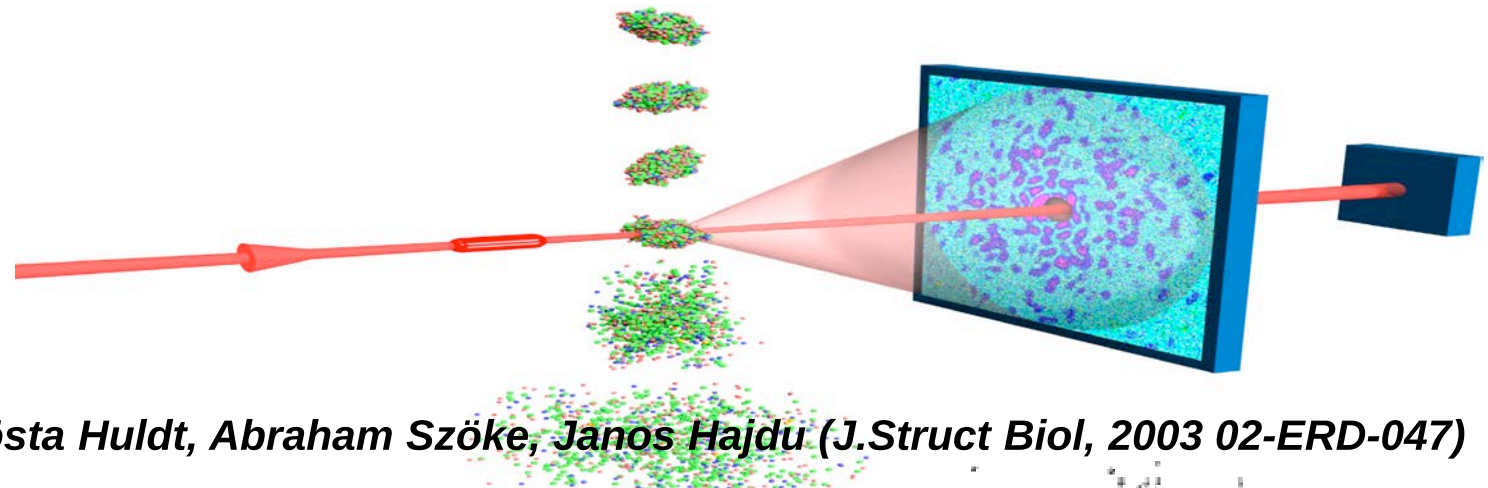

Gösta Huldt, Abraham Szöke, Janos Hajdu (J.Struct Biol, 2003 02-ERD-047)

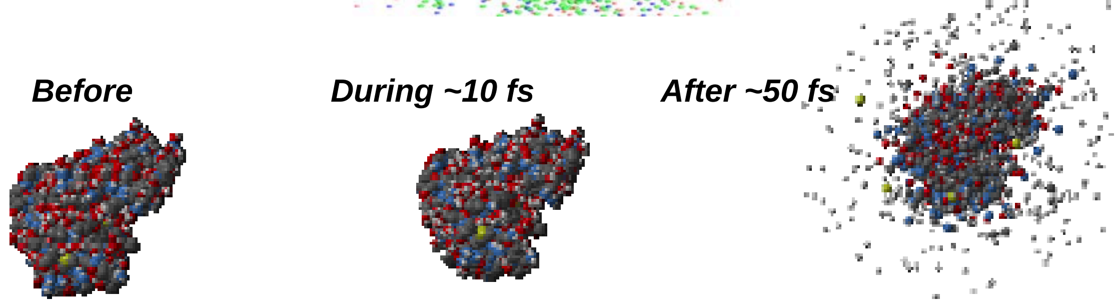

Neutze, Wouts, van der Spoel, Weckert, Hajdu   Nature 406, 752 (2000)

Single Mimivirus Particles Intercepted and Imaged with an X-ray laser

Seibert et al. Nature **470**, 78–81 (2011) *only 2D…..*

Coherent X-ray imaging of non-crystalized samples

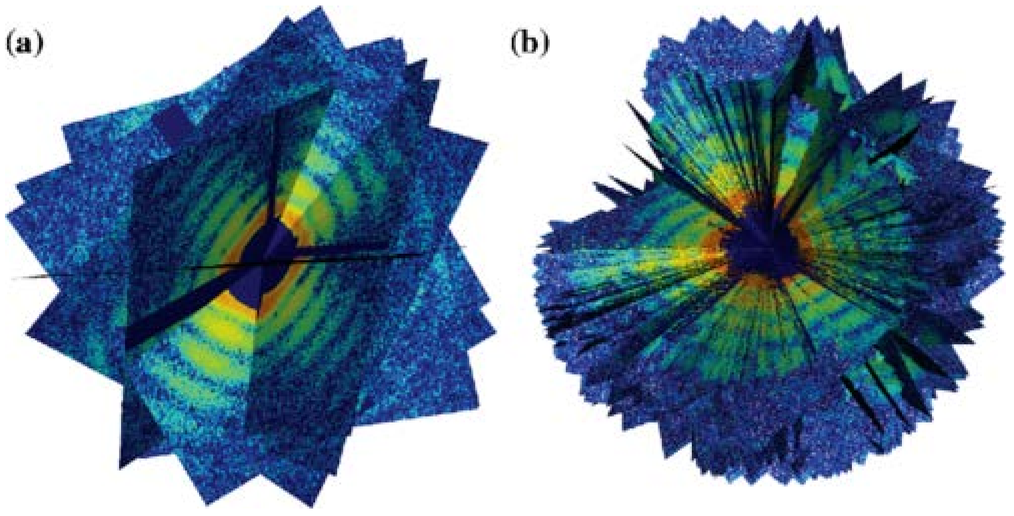

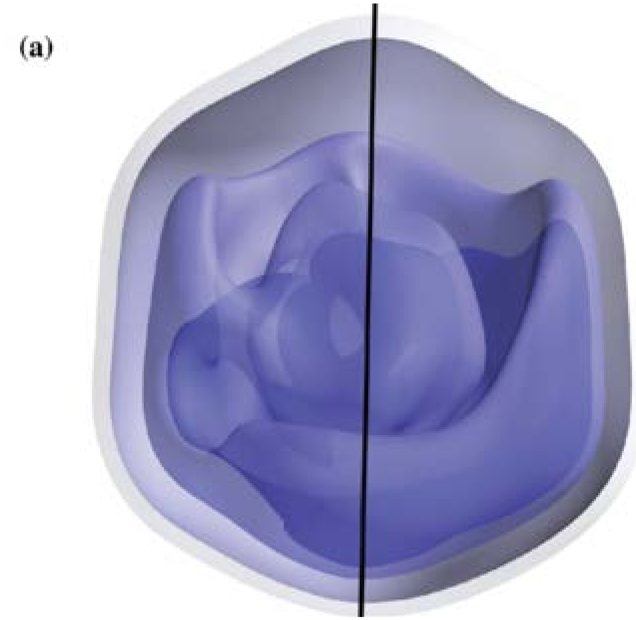

Three-Dimensional Reconstruction of the Giant Mimivirus Particle with an X-Ray Free-Electron Laser

Ekeberg *et al.* Phys. Rev. Lett. **114**, 098102 (2015)

Can we get 3D image from a single shot data?

Characteristic properties of FEL pulses

Intense and ultra-short pulses at **X –rays**

Why X-rays? structure determination at atomic resolution

*Femtosecond X-ray Protein Nano-crystallography, Chapman et al., Nature **470,** 73–77 (2011).*

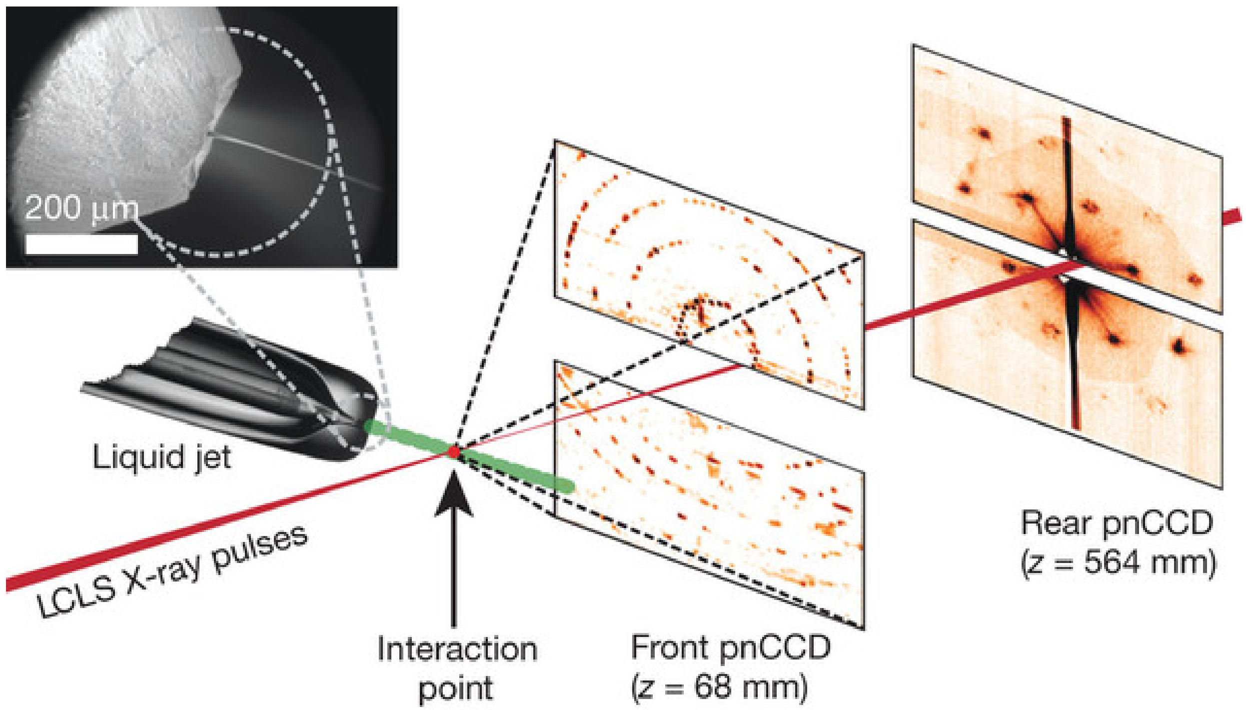

*High-Resolution Protein Structure Determination by Serial Femtosecond Crystallography, Boutet et al. Science **337,** 362 (2012).*

*Natively Inhibited Trypanosoma brucei Cathepsin B Structure Determined by Using an X-ray Laser, Redecke et al. Science **339**, 227 (2013).*

Photo-system II

Native structure of photosystem II at 1.95 Å resolution revealed by a femtosecond X-ray laser (SACLA)

Suga et al, Nature (2014)

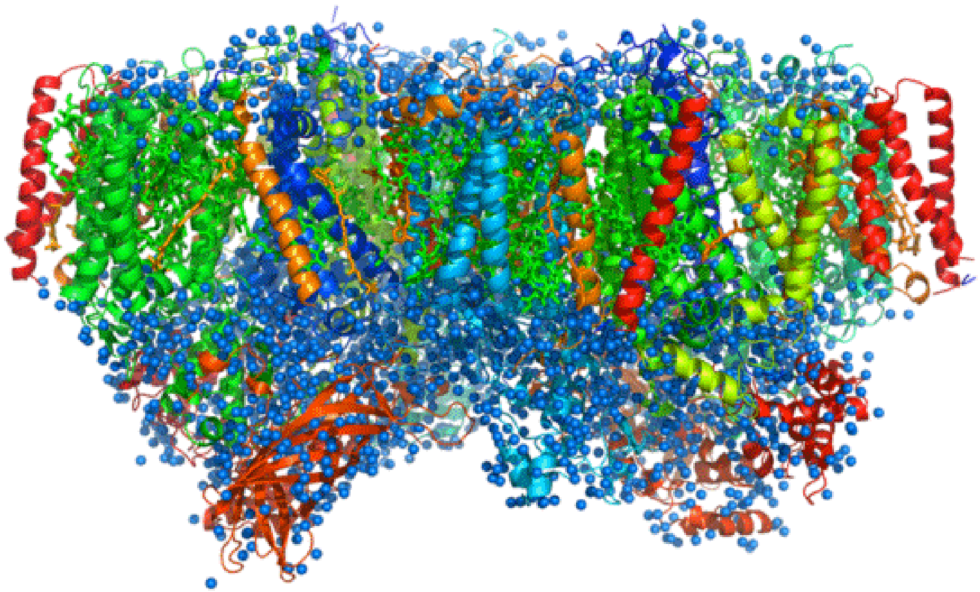

S_1

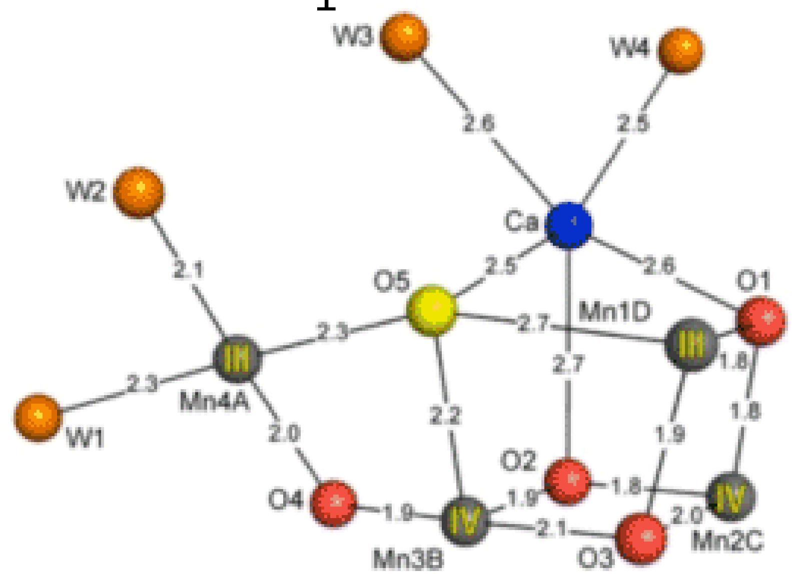

"Determination of damage-free crystal structure of an X-ray sensitive protein using an XFEL"
Nature Methods, 2014, doi:10.1038/NMETH.2962

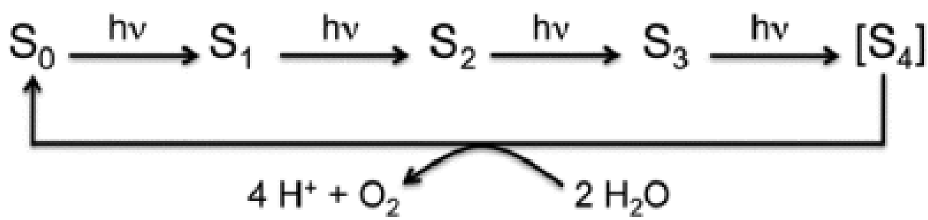

SR results (Nature 2011) had radiation damage….

Dynamic behavior of photo-system II

"The Mn_4Ca photosynthetic water-oxidation catalyst studied by simultaneous X-ray spectroscopy and crystallography using an X-ray free-electron laser"
Rosalie Tran et al
Phil. Trans. R. Soc. B 369 20130324 (2014) doi: 10.1098/rstb.2013.0324

"Taking snapshots of photosynthetic water oxidation using femtosecond X-ray diffraction and spectroscopy"
Jan Kern et al
Nature Comm. 5. 4371 (2014)

"Serial time-resolved crystallography of photosystem II using a femtosecond X-ray laser"
C. Kupitz et al
Nature (2014)
doi:10.1038/nature13453

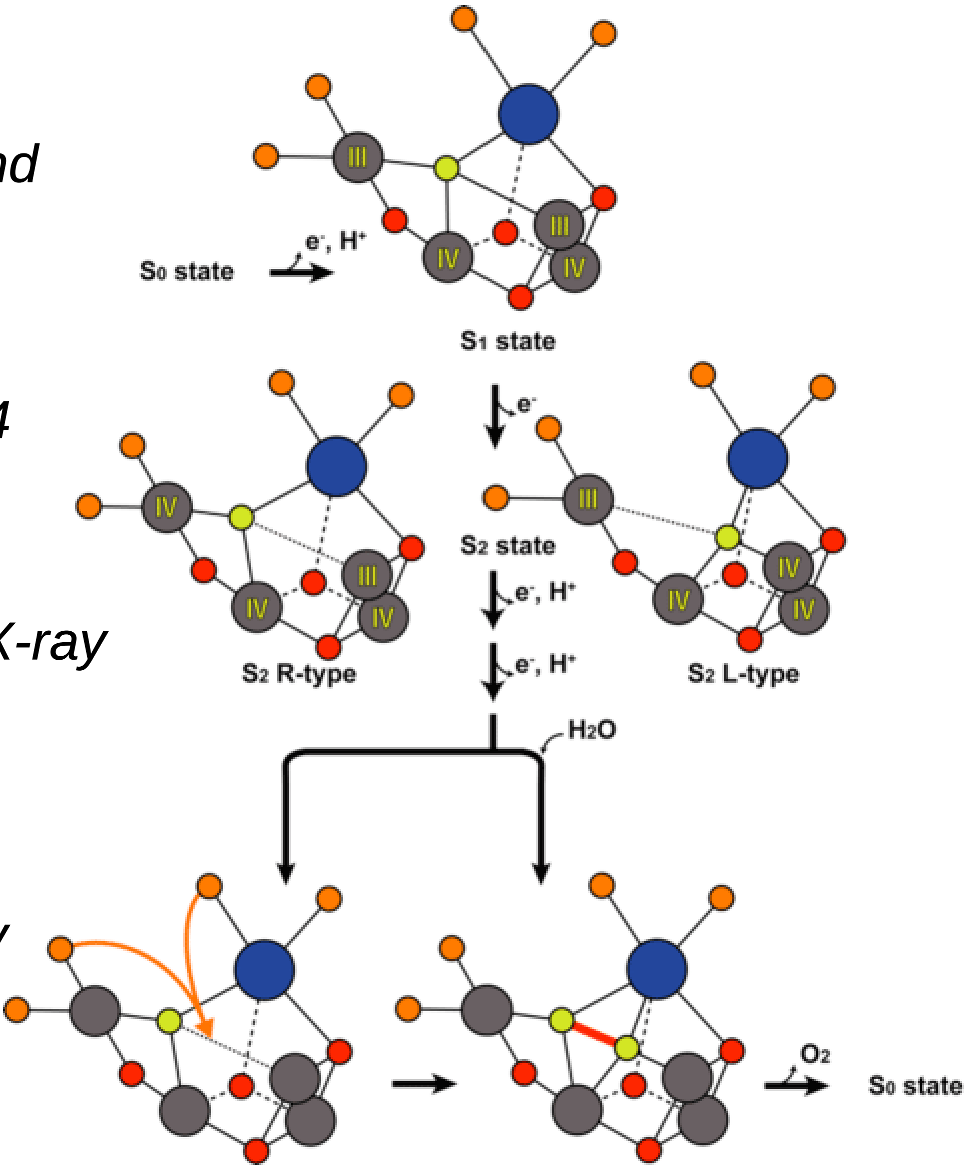

Suga et al, Nature

Towards artificial photosynthesis

Visualizing the non-equilibrium dynamics of photo-induced intramolecular electron transfer with femtosecond X-ray Pulses (SACLA) Canton et al. *Nature Comm. 6, 6359 (2015)*

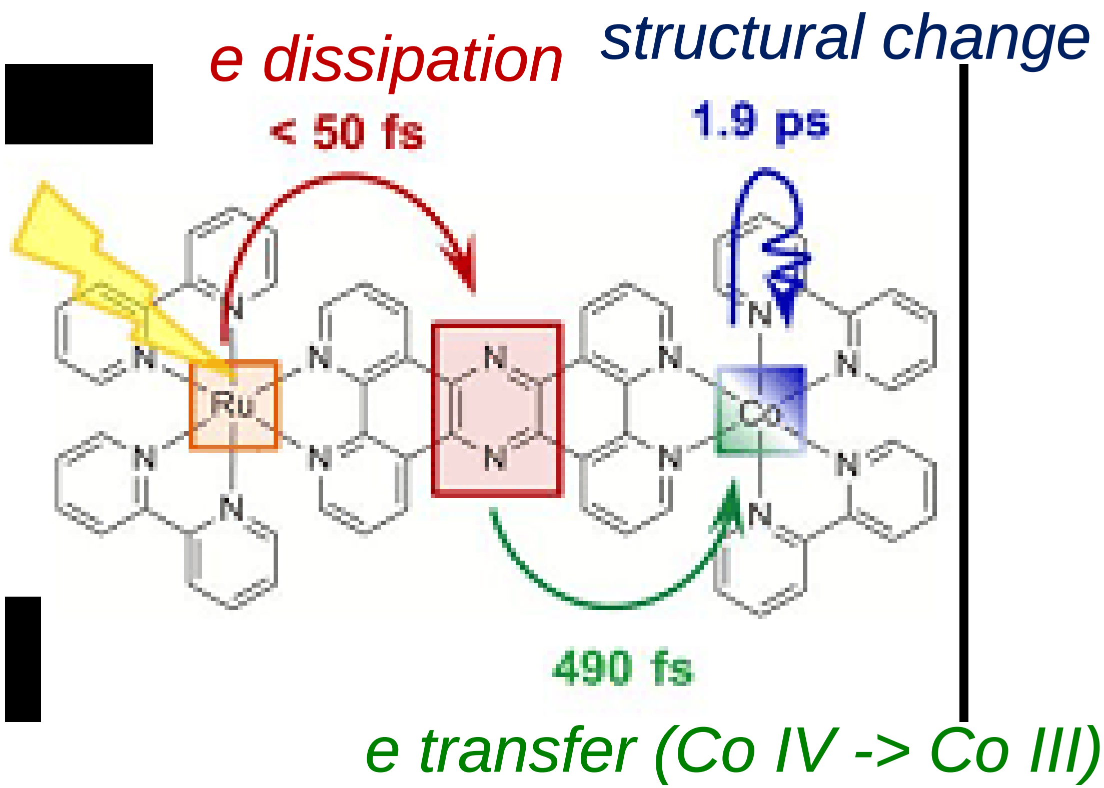

Serial femtosecond x-ray crystallography: phasing

Phasing of the serial femtosecond x-ray crystallography had been relying on molecular replacements…

If the structure is completely unknown, phasing approaches make use of anomalous dispersion in the scattering signals from specific atoms.

Anomalous signal from S atoms in protein crystallographic data from an X-ray free-electron laser

T.R.M. Barends, L. Foucar, R.L. Shoeman, …. K. Ueda and I. Schlichting

Acta Cryst. D ***69****, 838-842 (2013).*

One of the first experiments at SACLA

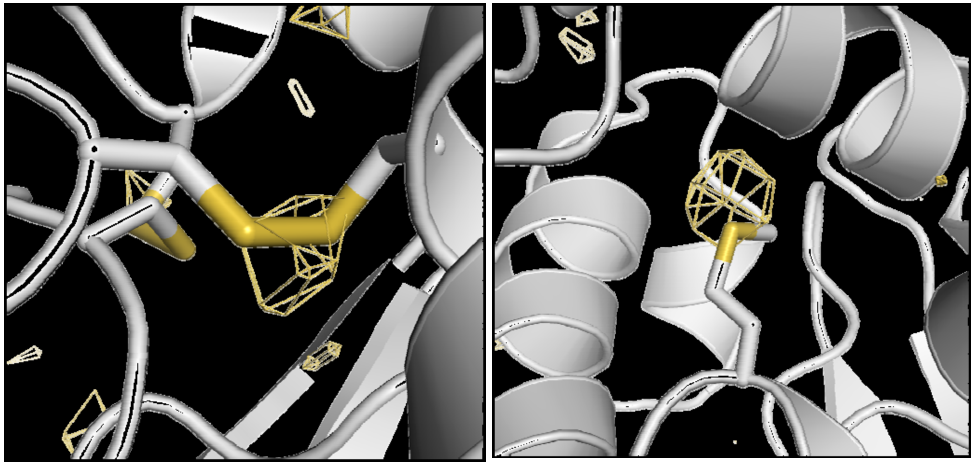

For phasing with a heavy atom, one has to take account of high x-ray intensity

Multi-wavelength anomalous diffraction at high X-ray intensity

S.-K. Son, H. N. Chapman, and R. Santra, Phys. Rev. Lett. ***107****, 218102 (2011).*

However…..

De novo protein crystal structure determination from X-ray free-electron laser data

T.R.M. Barends et al., Nature ***505,*** *244 (2014).*

Conventional phasing method based on anomalous dispersion worked….

Characteristic properties of FEL pulses

Intense 10^{14} W/cm^2 (EUV) - 10^{20} W/cm^2 (X)

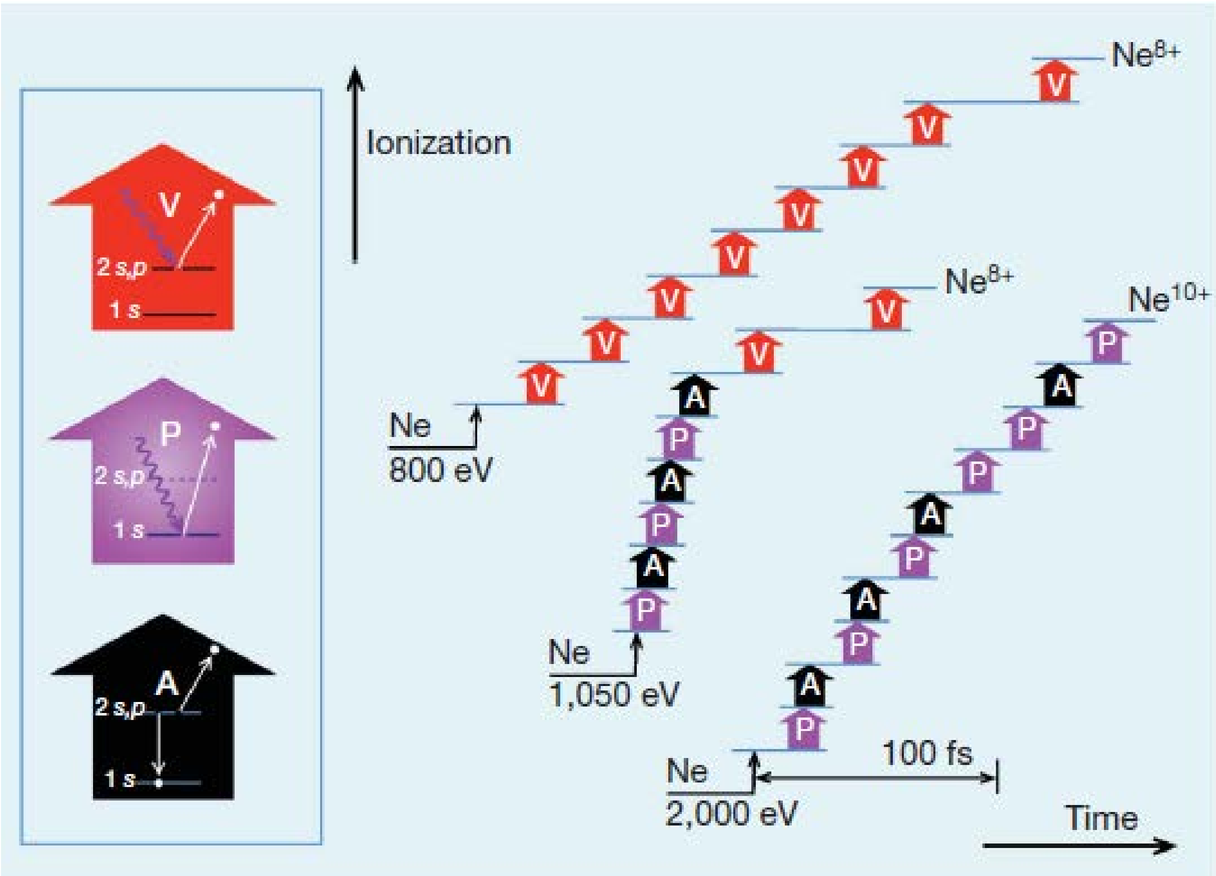

Femtosecond electronic response of atoms to ultra-intense x-rays
L. Young et al., Nature **466**, 56 (2010).

One LCLS pulse at 2 keV can remove all ten electrons from the neon atom.

The pulse is so intense that it causes electronic damage to the sample.

Non-linear X-ray atomic Physics

Ultra-Efficient Ionization of Heavy Atoms by Intense X-Rays

B. Rudek, S-K. Son, L. M. Foucar, S. W. Epp, B. Erk, R. Hartmann, M. Adolph, R. Andritschke, A. Aquila, N. Berrah, C. Bostedt, J. Bozek, N. Coppola, F. Filsinger, H. Gorke, T. Gorkhover, H. Graafsma, L. Gumprecht, A. Hartmann, G. Hauser, S. Herrmann, H. Hirsemann, P. Holl, A. Hömke, L. Journel, C.Kaiser, N. Kimmel, F. Krasniqi, K-U. Kühnel, M. Matysek, M. Messerschmidt, D. Miesner, T. Möller, R. Moshammer, K. Nagaya, B.Nielsson, G. Potdevin, D. Pietschner, C. Reich, D. Rupp, R.Santra, G. Schaller, I. Schlichting, C. Schmidt, F. Schopper, S. Schorb, C-D. Schröter, J. Schulz, M. Simon, H. Soltau, L. Strüder, ***K. Ueda****, G. Weidenspointner, J. Ullrich, A. Rudenko, and D. Rolles*

Nature Photonics 6, 858 (2012).

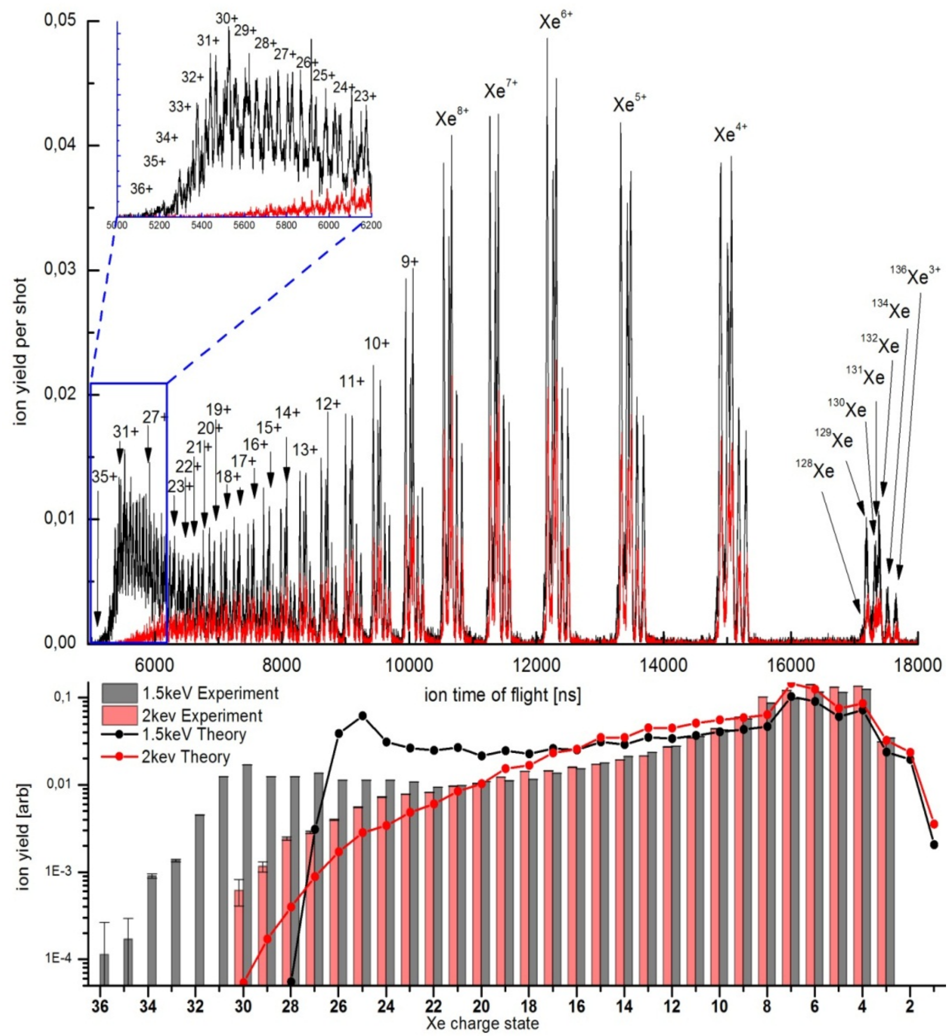

5-iodouracil ($C_4H_3IN_2O_2$)

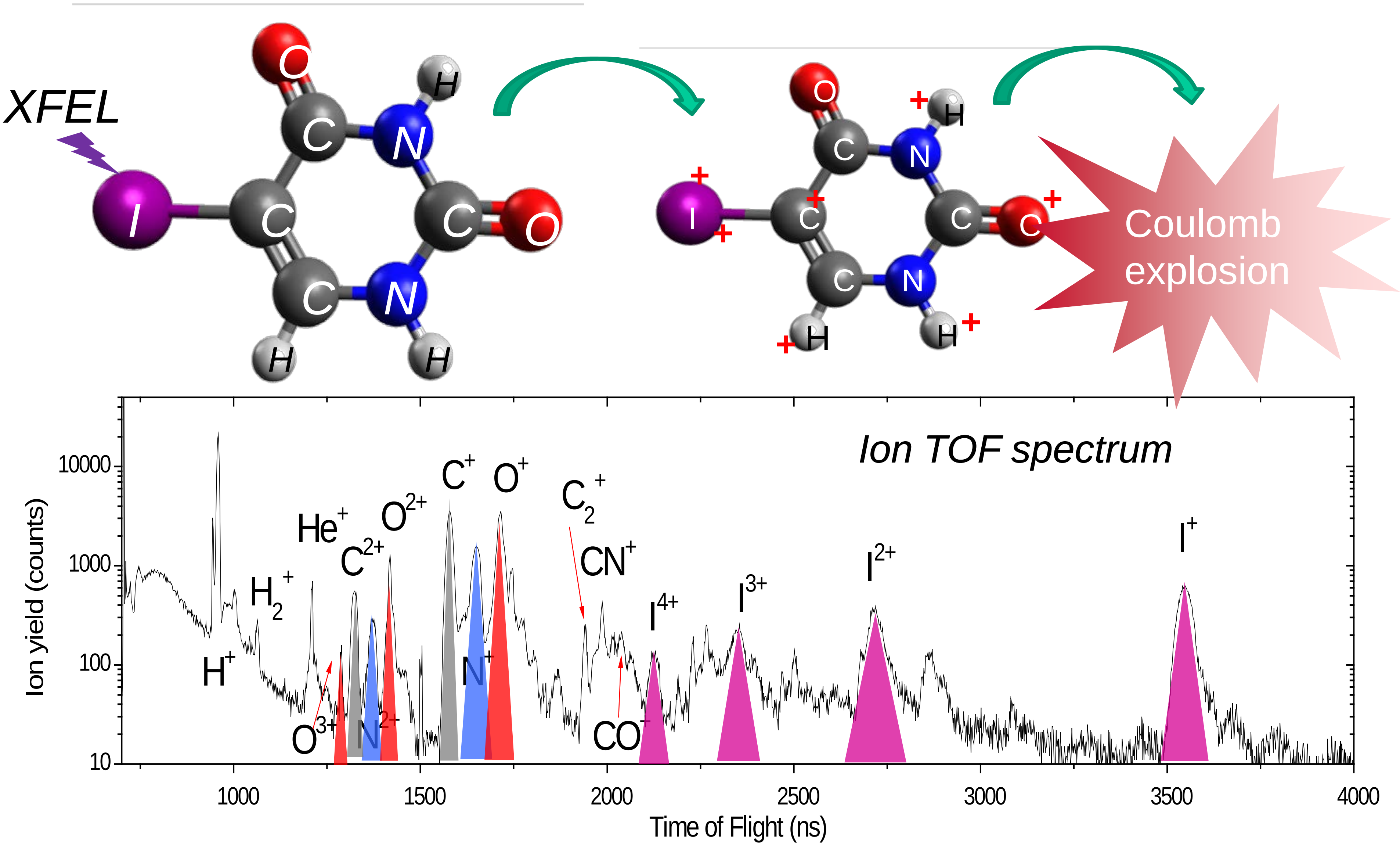

We observed iodine ions with the charge up to +4 and many more ions

2-body angular correlation

Black: I^{+}, Red: I^{2+}, Blue: I^{3+}, Green: I^{4+}

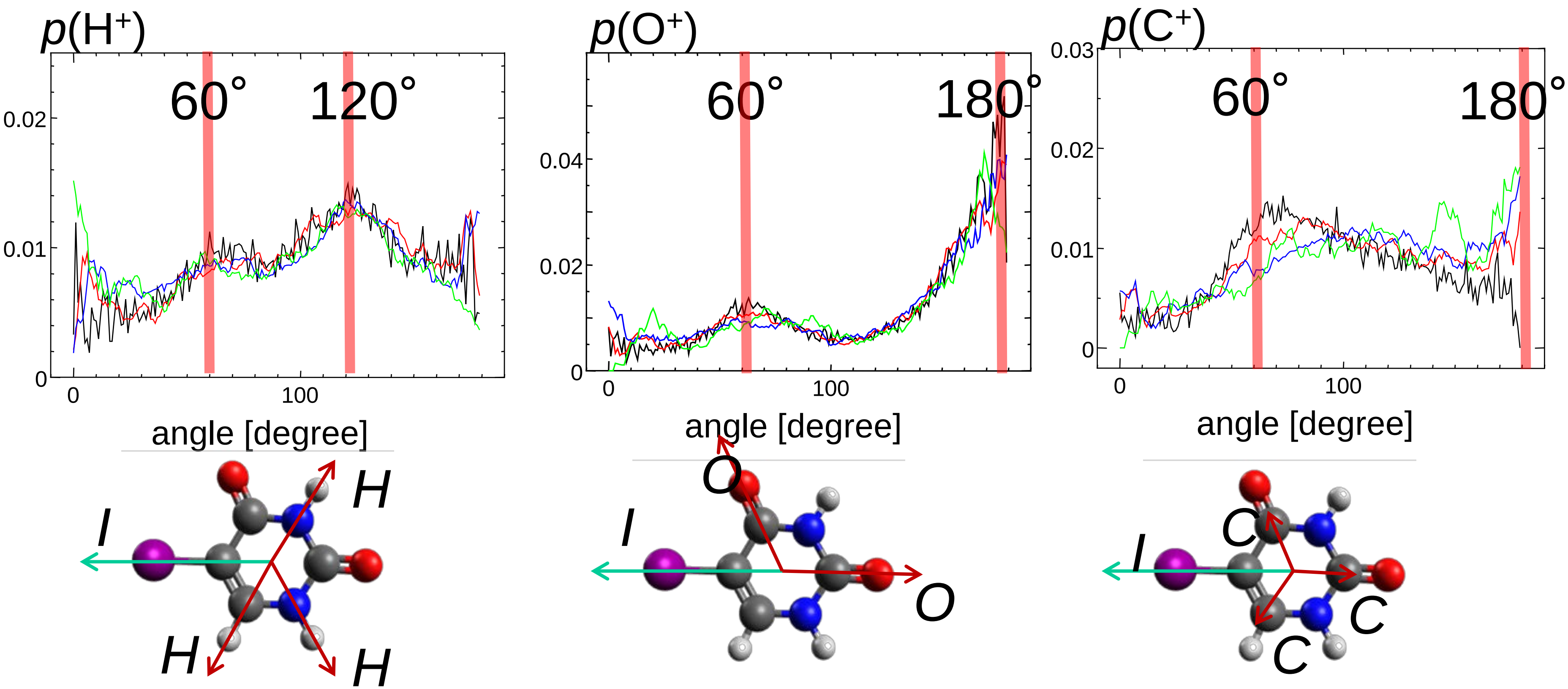

Red lines indicate angle between I direction and H, O, or C directions from the center of the aromatic ring in the neutral molecule.

Angular correlations of fragment ions (except carbon ions) reflect the shape of parent molecule.

2-body angular correlation

Black: I^{+}, *Red*: I^{2+}, *Blue*: I^{3+}, *Green*: I^{4+}

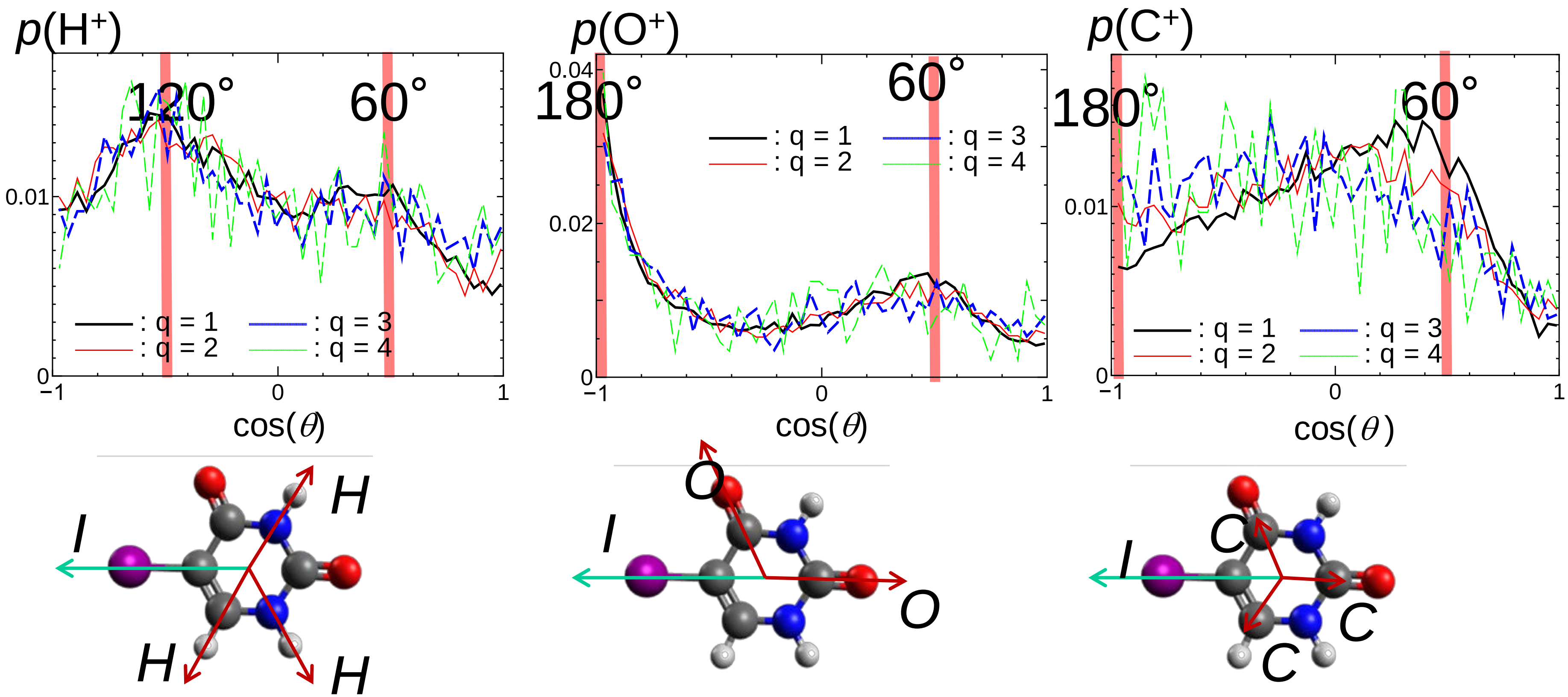

Red lines indicate angle between I direction and H, O, or C directions from the center of the aromatic ring in the neutral molecule.

Angular correlations of fragment ions (except carbon ions) reflect the shape of parent molecule.

3-body angular correlation

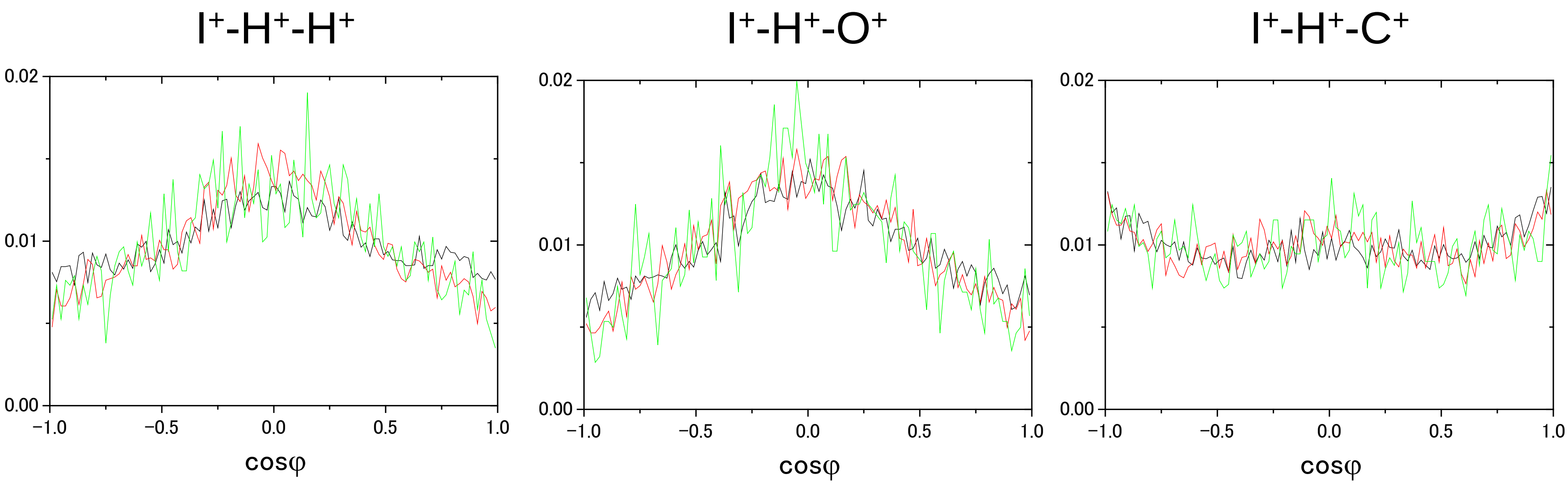

Black: I^+, Red: I^{2+}, Green: I^{3+}

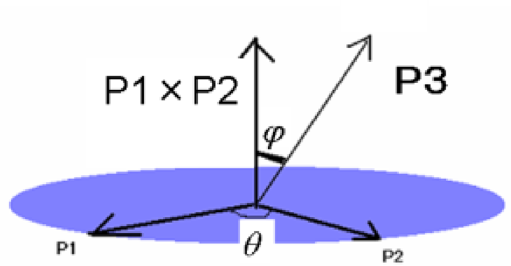

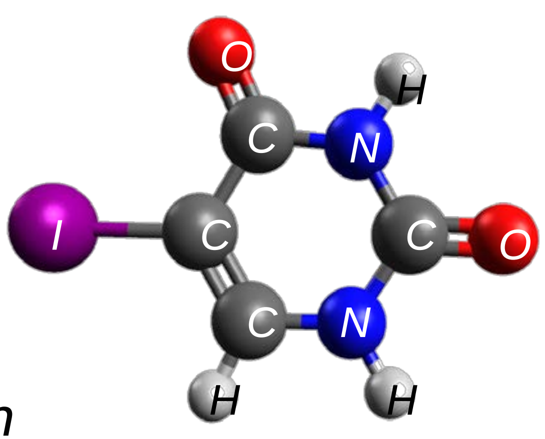

$$\cos(\varphi) = (\mathbf{P}_1 \times \mathbf{P}_2) \cdot \mathbf{P}_3 / (|\mathbf{P}_1||\mathbf{P}_2||\mathbf{P}_3| \sin(\theta)).$$

$\mathbf{P}_1$, $\mathbf{P}_2$ and $\mathbf{P}_3$ are momentum of ions.

$\cos(\varphi) = 0$ means that three momentum vectors are in the same plane.

These results suggest that carbon ions are released to off-planar direction.

3-body angular correlation

I^{+}-H^{+}-H^{+}

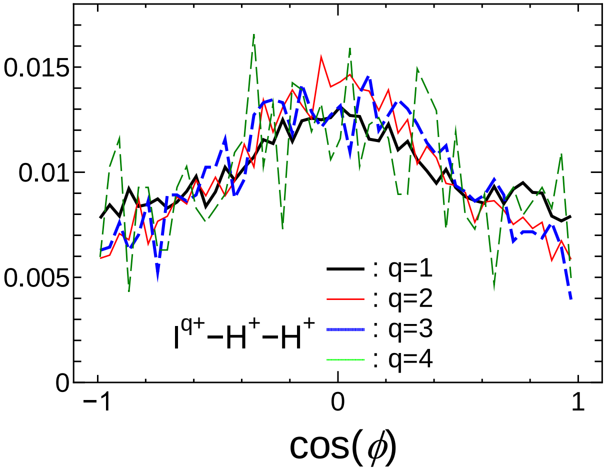

I^{+}-H^{+}-O^{+}

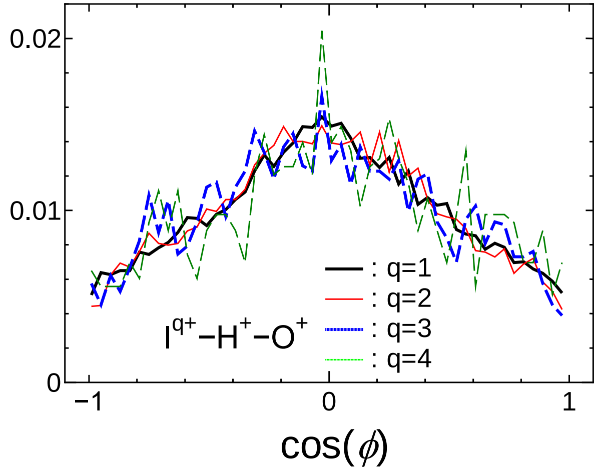

I^{+}-H^{+}-C^{+}

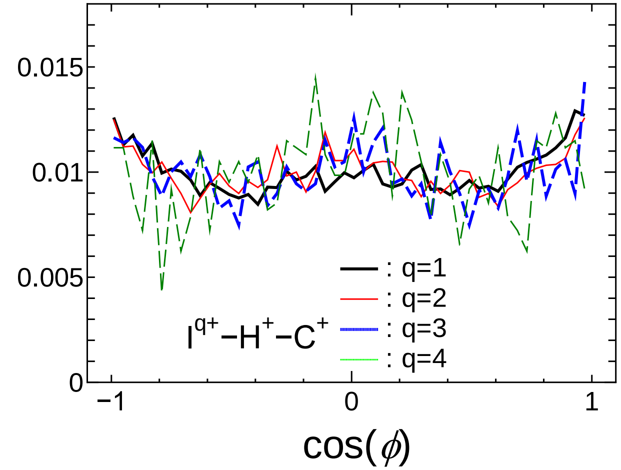

Black: I^{+}, Red: I^{2+}, Blue: I^{3+}, Green: I^{4+}

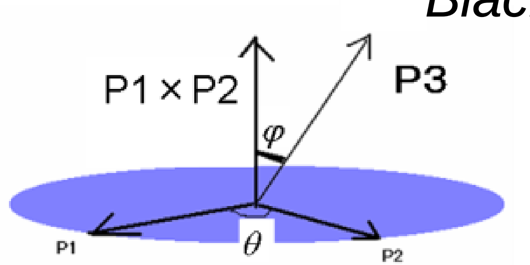

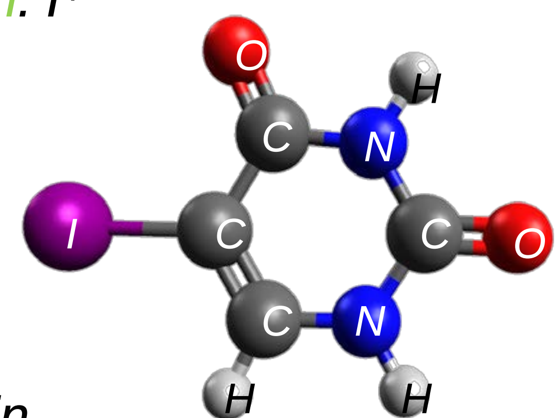

$$\cos(\varphi) = (\mathbf{P}_1 \times \mathbf{P}_2) \cdot \mathbf{P}_3 / (|\mathbf{P}_1||\mathbf{P}_2||\mathbf{P}_3|\sin(\theta)).$$

***P_1*, *P_2* and *P_3* are momentum of ions.**

$\cos(\varphi) = 0$ means that three momentum vectors are in the same plane.

These results suggest that carbon ions are released to off-planar direction.

DFT simulations for 5-iodouracil

We found charge transfer (localization) is completed within 6 fs.

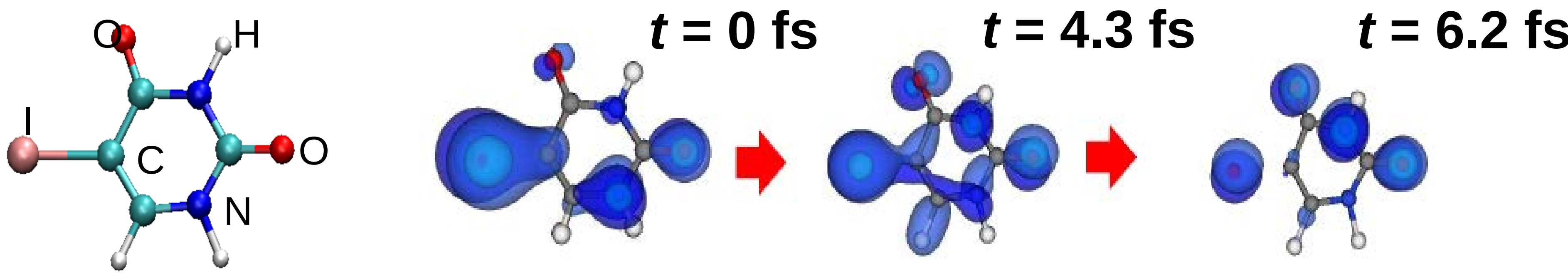

Protons are ejected within 10 fs.

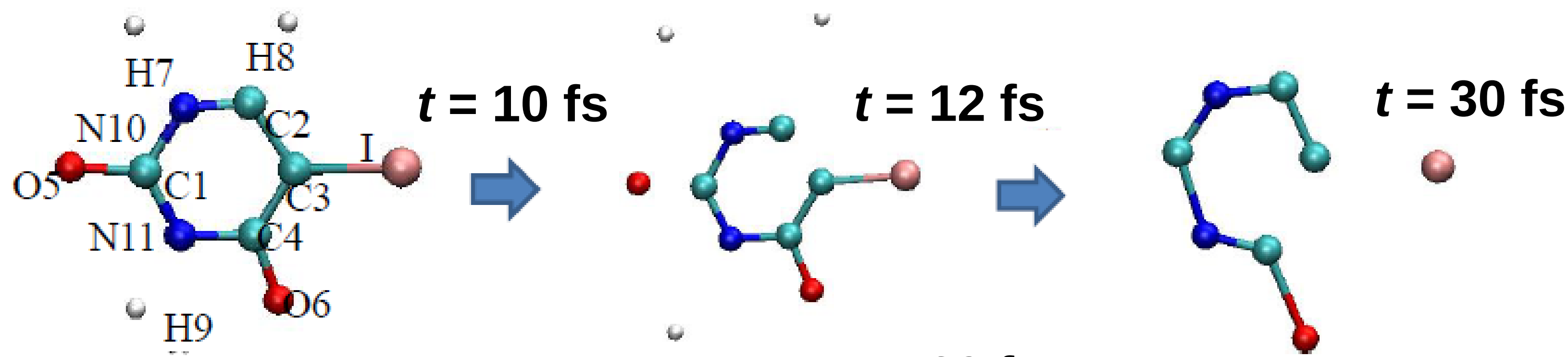

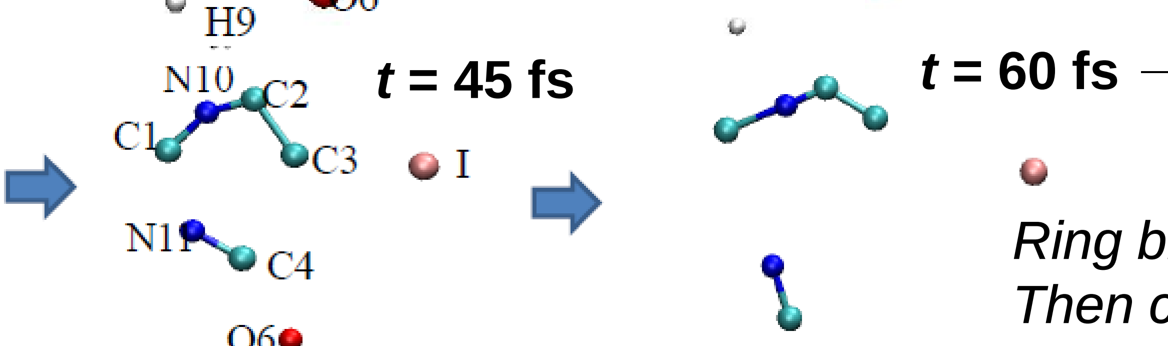

Ring breakup occurs later.
Then carbon ions can be released.

These calculation results support well the experimental findings.

IR energy absorption of nanoplasma

The energy absorbing rate per electron via surface plasmon resonance can be described by the Drude model,

Ponderomotive energy *Damping rate*

$$\frac{\partial E}{\partial t} = \frac{1}{n_e} E \cdot \frac{\partial \mathbf{D}}{\partial t} = 2\boldsymbol{U_p} \frac{\boldsymbol{\Gamma}}{\left(\boldsymbol{\omega_p^2}/3\boldsymbol{\omega}^2 - 1\right)^2 + \boldsymbol{\Gamma}^2/\boldsymbol{\omega}^2}$$

$$\omega_p = \sqrt{\frac{e^2 n_e(t)}{m_e \epsilon_0}}$$

ω_p: plasma frequency

$\boldsymbol{\omega}$: NIR Laser frequency

n_e : electron density $n_e(t) = 3ZN/4R(t)^3$

R : radius of nanoplasma $R(t) = \boldsymbol{v}t + R_0$

R_0 : cluster size $R_0 = 4.4$nm

$\Gamma(t) = \boldsymbol{\Gamma_0}\, x[R_0/R(t)]$ *$R(t) = \boldsymbol{R_{res}}$ @ $\omega_p = 3^{1/2}\omega$*

*T. Ditmire et al., Phys. Rev. A **53**, 3379 (1996)*

Fitting to the experimental data

$$\frac{\partial E^*}{\partial t} = \boxed{\frac{4\pi I_{\mathrm{NIR}}}{c}} \boxed{(R_0 + v_0 t_{\mathrm{Res}})^3 \Gamma_0} \frac{\left[\left(R_0 + v_0 t\right)/R_0\right]^{-1}}{\left[\exp\left(-\frac{t-t_{\mathrm{Res}}}{\tau_e}\right)\left(\frac{R_0+v_0 t}{R_0+v_0 t_{\mathrm{Res}}}\right)^{-3} - 1\right]^2 + \left[\Gamma_0\left(\frac{R_0+v_0 t}{R_0}\right)^{-1}/\omega\right]^2} \exp\left(-\frac{t-t_{\mathrm{Res}}}{\tau_e}\right)$$

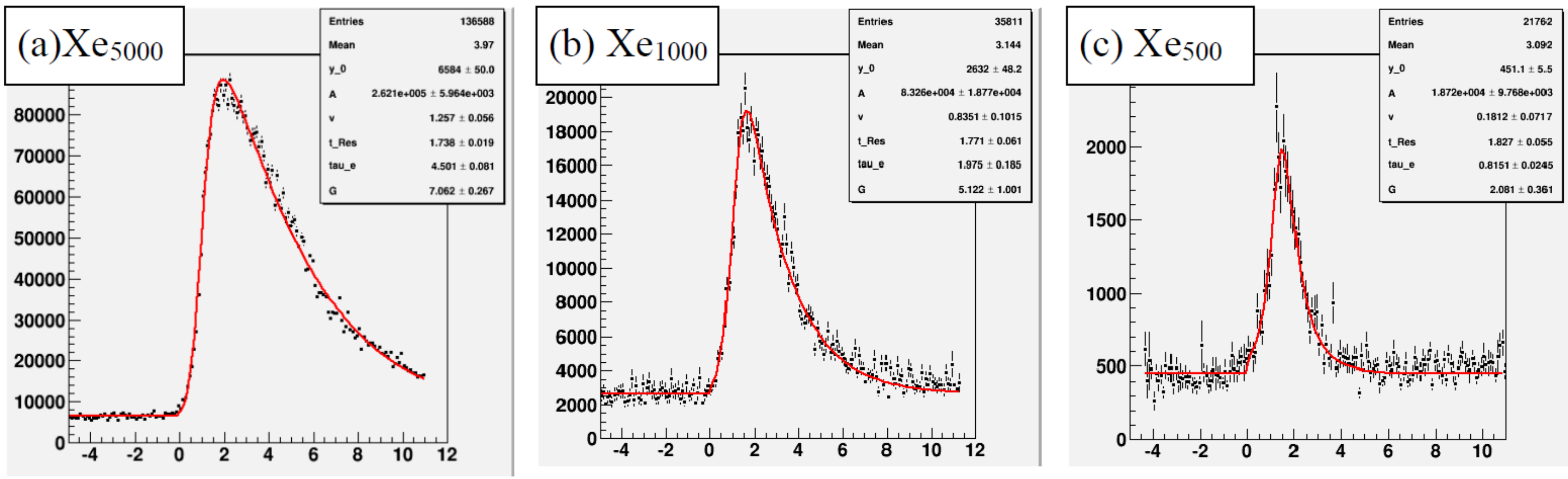

Fig3-1. Total energy absorption as a function of delay time. (a)Xe_{5000}, (b) Xe_{1000}, (c) Xe_{500}. Red curves show the fitting results by equation (4).

We can characterize XFEL-induced nanoplasma by investigating its expansion and recombination by IR probe !

Time of Flight spectrum of argon ions

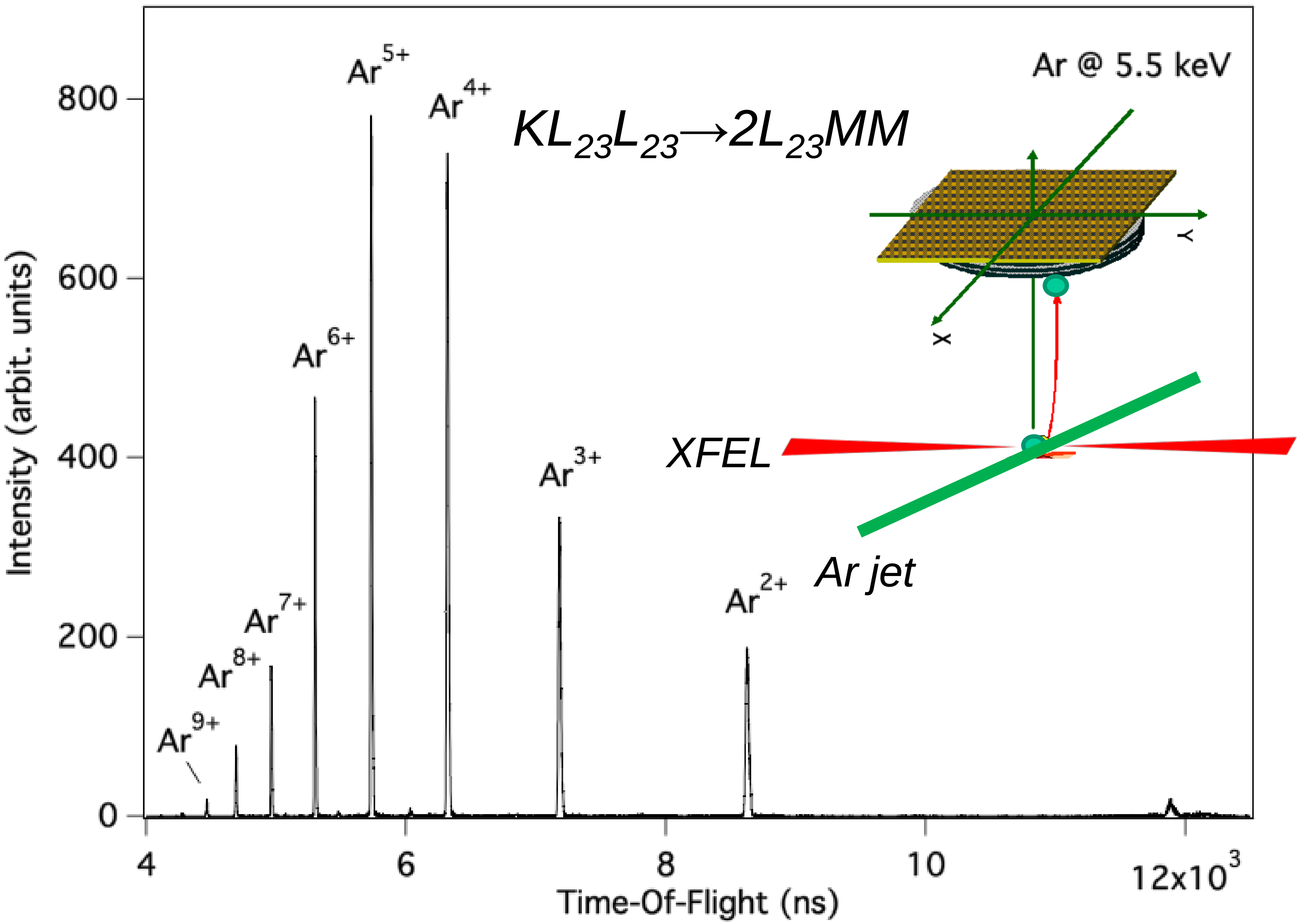

XFEL fluence dependence for Ar^{n+} yields

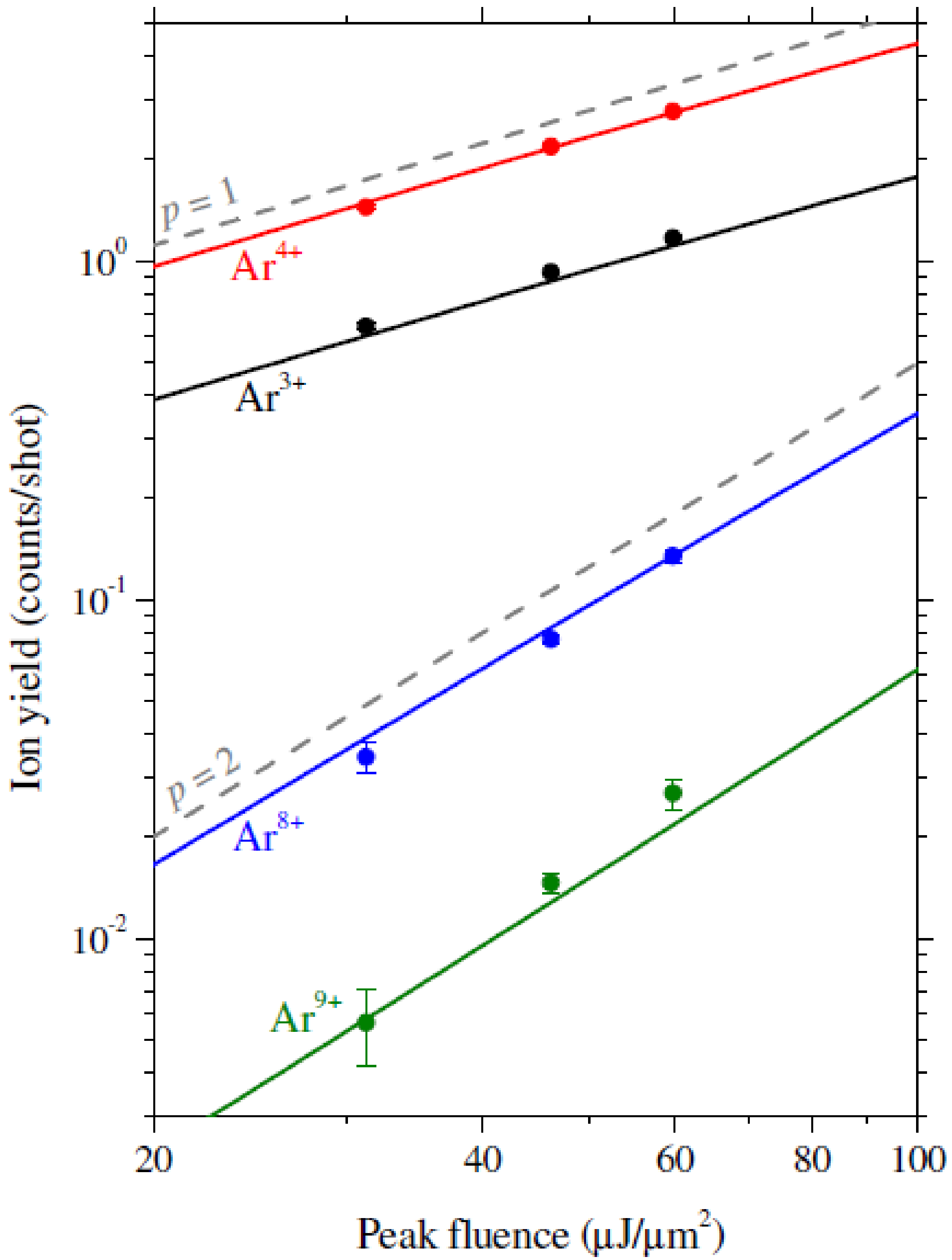

Ar^{4+}: single photon K-shell ionization $\rightarrow KL_{23}L_{23}$ Auger $\rightarrow 2L_{23}MM$ Auger

Ar^{3+}: single photon K shell absorption

$\rightarrow KL_{23}M$ Auger $\rightarrow L_{23}MM$ Auger

Ar^{8+}, Ar^{9+}: sequential two photon K shell ionization

Bench mark ab initio calculation reproduces fluence dependence and relative ratios.

In the theory, the pulse shape of Gaussian of 30 fs (FWHM), and Gaussian focal shape of 1 μm (FWHM) × 1 μm (FWHM) are assumed.

Charge state distribution of Ar: experiment and theory

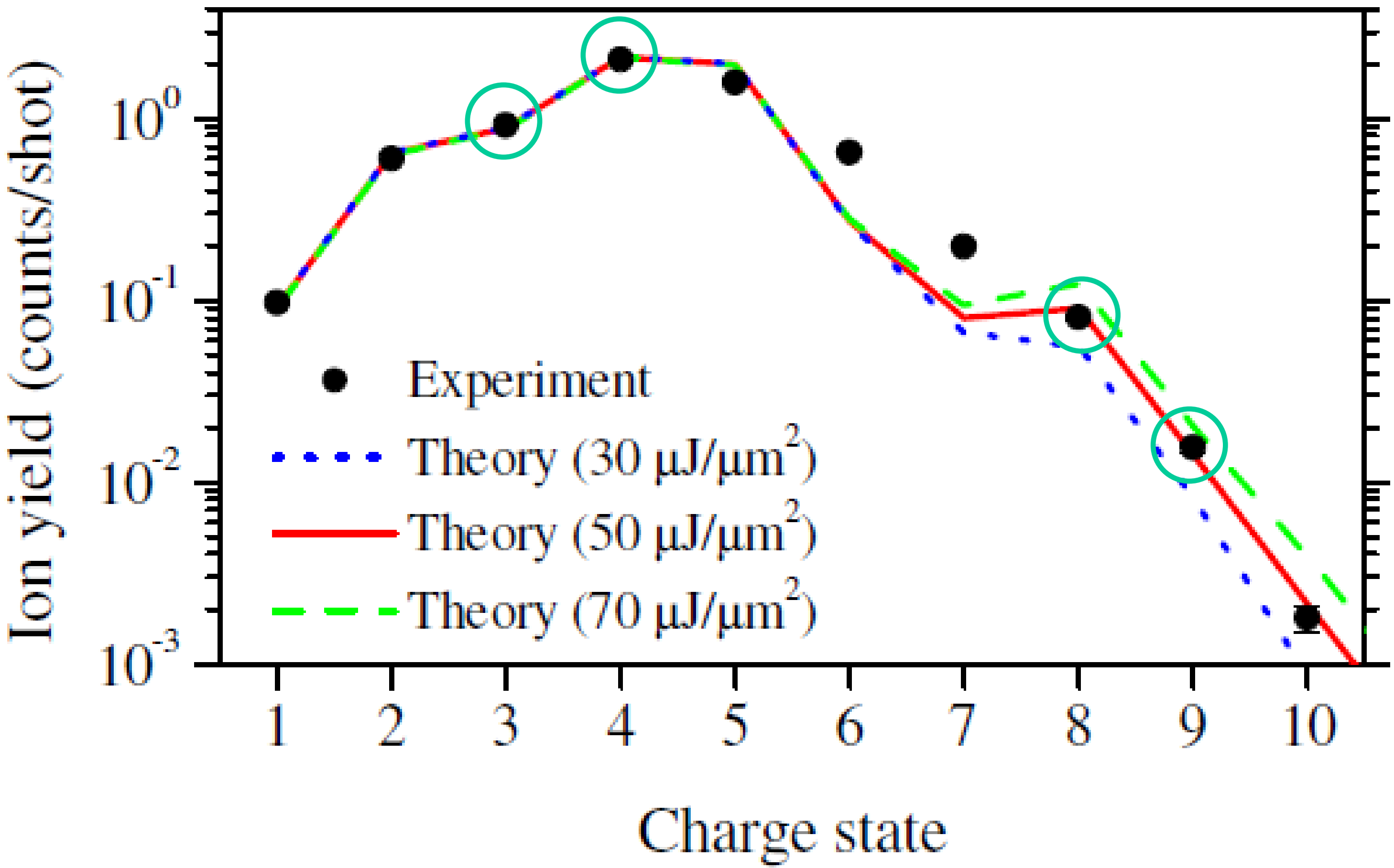

By comparison with theory, we obtained peak fluence of 50 μJ/μm^2 in the experiment!